NASA Contract Report CR-168023

COMPRESSION AND COMPRESSION FATIGUE TESTING OF COMPOSITE LAMINATES

T. R. Porter

Boeing Military Airplane Company
P.O. Box 3707
Seattle, Washington 98124

CONTRACT NAS3-22812

National Aeronautics and
Space Administration

Lewis Research Center
Cleveland, Ohio 44135

DISCLAIMER NOTICE

THIS DOCUMENT IS BEST QUALITY AVAILABLE. THE COPY FURNISHED TO DTIC CONTAINED A SIGNIFICANT NUMBER OF PAGES WHICH DO NOT REPRODUCE LEGIBLY.

NASA

NATIONAL AERONAUTICS AND

SPACE ADMINISTRATION

COMPRESSION AND COMPRESSION FATIGUE TESTING OF COMPOSITE LAMINATES

by

T. R. Porter

Advanced Airplane Branch

Boeing Military Airplane Company

A Division of the Boeing Company

Seattle, Washington

Prepared for

NATIONAL AERONAUTICS AND SPACE ADMINISTRATION

NASA Lewis Research Center

Contract NAS3-22812

Gordon T. Smith, Project Engineer

FOREWORD

This report summarizes the work accomplished on NASA Contract NAS3-22812 "Compression and Compression Fatigue Testing of Composite Laminates."

The program was sponsored by the National Aeronautics and Space Administration, Lewis Research Center, Cleveland, Ohio. Mr. G. T. Smith, NASA Lewis Research Center, was project manager.

Performance of this contract was under the direction of the Advanced Airplane Branch of the Boeing Military Airplane Company. Dr. R. R. June, who heads Advanced Composites Development, was the program manager. Mr. T. R. Porter was the technical leader, Pete Smith coordinated specimen fabrication, J. R. Vosper and M. C. Riley provided testing support, and L. R. Hause was responsible for ultrasonic inspection support.

TABLE OF CONTENTS

LIST OF TABLES

LIST OF FIGURES

LIST OF FIGURES

INTRODUCTION

The objective of this program was to obtain data to experimentally evaluate the effects of moisture and temperature on the integrity of fiber composite components. In particular, the static and cyclic performance of composite laminates containing flaws was investigated at room temperature, 394K (250^{o} F) and 422K (300^{o} F) in wet and dry conditions. This program extends the results developed under contracts NAS3-19709 and NAS3-20405 reported in NASA CR-135403 and NASA CR-165213 (references 1 and 2).

The experimental program was performed in three tasks: (1) Static-Compression Tests, (2) Tension-Compression Fatigue Tests and (3) Residual-Compression Tests.

The static-compression fracture strength was evaluated on laminates that had been moisture conditioned and in the as-prepared condition. In addition to unnotched specimens, panels containing through-the-thickness slits 3.18 mm (0.125 in), 9.52 mm (0.375 in), and 15.87 mm (0.625 in) long were tested.

The tension-compression fatigue testing was performed on specimens that had 15.87 mm (0.625 in) slits and impact-produced delaminations. As-manufactured and moisture-conditioned specimens were evaluated at room and elevated temperatures.

The residual-compression strength was evaluated for test specimens after cyclic loading. Both tension-compression and compression-only cyclic loading ratios were included.

Previous testing under NASA Lewis Contracts NAS3-19709 and NAS3-20405 with The Boeing Company had demonstrated the importance of compressive loading on the fatigue and static response of these graphite-epoxy structural laminates. The compression loads were especially critical for the elevated-temperature and wet environments.

Test materials available from NASA Contract NAS3-20405 were used for this program. These results are directly comparable to the available data since they are from the same material batch and have the same processing history.

SPECIMEN DESIGN AND MANUFACTURE

The specimens used in this test program were cut from panels that had been fabricated under Contract NAS3-20405 (reference 2). The majority of the available materials were the general purpose laminate (L1) with a small panel of the all-graphite turbine engine fan-blade laminate (L3-B). The list of these available materials is given on table 1.

Laminate Materials

The materials used for the program were Thornel T-300 graphite fiber, and Fiberite 934 epoxy resin. This is an intermediate stiffness graphite-epoxy composite and was selected as the basic material for the program because of its wide use, moderate cost, and established structural performance. The Fiberite 934 resin system satisfied the requirements of a general purpose epoxy and also has a wide range of applications in aerospace structures. The stacking sequence selected for layup L1, based on symmetry and load transfer requirements, was $((0/\pm 45/0/90)_S)_2$. Note that this stacking is not quasi-isotropic since it contains twice as many 0^o plies as the other orientations.

The stacking sequence for layup L3 is representative of those considered for use in composite turbine engine fan blades. Two possible layup approaches are the dispersed-ply approach and the core-shell approach. The dispersed-ply approach was used because such layups are less subject to delamination from foreign object impact.

Specimen Configuration

Two test specimen configurations were used. A 76-mm (3.0-in) wide specimen shown in figure 1 was used for the notched tests and a 12.6-mm (0.5-inch) wide specimen (figure 2) was used for the unnotched compression tests.

The 76-mm (3.0-in) width used for the majority of the tests was chosen to provide specimens large enough to preclude significant interaction between the stress concentration and stress-free specimen boundaries. The specimen was designed so that the stress concentration factor for the largest defect would be within 5% of the corresponding stress concentration factor for a plate of infinite width. The potential effect of the free edge on the fracture behavior has been investigated experimentally by static testing specimens of various widths that contained the largest defects (reference 2). The 0-degree laminate direction corresponds to the axial direction of the specimen. Woven fiberglass grip tabs were secondarily bonded to the specimen using a 394K (250^{o}) cure adhesive. The 12.6-mm (0.5-in) compression coupon has been shown to produce reliable results for unnotched laminate testing.

Both test specimens were prevented from buckling by using support plates against the specimen faces. The support plates for the 76-mm. (3.0-in) wide specimen had a 50.8-mm (2.0-in) diameter central hole located over the defect to allow local out-of-plane deformations and monitoring of damage growth.

Test Specimen Fabrication and Processing

Specimen layup and fabrication steps are illustrated in figures 3 and 4. Laminates were laid up and cured in 81-cm (32-in) wide panels up to 293 cm (120-in) in length. After curing, fiberglass end tabs were bonded to the basic laminates and then the panels were sawed into specimen blanks. The laminates were debulked after 4th, 8th, 12th, 16th, and 20th ply by holding the laminate under vacuum for 15 to 20 min. The autoclave cure cycle used was:

1. Apply vacuum.

2. Increase autoclave temperature so that laminate temperature increases at a rate of $0.5^{o}C$ to $2.8^{o}C$ ($1^{o}F$ to $5^{o}F$) per min.

3. Hold 60 min at $121^{o}C \pm 5.5^{o}C$ ($250^{o}F \pm 20^{o}F$).

4. Apply 689 kPa (100 lb/in^2) pressure 15 min after the laminate reaches temperature.

5. Increase laminate temperature to $177^{o}C \pm 5.5^{o}C$ ($350^{o}F \pm 10^{o}F$) at a rate of $0.5^{o}C$ to $2.8^{o}C$ ($1^{o}F$ to 5^{o} F) per min.

6. Hold at temperature for 120 min $\pm$5 min, then cool under pressure.

The specimens were tested with no defects, full-penetration slits, half-

penetration slits, and impact-produced delaminations. These defects were selected from a more extensive list used in the previous (reference 1 and 2) programs shown in table 2. For the data presentation in the tables and figures a code is used to identify the type and nominal size of defect as defined in table 2. Figure 5 illustrates the defect types tested in this program.

The slit sizes selected for test were 3.18 mm (0.125 in), 9.52 mm (0.375 in), and 15.87 mm (0.625 in). These sizes, coded as 1/8, 3/8, and 5/8 (in) respectively encompass most practical fastener diameters. They are also at the threshold of detectable damage sizes for many common inspection procedures. The same sizes were used for the surface length of the half-penetration defects, because when partial penetration damage exists in structures, the most obvious dimension is the length of the damage on the surface. All slits were perpendicular to the primary load-carrying direction of each laminate. This means that they were perpendicular to the 0-degree fibers.

The slits were fabricated by ultrasonic machining. Circular cutter tips were machined to a thickness of 1.52 mm (0.06 in) and a sharp radius. The ultrasonic vibrations of the cutter produce a lapping action in an abrasive slurry that carries away the excess material as the cutter penetrates the part. The slit radius in the composite laminate was typically about 0.127 mm (0.005 in) with a smooth surface. Figure 6 shows a typical partial penetration flaw that has been sectioned to illustrate the root geometry.

The impact-damage defect was produced by impacting the specimens with a 0.91-kg (2-lb) weight dropped from a height of 0.38m (15 in). Figure 7 is a photograph of the impact stand used. There was almost no visible evidence of damage to the test specimen after impact. The surface dent depth was less than 0.13 mm (0.005 in) and there was no evidence of broken filaments. The test specimen was supported on a circular support containing a 15.9 mm (0.625-in) hole. This support condition, together with the 15.9 mm (0.625-in) diameter hemispherical impactor, produced a delamination damage diameter of approximately 15.9 mm (0.625 in). Examination of sectioned specimens damaged in this manner showed delamination damage throughout the laminate thickness. Figure 8 shows the typical impact produced delaminations.

MOISTURE CONDITIONING

The specimens in this program were tested in two moisture conditions: dry and wet. The dry condition resulted from office-room-air storage of the laminates from the time of cure until specimen fabrication and laboratory storage before testing. Since these laminate materials were fabricated for a previous program, the storage time for the materials was approximately two years between cure and test. The humidity during this storage was generally in the range of 40% to 50%.

The wet moisture condition was produced by soaking in a 355K ($180^{o}F$) water bath for 8 weeks. This time and temperature, established from previous testing, produces a near-equillibrium condition with a weight gain of about 1.3% to 1.5%. During the elevated-temperature soak, test specimens were taken from the water bath at intervals, towel dried, and weighed to determine the amount of moisture gain. To minimize variances due to conditioning procedures, all specimens were conditioned together in one tank. Previous exposure testing of similar configuration specimens has shown that the glass tabs absorb moisture at a higher rate than the graphite-epoxy, making the actual weight-gain values hard to interpret. To offset this problem, untabbed test laminate traveler material from each of the laminate types was soaked and weighed along with the test samples. The weight of these traveler coupons was used to monitor the conditioning treatment.

Figure 9 shows the weight gain for these traveler coupons. Similar moisture absorption data developed in previous conditioning is included for

comparison. The data indicate that the coupons conditioned in this program absorbed slightly less moisture (about 0.1% to 0.2% less) during conditioning than those conditioned previously. The result is anticipated because of the moisture absorbed by the panel during storage between programs.

STATIC FRACTURE RESULTS

The static-fracture strength under compression loading was evaluated for laminate L1 and a limited number of L3-B laminate specimens. The test conditions are presented in table 3. The testing included room and elevated temperatures. All static tests were performed in a load-controlled test machine using friction specimen grips. The specimens were loaded at a rate of 1100 N/S (250 lb/s). This rate resulted in failure in about 1 min after the onset of loading. The flawed test specimens were instrumented using a crack opening displacement (COD) gage across the defect. The COD gage was placed across the defect against bonded knife-edge supports. COD versus load was recorded for each test. These curves are included in appendix D.

The specimen heating procedures were developed in previous testing using temperature survey specimens. The test specimens were heated through a combination of resistance heaters on the stabilizing plates and a radiant heater. In this manner the specimen temperature is controlled to within 3K ($5^{o}F$) of the desired temperature in the region of the defect. These procedures allowed access to the specimen for inspection and COD instrumentation. Access to the specimen face was through the 50.8-mm (2-in) diameter central holes in the stabilization plates.

The compression-fracture test results and how they compare with previous tension results are presented in figures 10 through 18.

The effect of defect size on the dry-compression-fracture strength is shown in figure 10. The results show there is a significant effect of defect size in the compression strength at all test temperatures with temperature having only a minor effect. With the wet-test specimens however, elevated temperatures significantly degrade the compression strength (figure 11).

These wet- and dry-test results are compared with the available tension data (reference 1 and 2) in figures 12, and 14. At room temperature (figure 12) the tension and compression results are similar in magnitude. The compression data specimens are slightly lower in strength when wet while the tensile data specimens are lower in strength when dry. At elevated temperature (figure 14) the dry specimen compression strength is lower than the tension strength and the wet compression strength is greatly reduced.

These temperature effects are illustrated for dry and wet laminates in figures 15 and 16 for the through slits (FP) and figure 17 for the half penetration (HP) slit. As shown in figure 17, elevated temperature can reduce the notch effect for tension-loaded HP slits leading to an increase in fracture strength. Under compression loading, however, the elevated-temperature dry and the elevated-temperature wet specimens display a significant reduction in strength.

The test data for laminate L3 (figure 18) shows the notch effect was similar for both tension- and compression-loaded specimens. In general, the compression strength was lower than the tension strength.

Comparison of typical crack opening/closing records from these compression tests with results from previous tension testing are shown in figure 19.

FATIGUE RESULTS

Tension-compression (R= -1.0) and fatigue testing was conducted to extend the available tension fatigue test data. Table 4 presents the test matrix for these specimens. All testing was with specimens from laminate L1 containing 5/8-in defects.

The fatigue data for the wet- and dry-slit specimens at 394K ($250^{o}F$) is shown in figure 20. The test data indicate that the absorbed moisture has a greater effect on the initial strength than on the long-life fatigue behavior. The hot wet reduction in static strength was shown earlier in the results in figure 16. The long cyclic life in the hot wet condition could be the result of specimen drying during cyclic test.

The impacted test specimen fatigue data is presented in figure 21 and the HP slit data in figure 22. Because there were only limited test specimens for each condition, when the test specimen did not fail in 1.5×10^{6} cycles the cyclic load was raised to a higher level for continued test. This permitted cyclic test failure data to be developed for all conditions. These points are labeled as a retest in the figure.

A comparison of fatigue results for different types of 5/8-in defects is shown in figure 23. These results are for room air tests of dry specimens cycled under tension-compression loading (R = -1.0). These data indicate that a built-in disbond (a circular teflon insert 1/4 thickness from surface) was the least severe of all defects tested and a through-the-thick-

ness slit was the most severe. The results indicate that an impact-produced delamination is relatively more critical to the static-compression strength and less critical to the fatigue life than the other defects. This result may be true only for those tests with a tension cyclic component ($R = -1.0$). The tension portion of the cycle would contribute to damage growth in the slit and hole specimens, but would not contribute to damage growth when the delamination defect was produced by impact.

RESIDUAL STRENGTH RESULTS

The compression static strengths of cyclic-loaded test specimens were evaluated as defined in table 5. In these tests, cyclic load levels were selected to produce an estimated life of 10^6 cycles. The testing was stopped at the defined lives and the residual static-compression strength was evaluated. Through-transmission C-scan records before and after cycling were used to monitor damage. Figure 24 presents the C-scan results after cycling for room temperature, dry-test specimens. The longer life test specimens show delamination growth in the region of the initial slit. The residual-compression strengths for these specimens are shown in figure 19. There is a reduction in the compression-residual strength in specimens where the C-scans show damage growth.

The available tension-residual strength results and cyclic-fatigue-life data are also included in figure 25 for reference. From these results it can be seen that the initial tension and compression strengths in these panels are nearly identical. With cyclic loading, however, the tension-residual strength raises while the compression-strength lowers.

Figures 26 through 30 present similar residual strength results for the other test conditions. Similar conclusions apply to the other test conditions with the exception that the compression strengths did not always decrease. This was most evident for the elevated-temperature test data. A potential reason could be specimen drying during the cyclic test.

CONCLUSIONS

Tests were performed on two composite laminates to provide additional data on the static-compression and tension-compression fatigue behavior. These results extend the data generated in prior programs. The test results apply to the specific laminates and test conditions evaluated but the trends should have a wider application. Some of the conclusions made from the test data, and which are discussed in more detail in the report, are as follows:

a. Defects in the composite laminates that cut filaments significantly reduced their tensile and compressive strength.

b. The failure in the test specimens with cut filaments initiated at the stress concentration and propagated across the specimen width. The failure mode and failure stress were similar for both tension and compression loading and the fracture strength was a direct function of defect size.

c. Absorbed moisture had a small effect on the static-fracture strength at room temperature.

d. Test temperature had a significant degredation effect on compression-fracture strength and the combination of moisture and temperature had the greatest degredation effect on compression strength.

e. Moisture and temperature, independently and in combination, had a significant degredation effect on tension-compression fatigue behavior.

f. Under tension-compression fatigue loadings full penetration slits were the most critical while built-in disbonds were the least critical. Impact-produced delaminations were as critical as slits for compression-static loading, but less severe for longer term cyclic testing under tension-compression loading.

g. Cyclic-loading of notched test specimens could produce reductions in the compression-residual strength. This is in contrast to the tension-residual strength which would generally increase.

Table 1. Materials Available for Testing

Laminate	Layup	Specimen Number	Panel Size m x m (in x in)
L1	$((0/\pm45/0/90)_S)_2$	L1 - 21 - x	0.41 x 0.79 (16 x 31)
L1	$((0/\pm45/0/90)_S)_2$	L1 - 34 - x	0.81 x 1.52 (32 x 60)
L1	$((0/\pm45/0/90)_S)_2$	L1 - 35 - x	0.81 x 1.52 (32 x 60)
L3-B	$((0/+30/0/-30/0)_2)_S$	L3 - 22B - x	0.41 x .30 (16 x 12)

Table 2. Defect Type and Size Code

Defect type \ Approximate diameter or surface length d mm (in)	3.18 (0.125)	9.52 (0.375)	15.9 (0.625)
Full-penetration hoie	1/8 FP HOLE	3/8 FP HOLE	5/8 FP HOLE
Half-penetration hole [1]	1/8 HP HOLE	3/8 HP HOLE	5/8 HP HOLE
Full-penetration slit	1/8 FP SLIT	3/8 FP SLIT	5/8 FP SLIT
Half-penetration slit [1]	1/8 HP SLIT	3/8 HP SLIT	5/8 HP SLIT
100-degree full-depth countersink hole	1/8 CSK HOLE	3/8 CSK HOLE	5/8 CSK HOLE
Circular disbond defect between 15th and 16th plies	–	–	5/8 DISBOND
Low velocity impact damage 3.38 N-m (30 in-lb')	–	–	IMPACT

[1] HP defects are 1.5 mm (0.060 in) deep

Table 3. Static Compression Tests

Laminate configuration	Test conditions			Number of test specimens				
				Slit length				
	Moisture	Temperature °F		0	1/8"	3/8"	5/8"	
L_1 $\left(\left[0/\pm45/0/90\right]_S\right)_2$	Dry	75		1	1	1	1	
		250		1	1	1	1	
		300		1	1	1	1	
	Wet	75		1	1	1	1	
		250		1	1	1	1	
		300		1	1	1	1	
	Dry	75					1*	
		250					1*	
		300					1*	
	Wet	75					1*	
		250					1*	
		300					1*	
L_{3-2} $\left(\left[0/+30/0/-30/0\right]_2\right)_S$	Dry	75		1	1	—	1	
		75		—	—	—	1*	

*Half penetration slits

Table 4. Tension-Compression Fatigue Tests

Laminate configuration	Test conditions		R	Number of specimens			
				Defect size			
	Moisture	Temperature °F	Pmax / Pmin	0	1/8"	3/8"	5/8"
L_1 $([0/+45/0/90]_S)_2$	Dry	75	-1				2*
		250	-1				5
		300	-1				2*
	Wet	75	-1				2*
		250	-1				5
		300	-1				2*
	Dry	75	-1				2**
		300	-1				2**
	Wet	75	-1				2**
		300	-1				2**

* Impact delamination defects

** Half-penetration slits

Pmax values for 250° F tests selected for uniform distribution along S/N curve to 1.5×10^6 cycles

Pmax values for 75° F and 300° F tests selected based on NAS 3-20405 failure data

Table 5. Residual Compression Strength Tests

Laminate configuration	Test conditions		Applied load cycles	R. $\frac{P_{min}}{P_{max}}$	Max load	Number of specimens 5/8" slit
	Moisture	Temperature				
L_1 $\left([0/\pm45/0/90]_S\right)_2$	Dry	75	1 10 1,000 100,000 1,000,000	-1 -1 -1 -1 -1	①	1 1 1 1 1
	Wet	75	1 10 1,000 100,000 1,000,000	20 -1 20 -1 20 -1 20 -1 20 -1	①	1 1 1 1 1 1 1 1 1 1
	Dry	300	10 1,000 100,000	-1 -1 -1	①	1 1 1
	Wet	300	10 1,000 100,000	20 -1 20 -1 20 -1	①	1 1 1 1 1 1

① Max load as determined for life of 10^6 cycles

$R = 20 = \frac{-P_{max}}{-.05P_{max}}$ (Compression—compression loading)

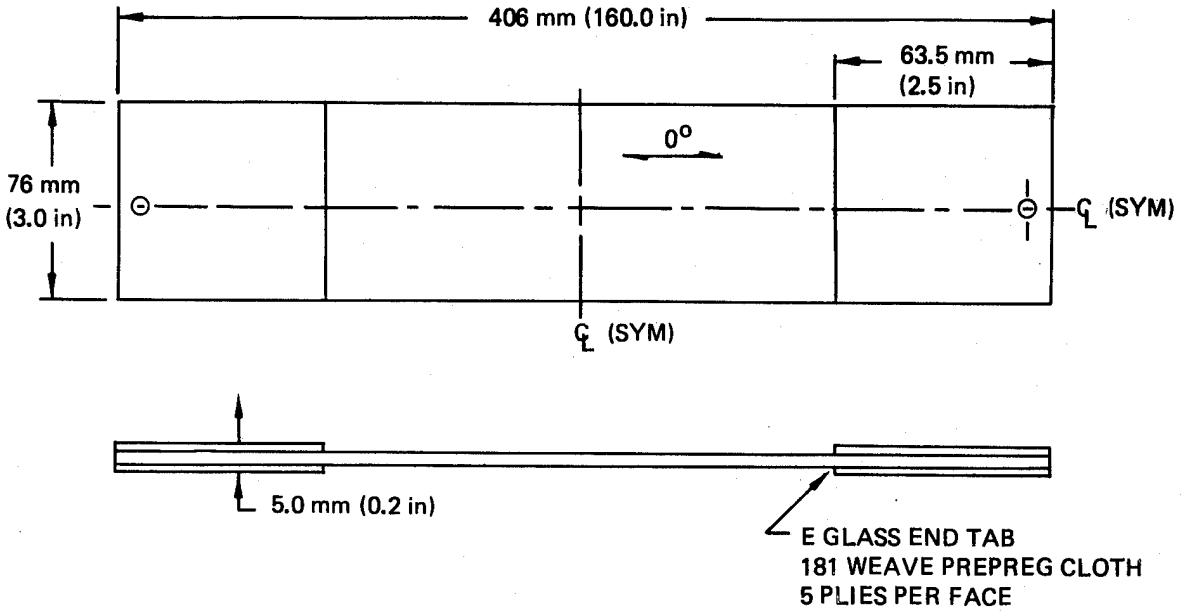

Figure 1. Notched Specimen Configuration

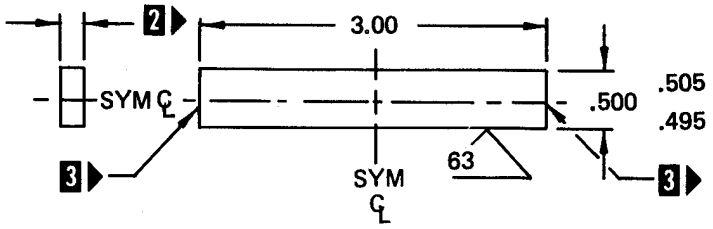

2 THICKNESS AS RECEIVED

3 ENDS TO BE SQUARE AND PARALLEL WITHIN ± .0005 AND PERPENDICULAR TO THE LONGITUDINAL AXIS OF THE SPECIMEN WITHIN ± .001. REMOVE BURRS BUT DO NOT CHAMFER NOR BREAK EDGES

Figure 2. Unnotched Compression Static Specimen

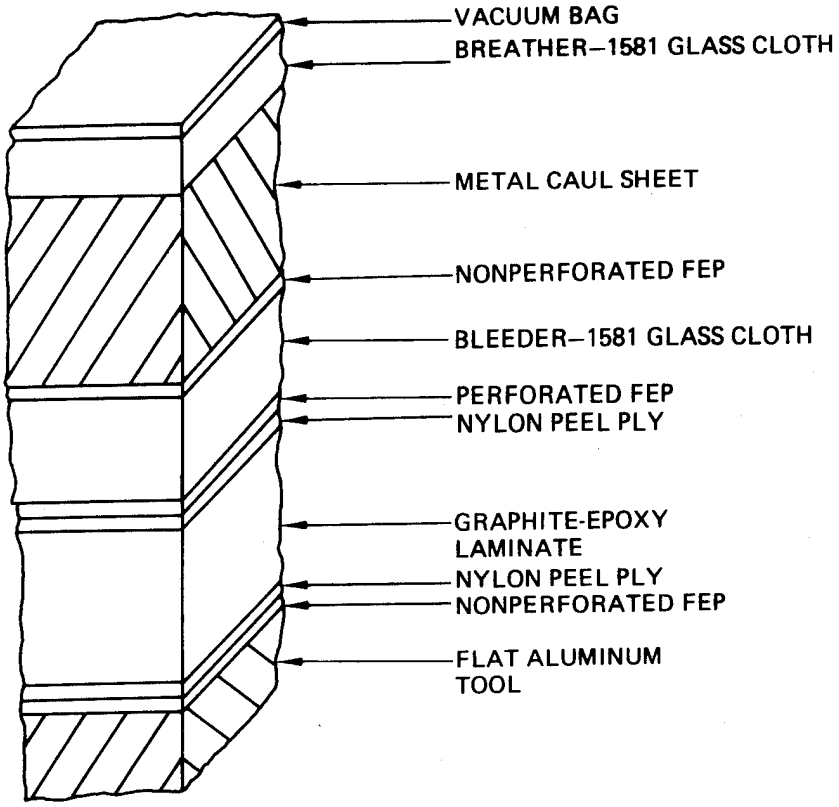

Figure 3. Specimen Laminate Layup Sequence

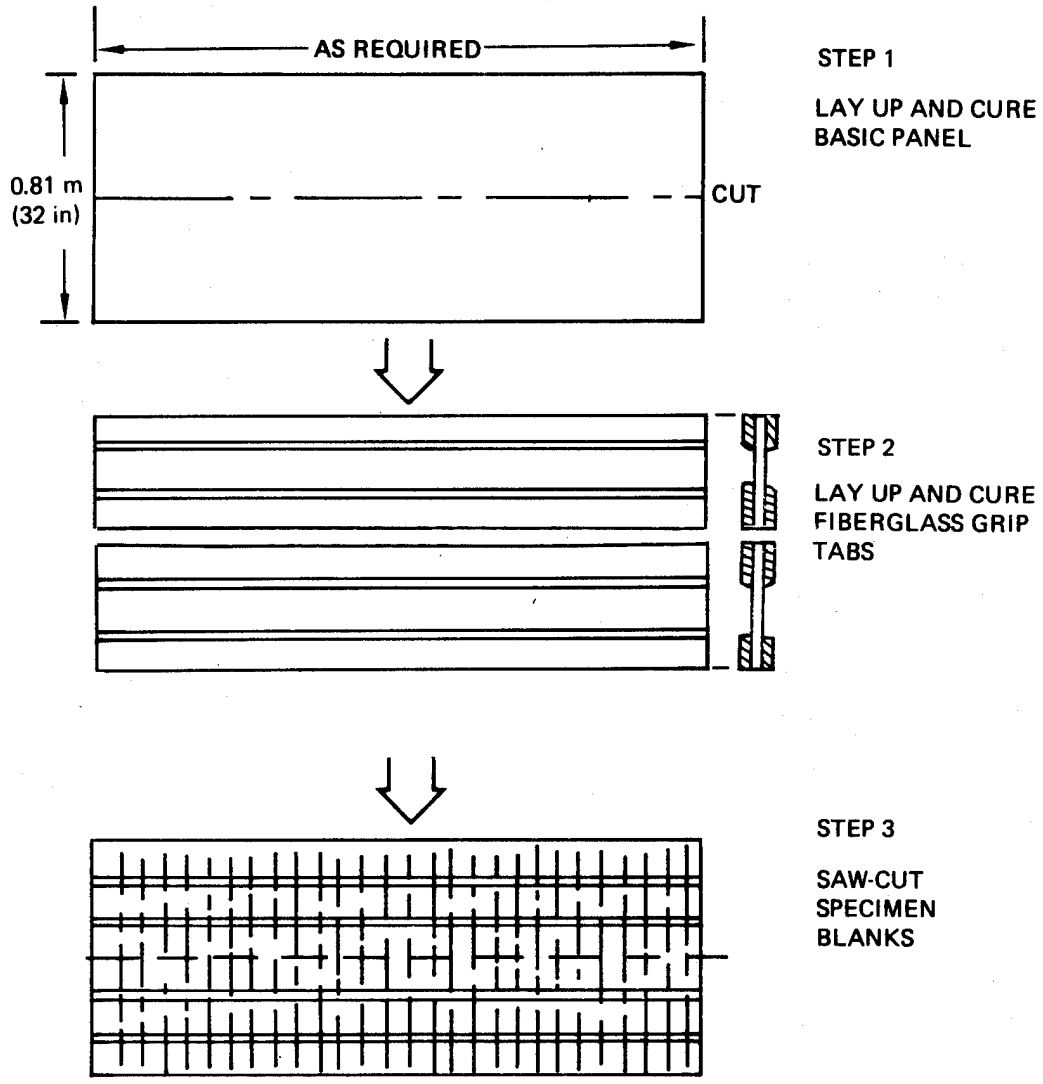

Figure 4. Specimen Cutting Procedure

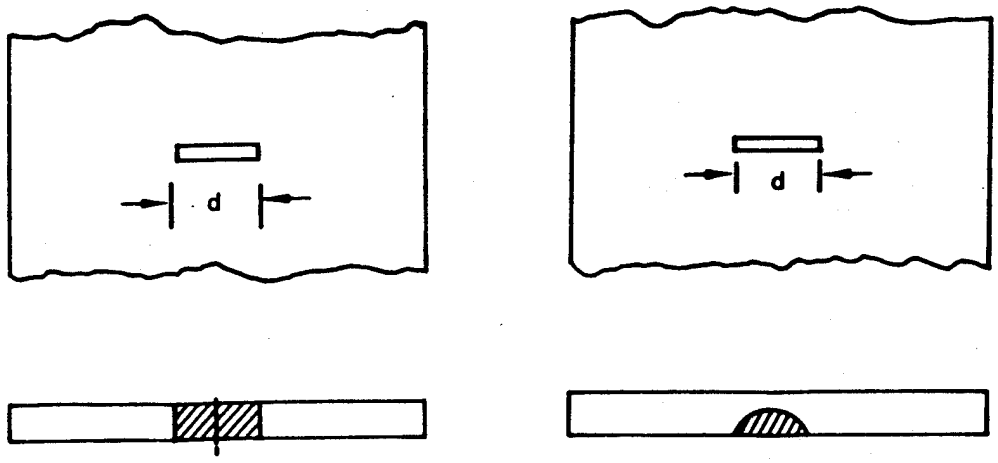

FULL-PENETRATION SLIT (FP)

HALF-PENETRATION SLIT (HP)

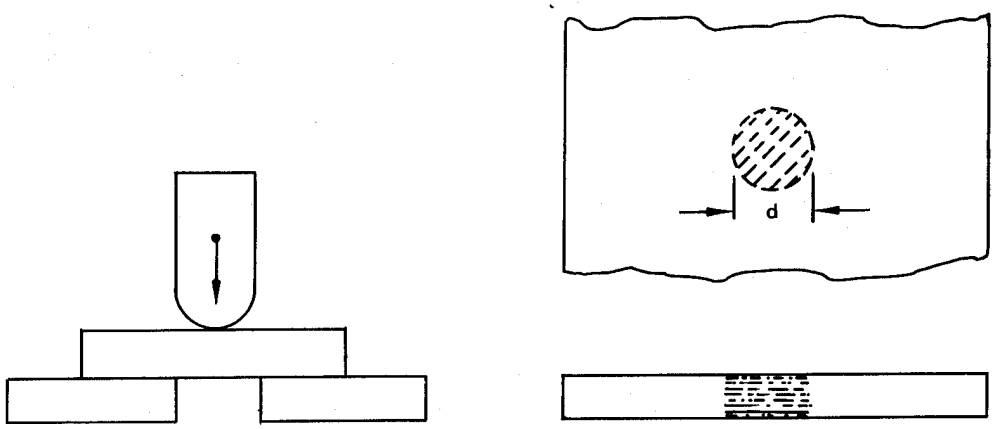

IMPACT-PRODUCED DELAMINATION (IMPACT)

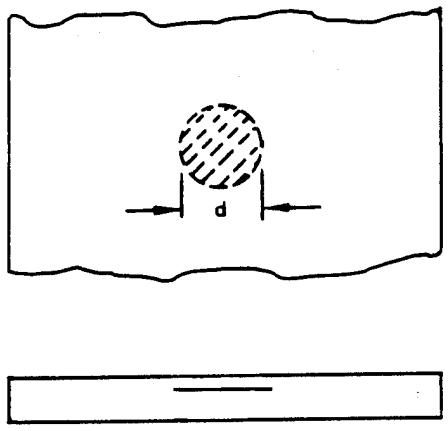

DISBOND AT QUARTER PLANE

Figure 5. Stress Concentration Configurations Tested

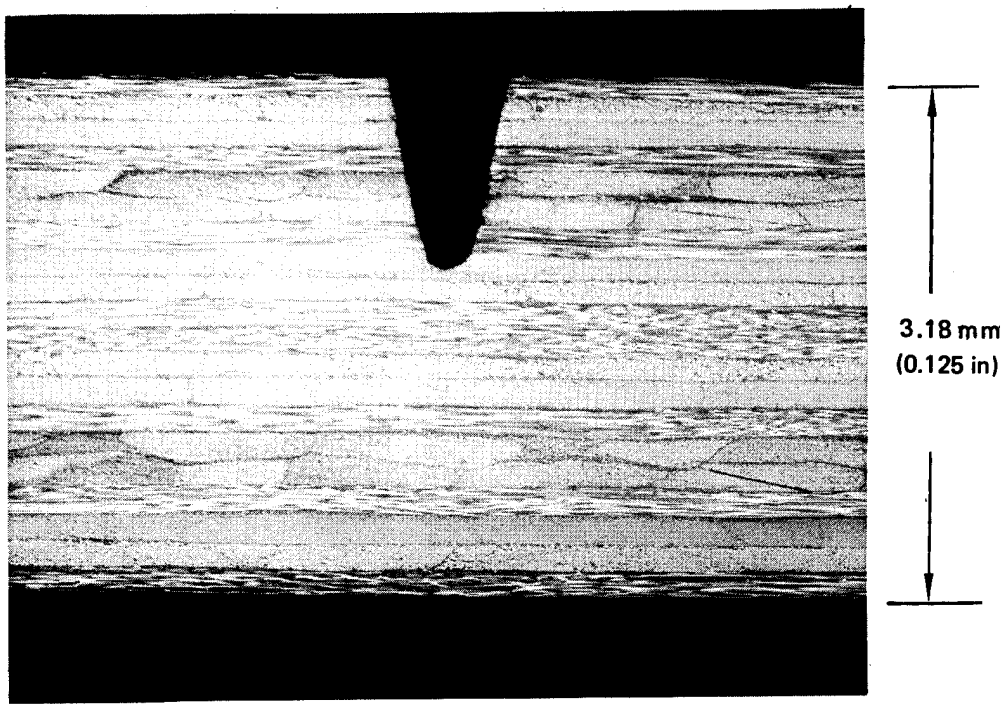

Figure 6. Photomicrograph Showing Root of Ultrasonically Machined Flaw

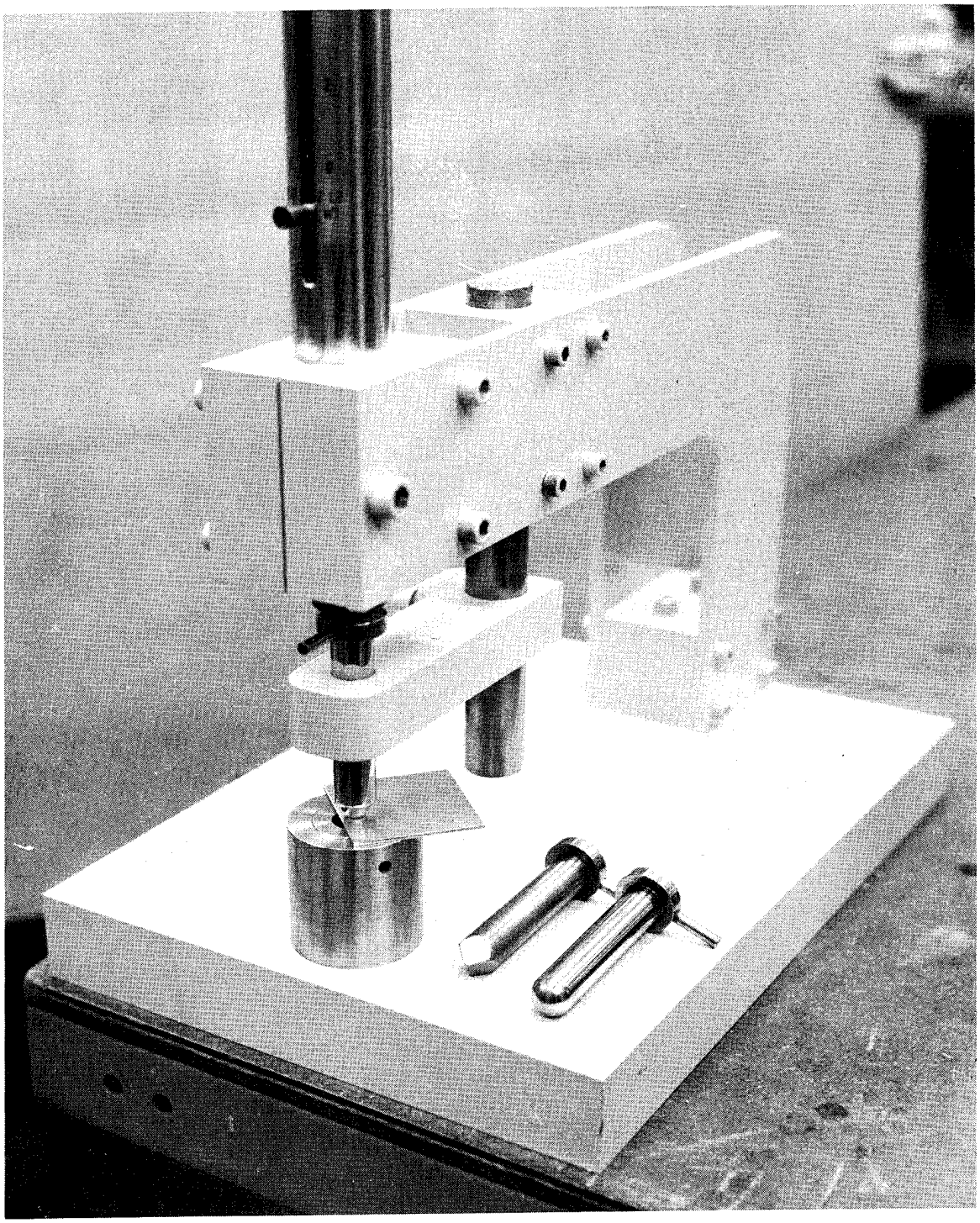

Figure 7. Impact Test Machine

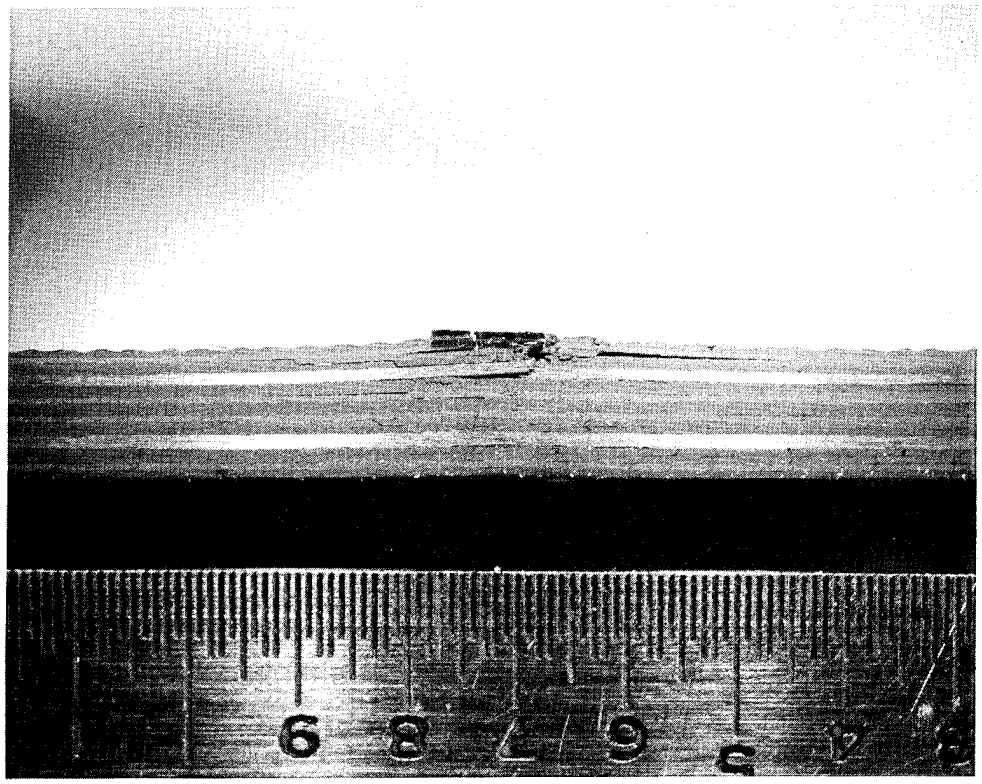

5X MICROGRAPH

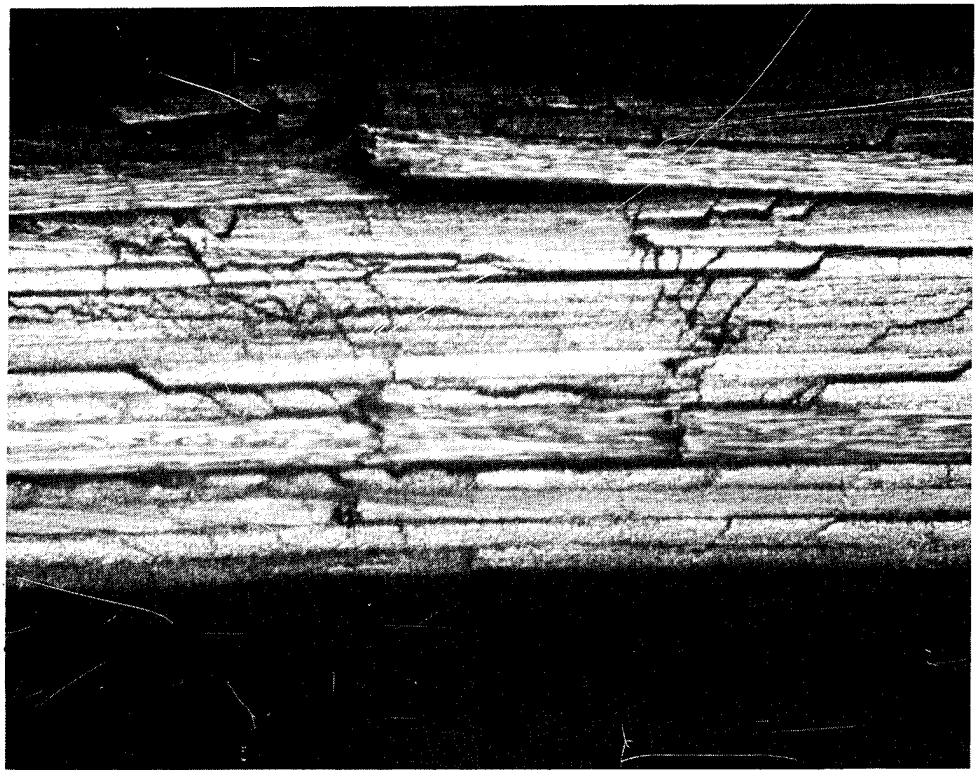

20X MICROGRAPH

Figure 8. Impact Produced Delamination

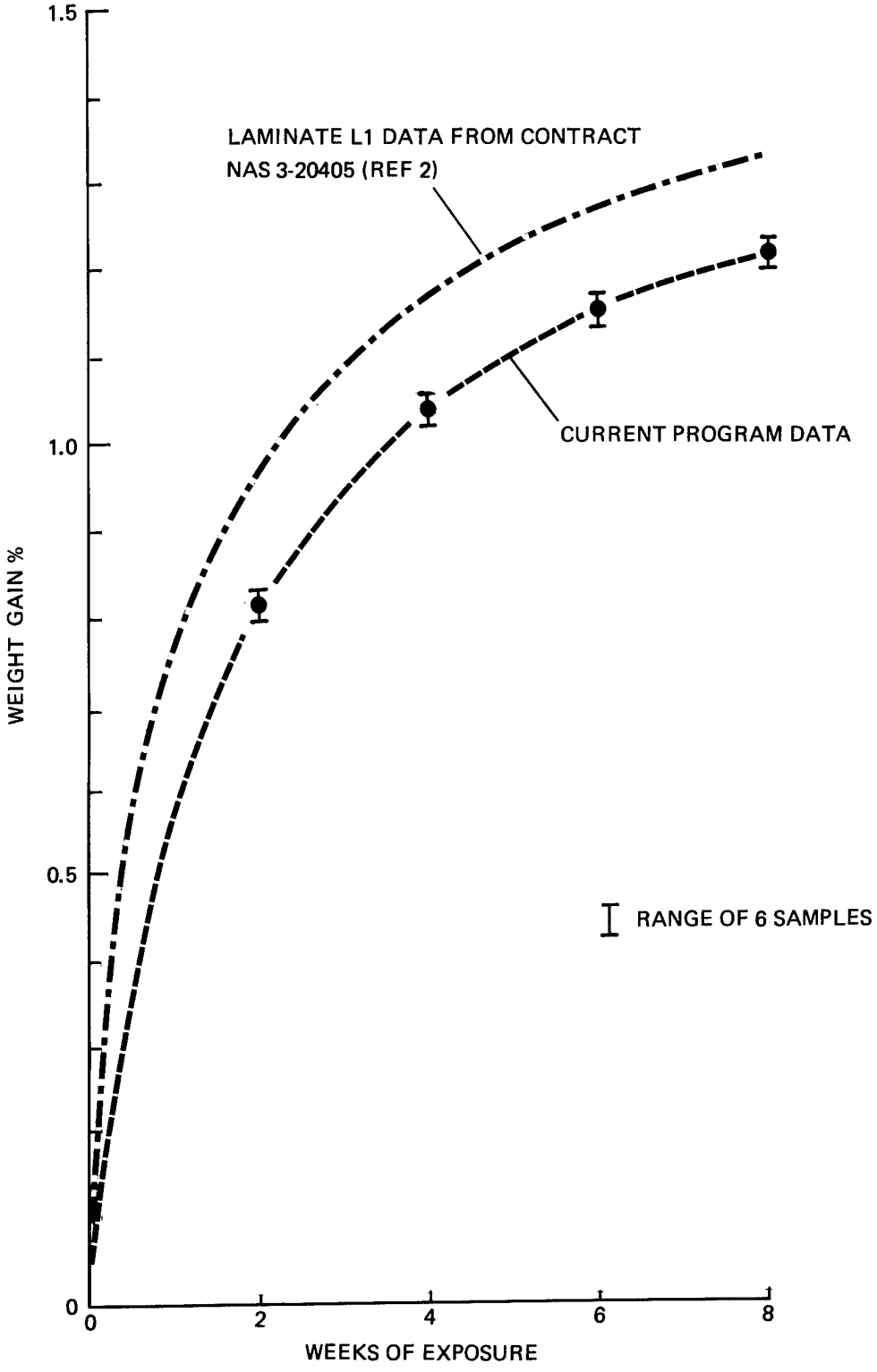

Figure 9. Moisture Conditioning Data

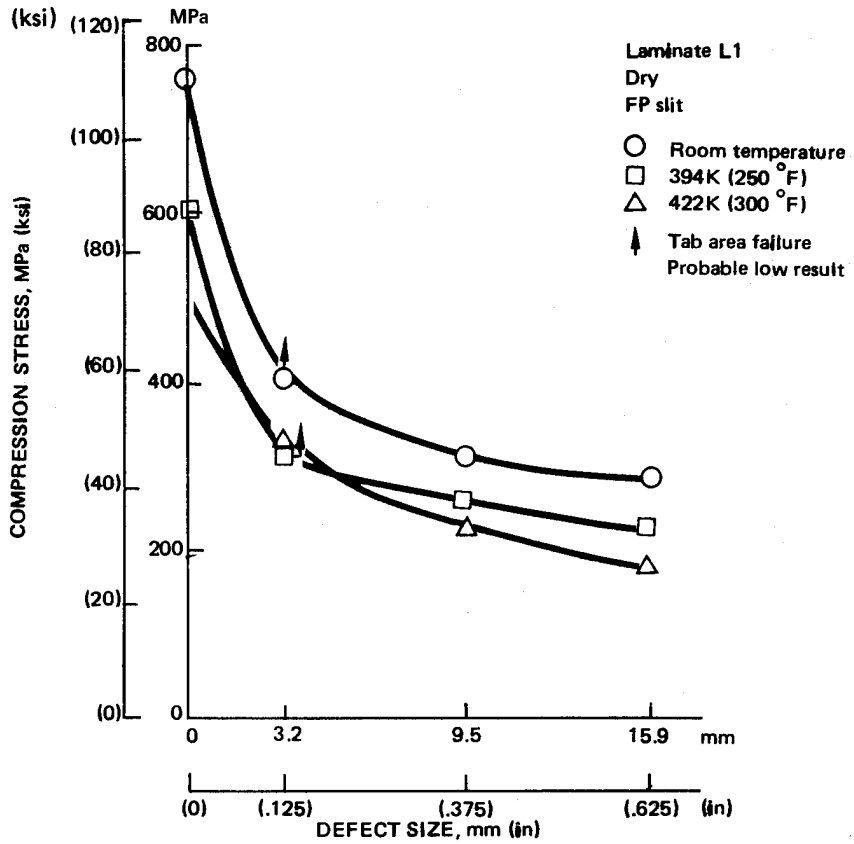

Figure 10. Compression-Fracture Strength of Dry L1 Laminates

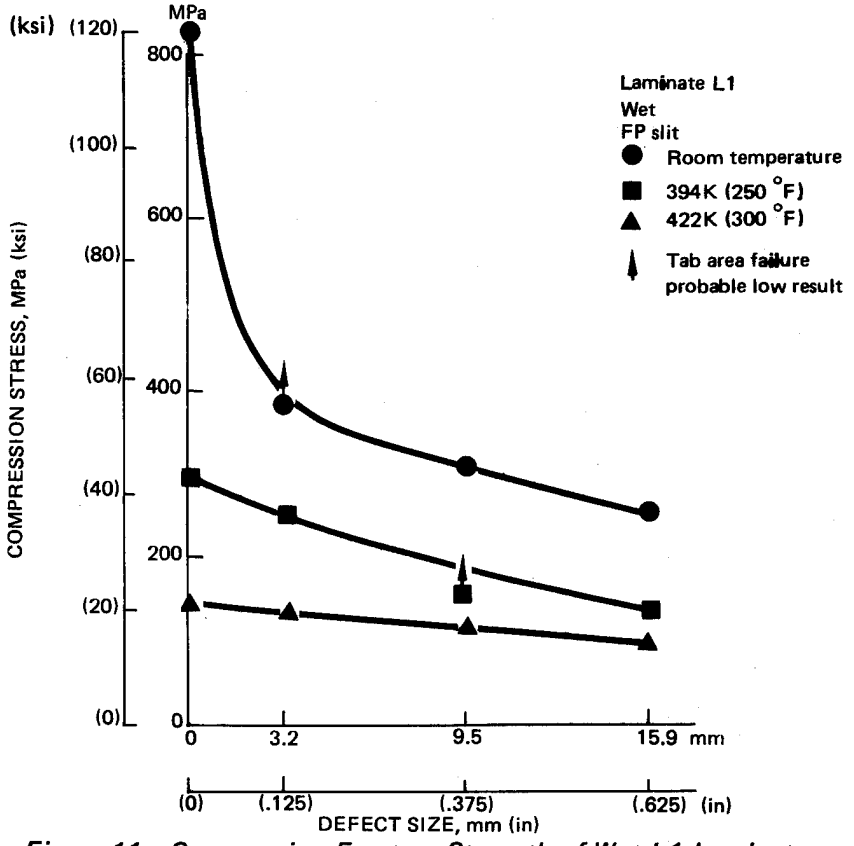

Figure 11. Compression-Fracture Strength of Wet L1 Laminates

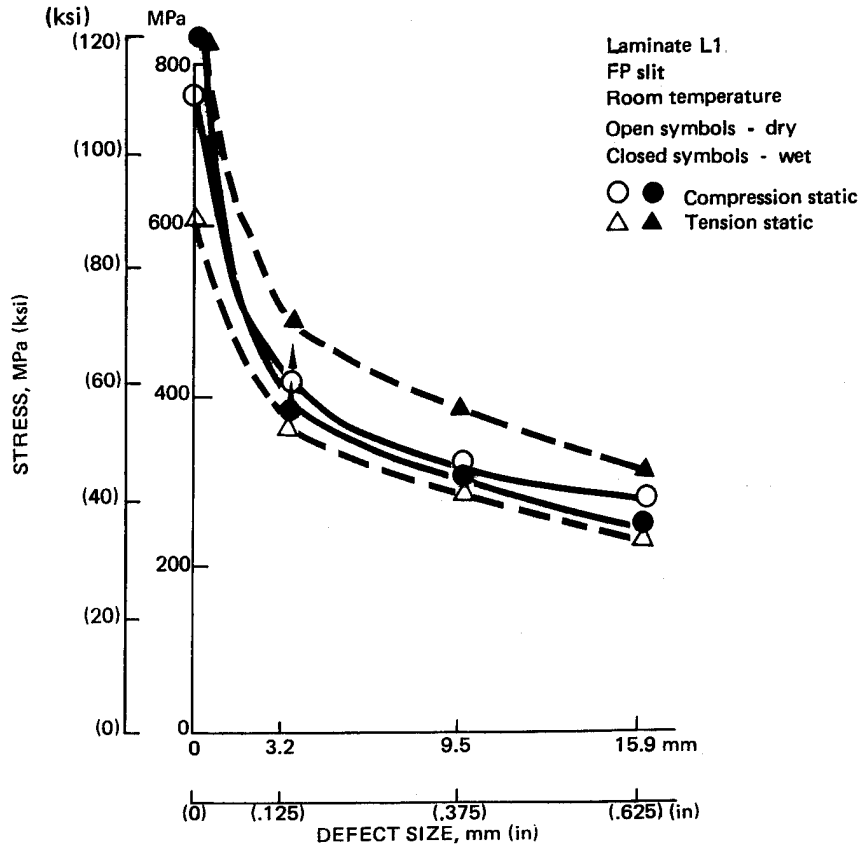

Figure 12. Comparision of Wet and Dry Fracture at Room Temperature

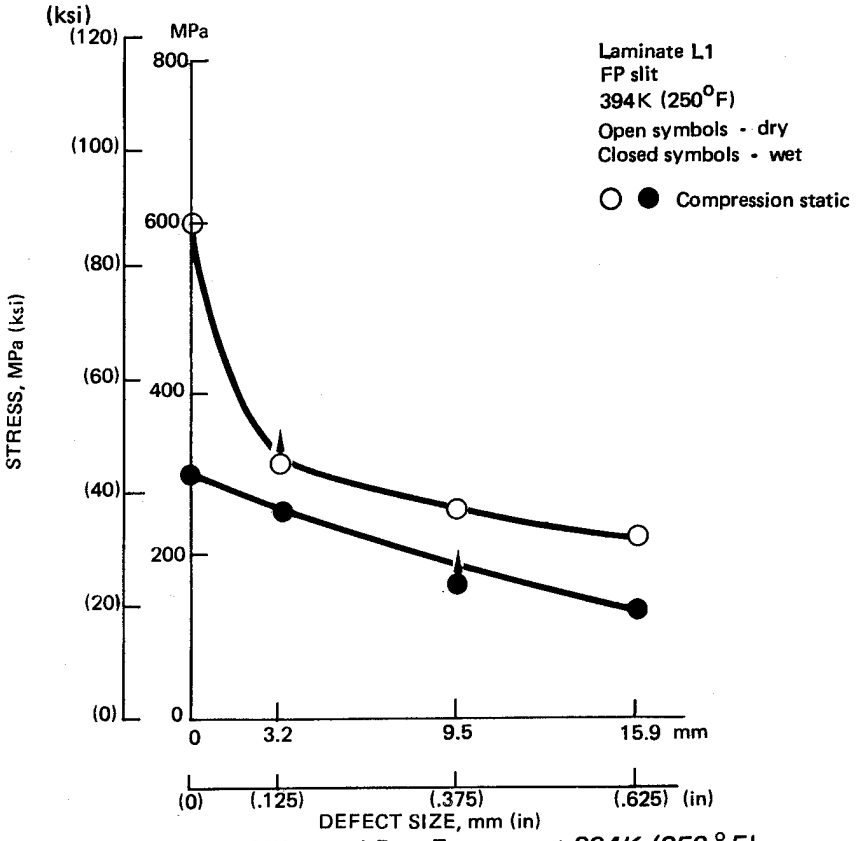

Figure 13. Comparison of Wet and Dry Fracture at 394K (250 °F)

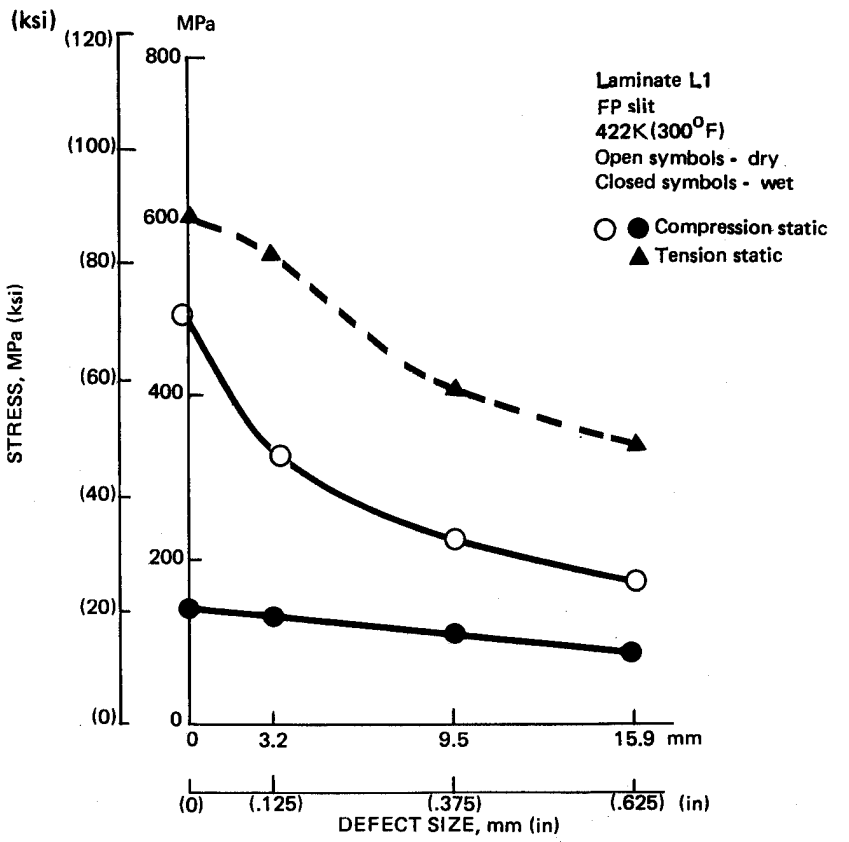

Figure 14. Comparison of Wet and Dry Fracture at 422K (350 °F)

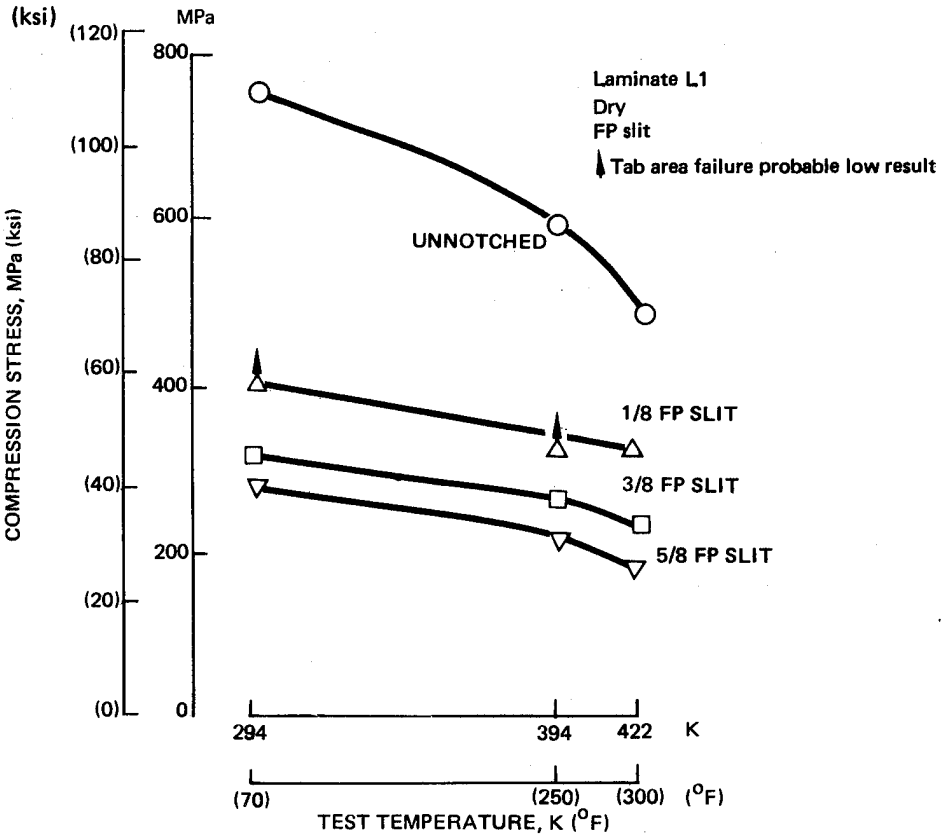

Figure 15. Effect of Test Temperature on the Dry-Compression Fracture Strength

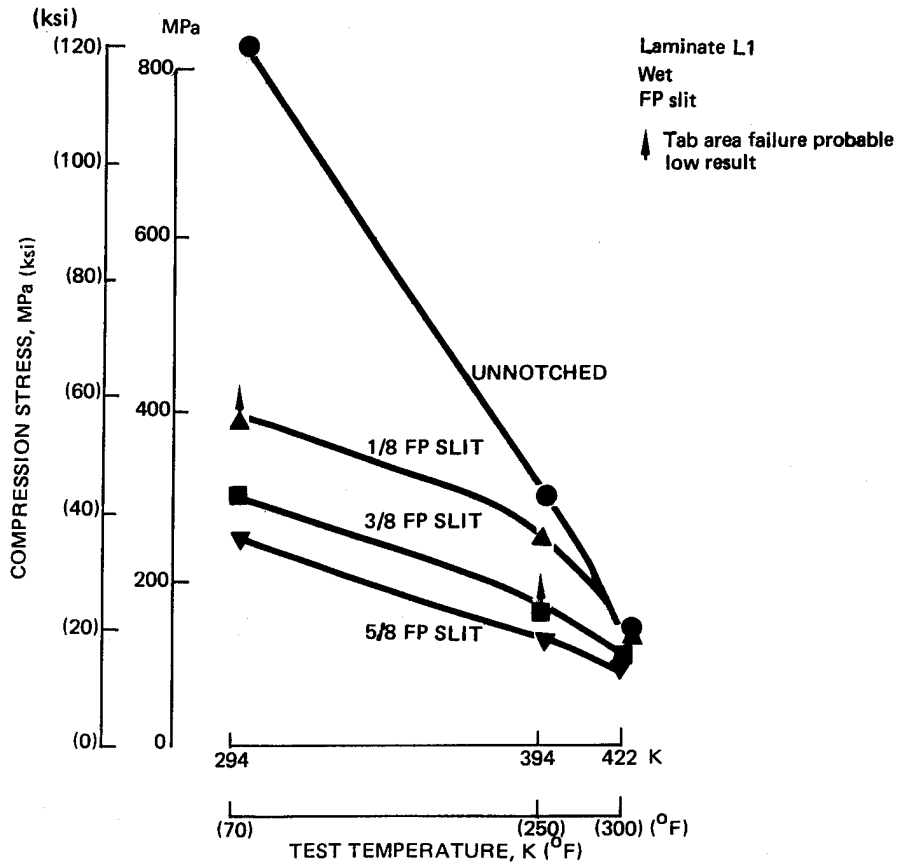

Figure 16. Effect of Test Temperature on the Wet-Compression Fracture Strength

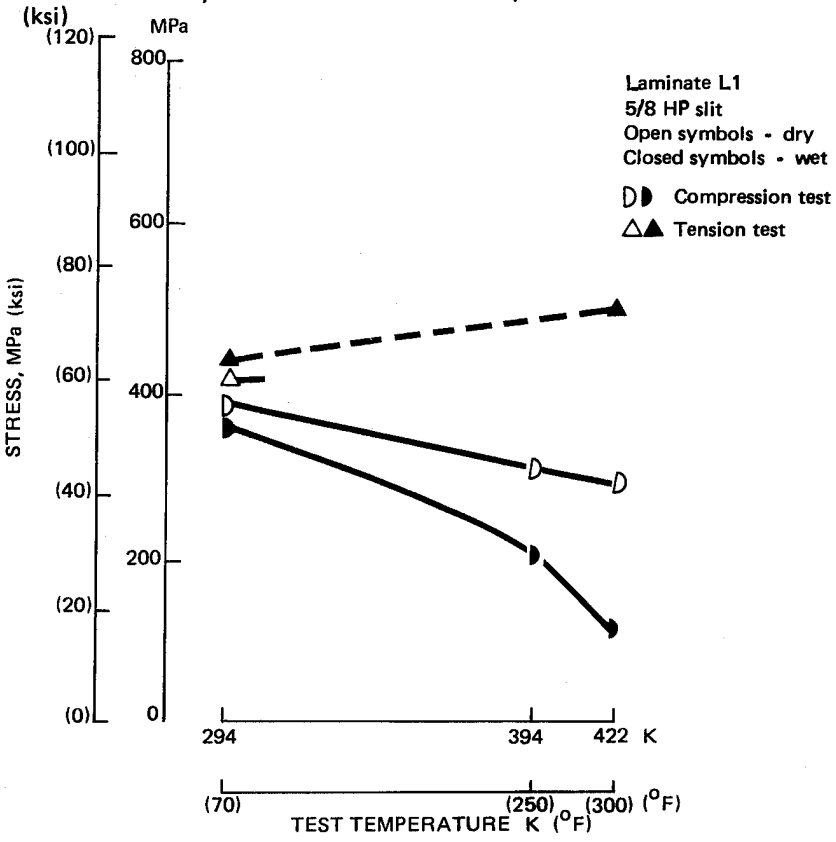

Figure 17. Effect of Test Temparature on Fracture of Half Penetration Slit Specimens

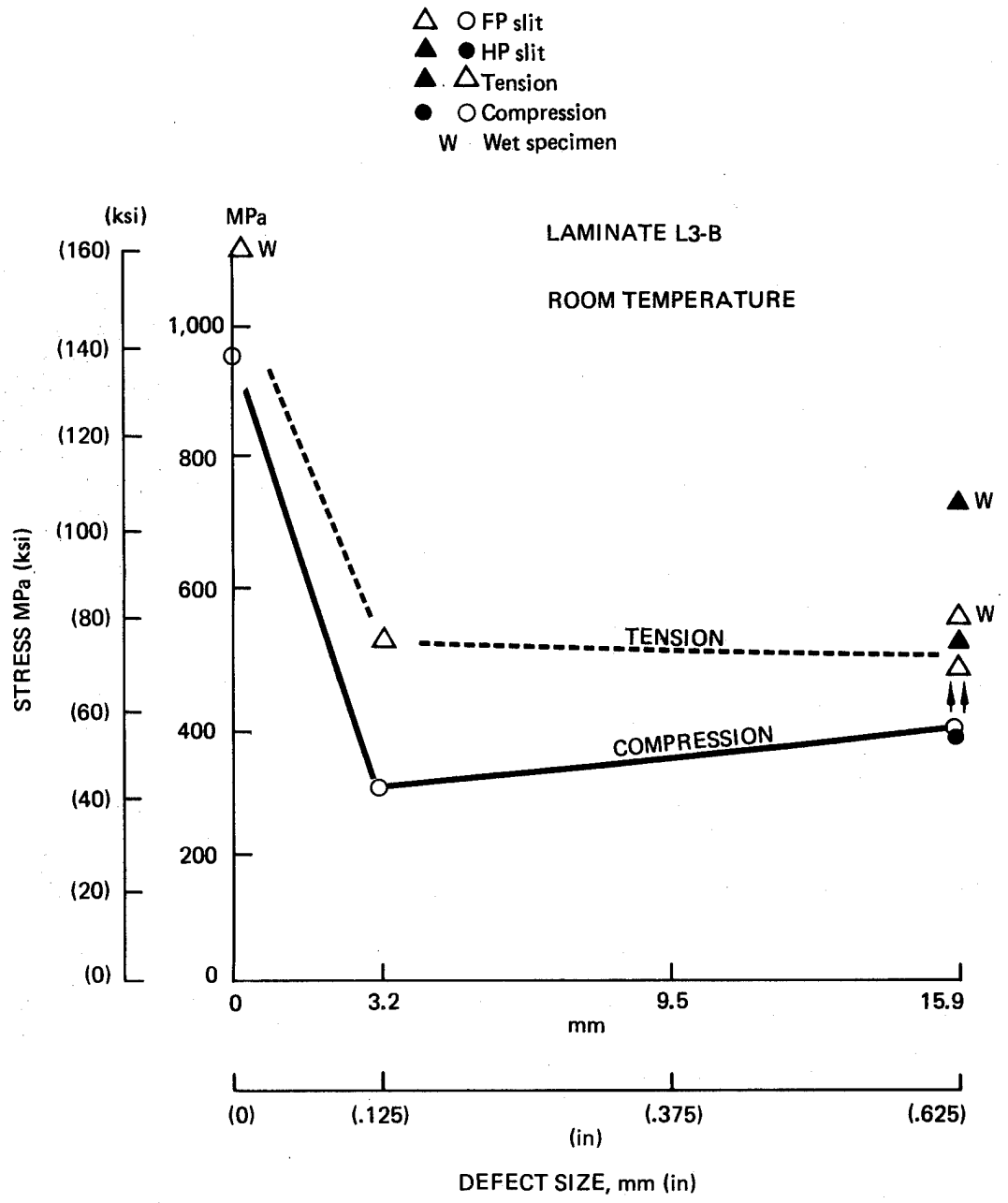

Figure 18. Fracture Strength of L3-B Laminates

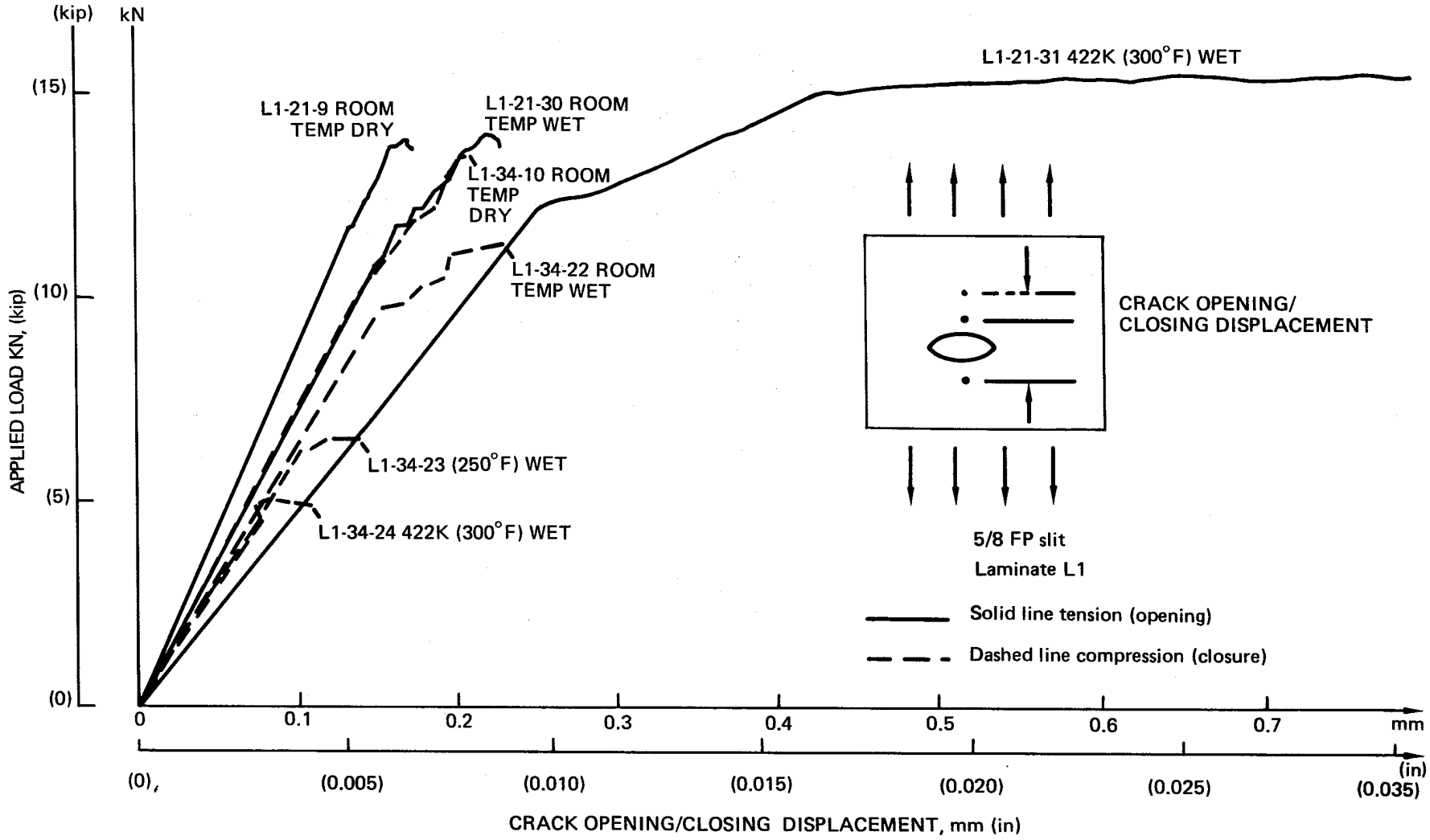

Figure 19. Typical Crack Opening/Closing Displacement Records for Test Specimens

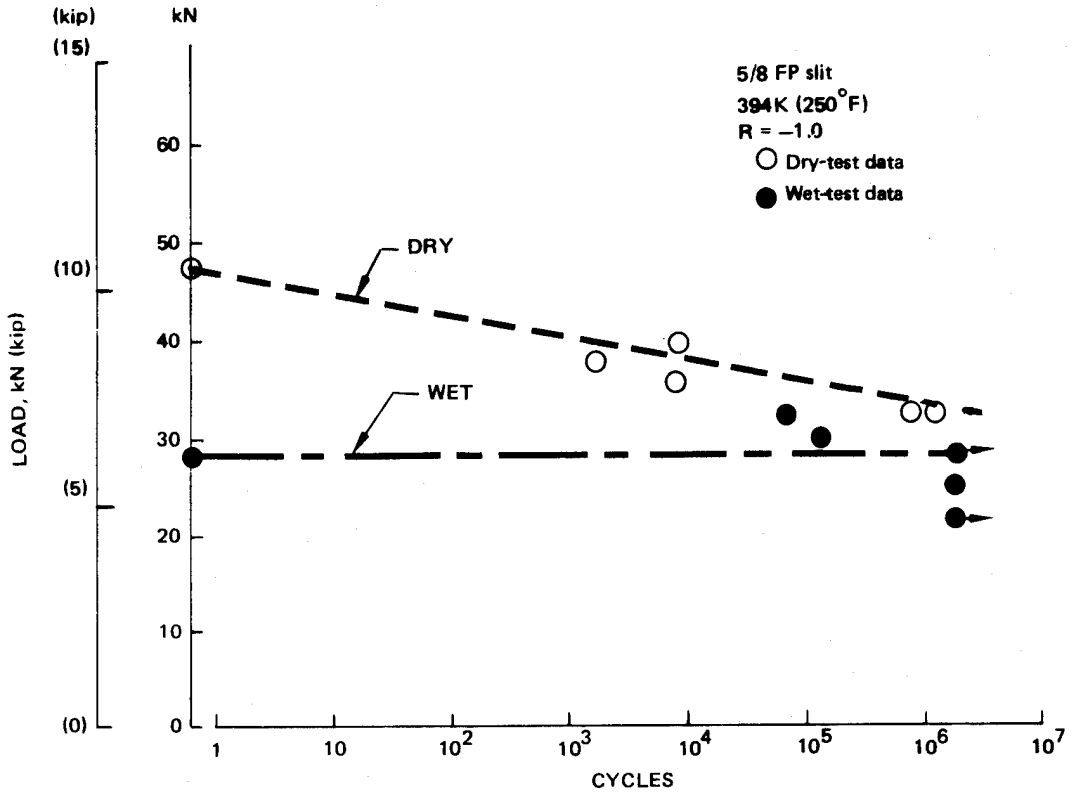

Figure 20. Fatigue Test Data for 5/8 FP Slit Specimens at 394K (250° F)

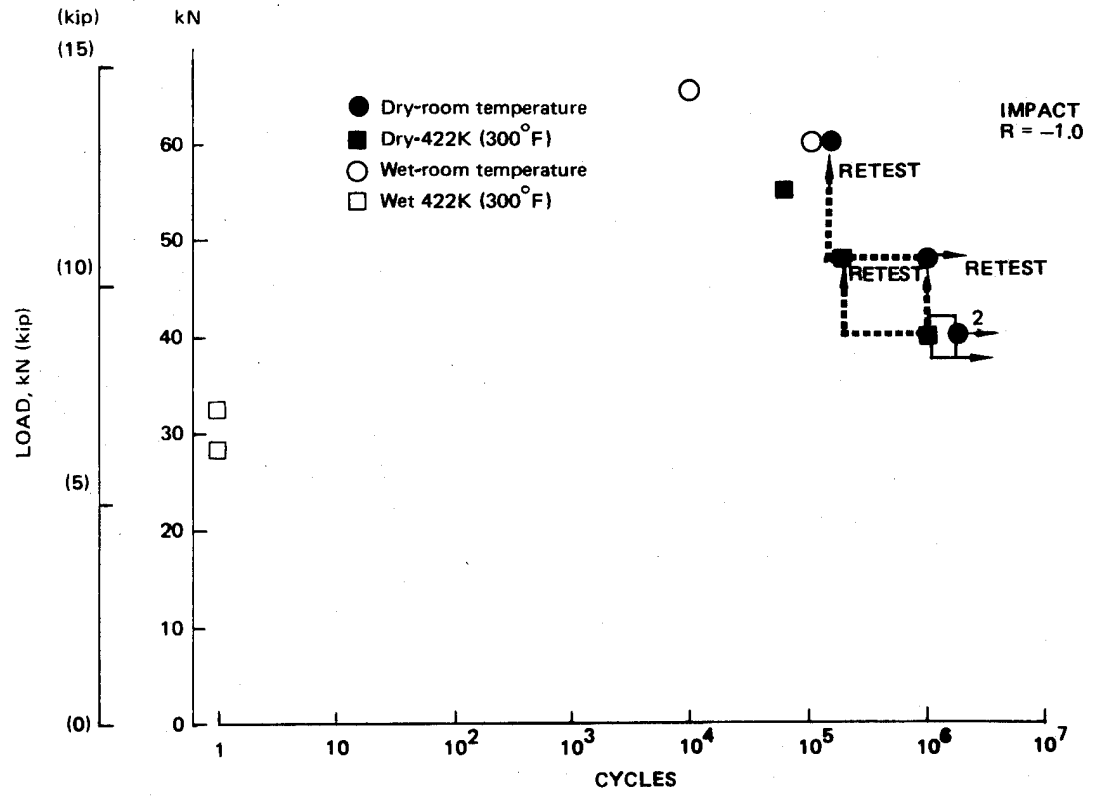

Figure 21. Fatigue Test Data for Specimens With Impact-Produced Defects

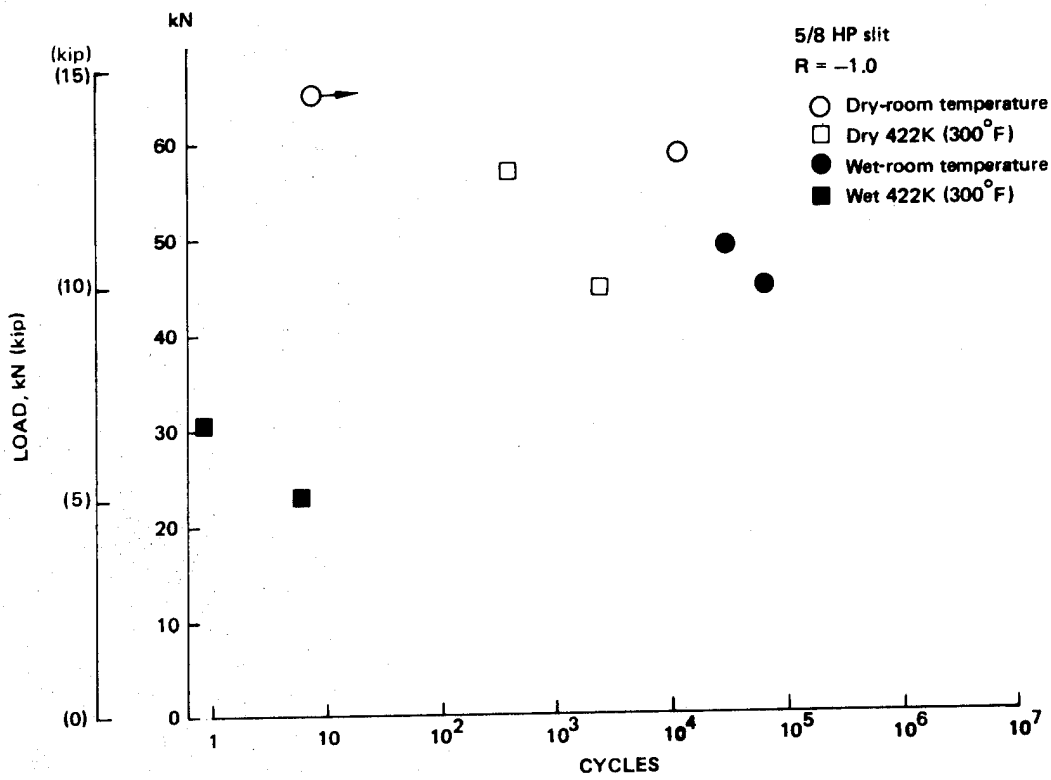

Figure 22. Fatigue Test Data for Specimens With 5/8 HP Slit

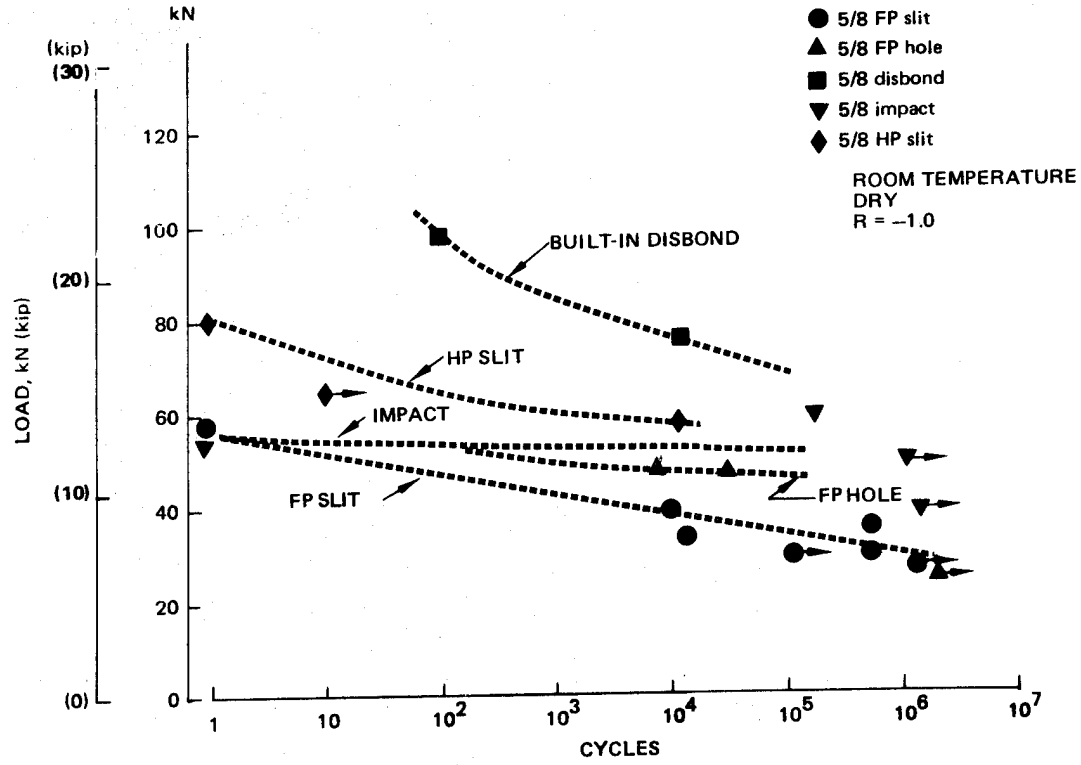

Figure 23. Comparison of R = –1.0 Fatigue Behavior of 5/8 Defects

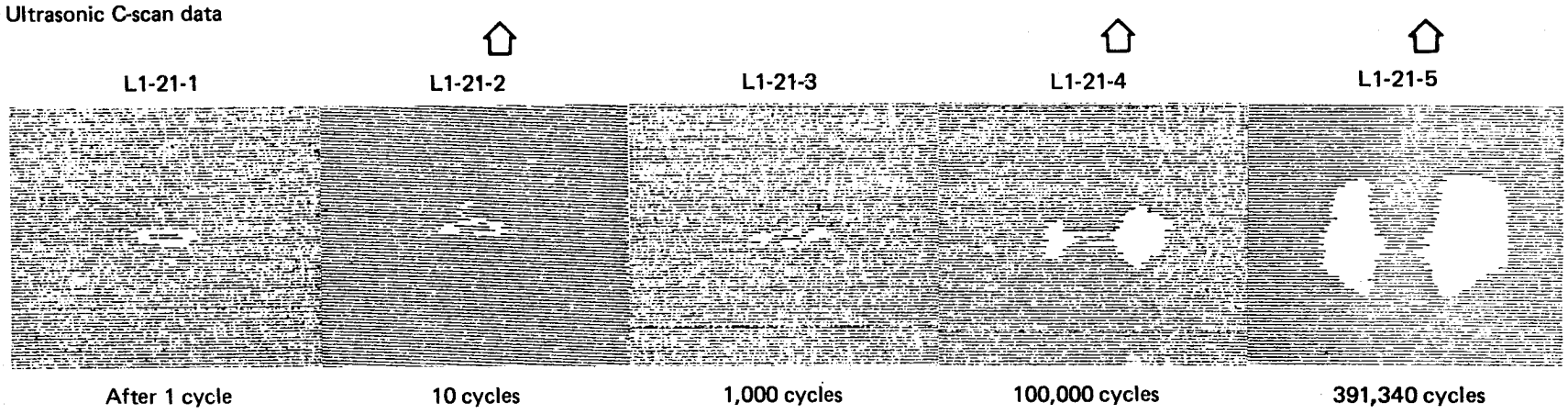

Figure 24. Through-Transmission Ultrasonic C-Scan Records of 5/8 FP Slit Residual-Strength Specimens

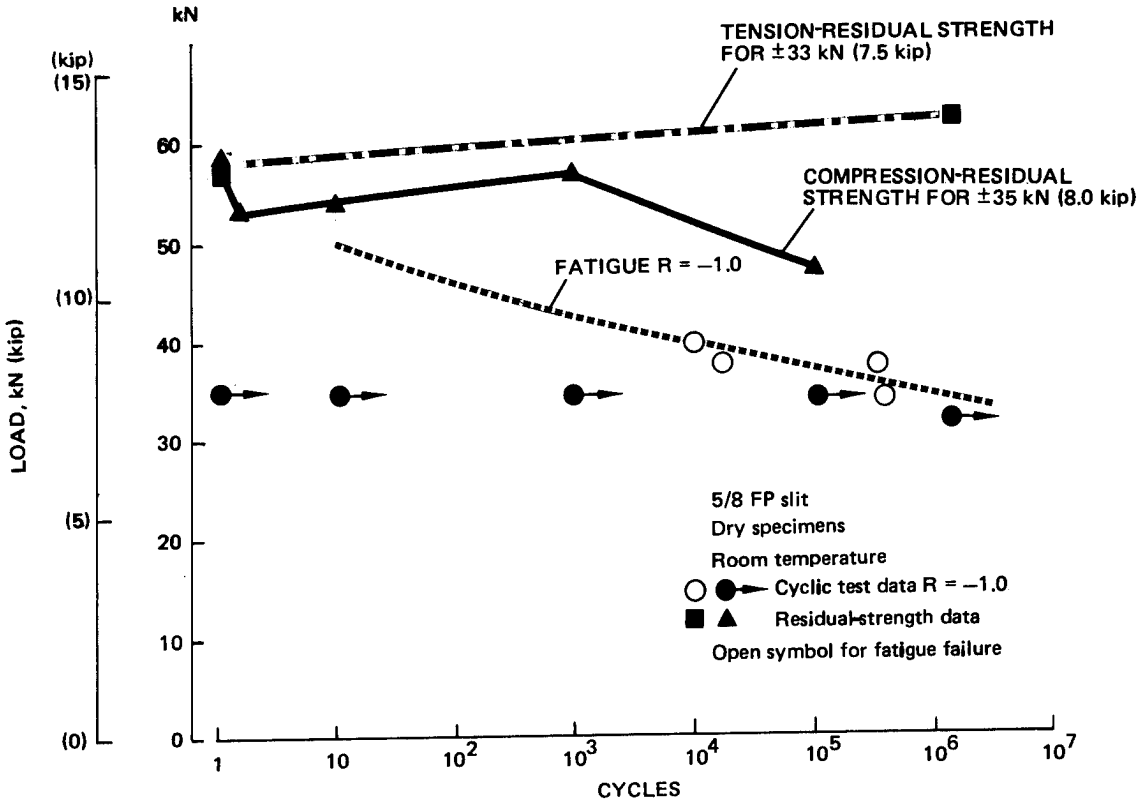

Figure 25. Dry-Slit Specimen Residual-Strength Test Data, R = –1.0

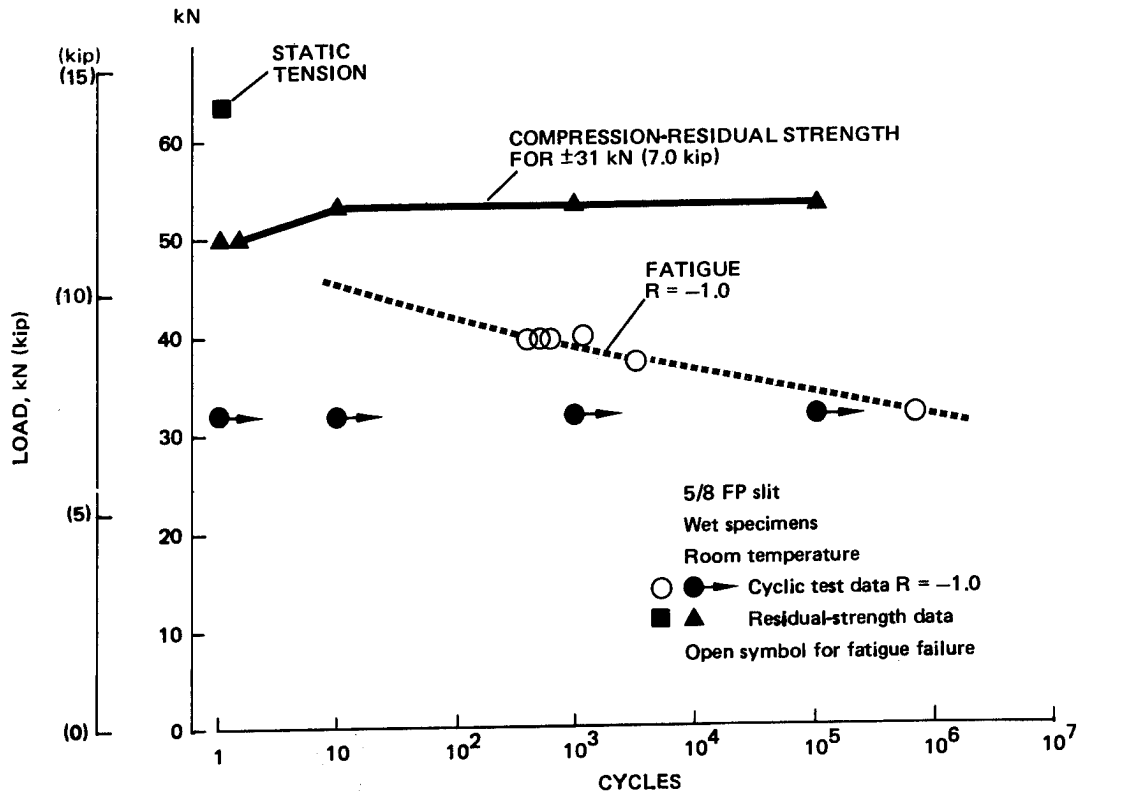

Figure 26. Wet-Slit Specimen Residual-Strength Test Data, R = –1.0

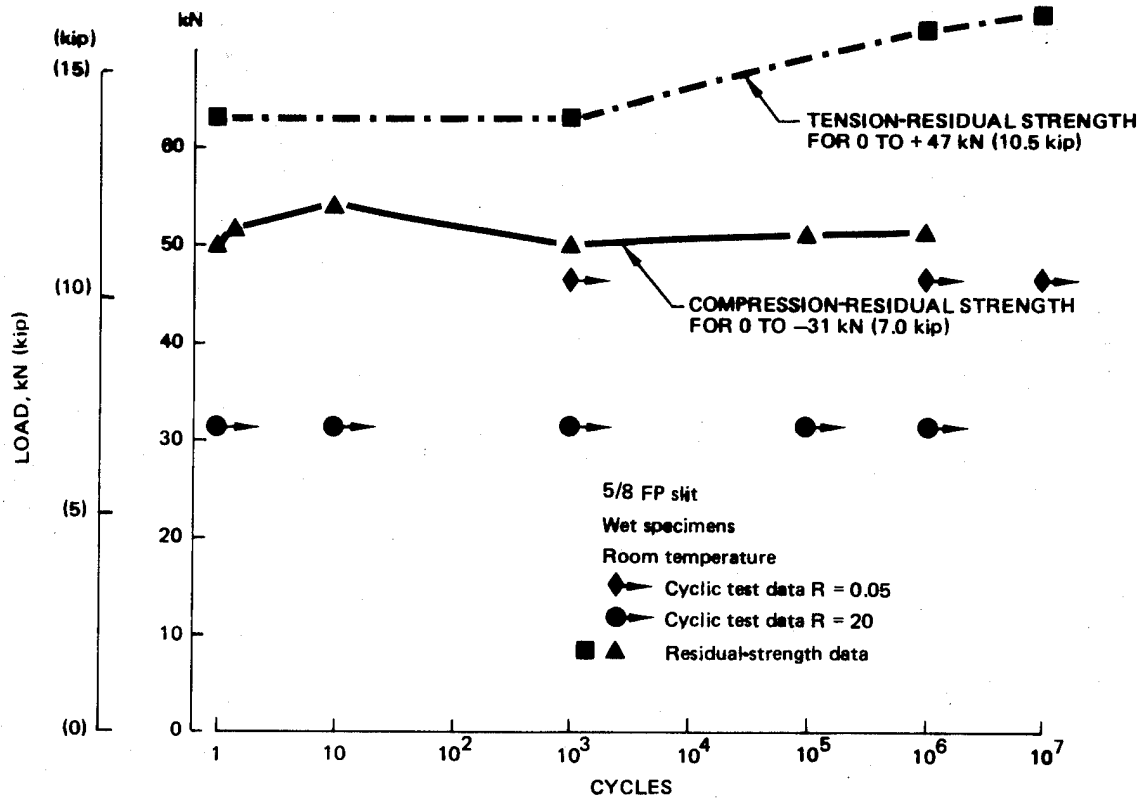

Figure 27. Wet-Slit Specimen Residual-Strength Test Data, R = .05 and 20

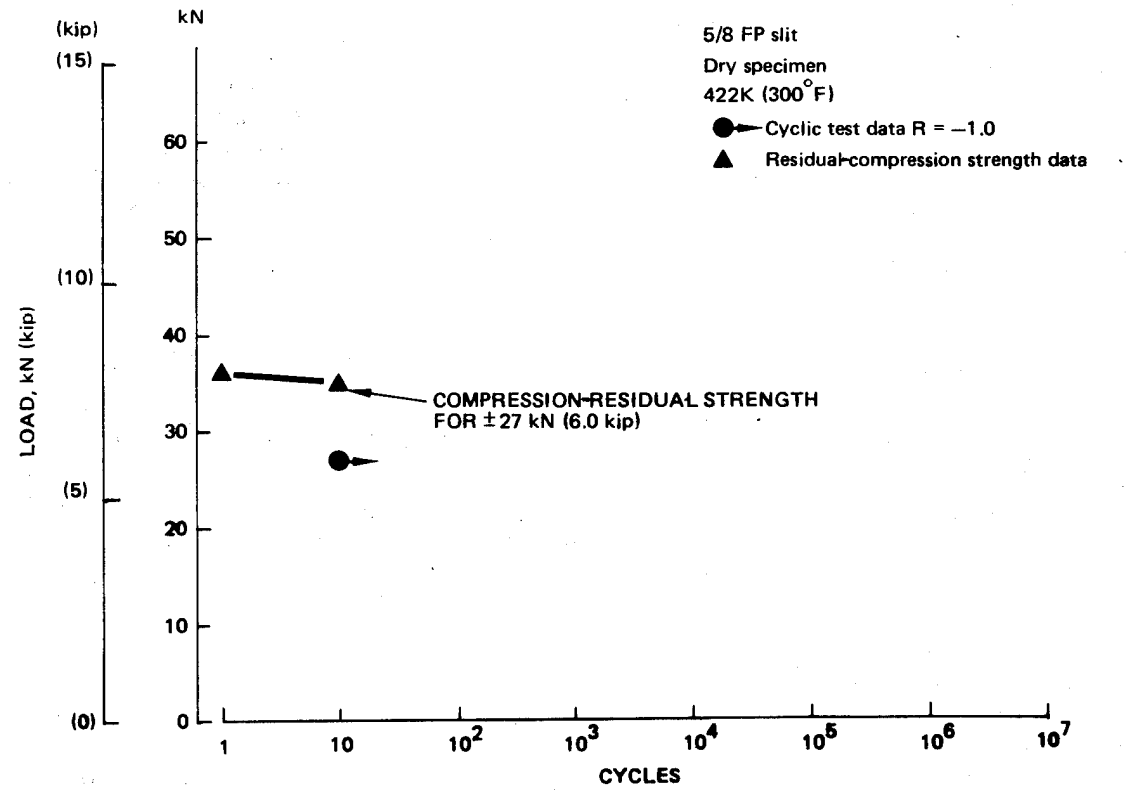

Figure 28. 422K (300°F) Dry-Specimen Residual-Strength Test Data, R = –1.0

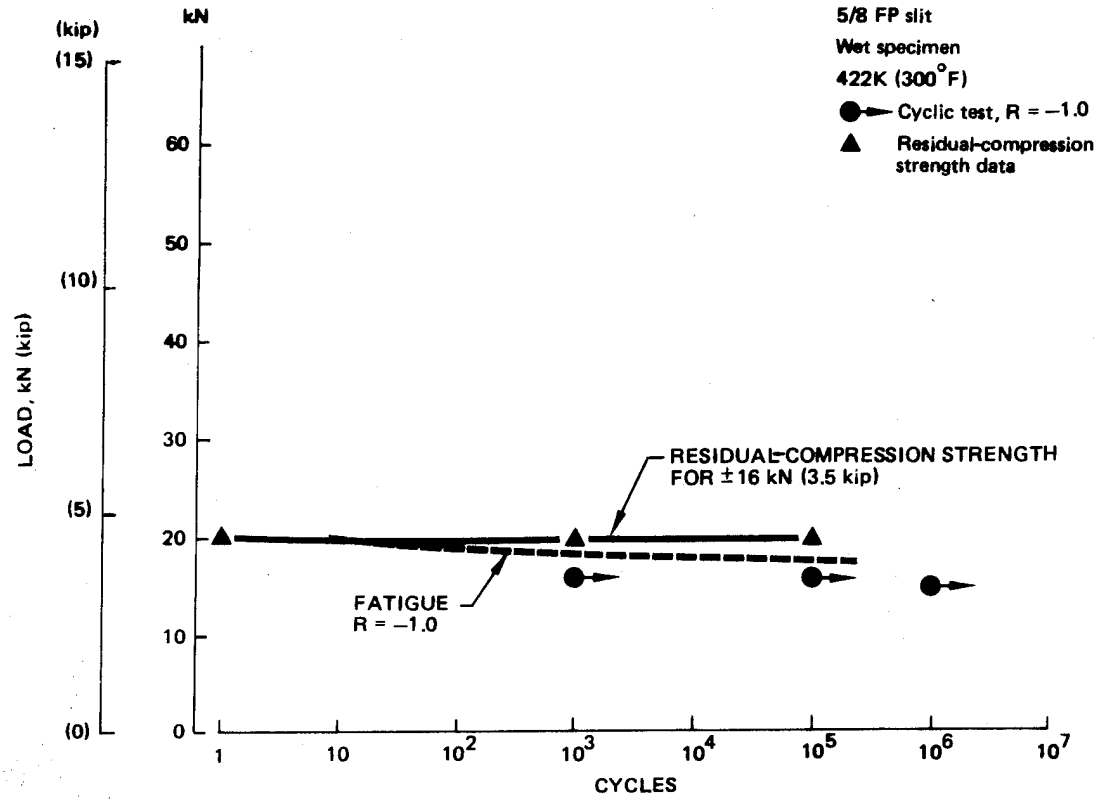

Figure 29. 422K (300°F) Wet-Specimen Residual-Strength Test Data

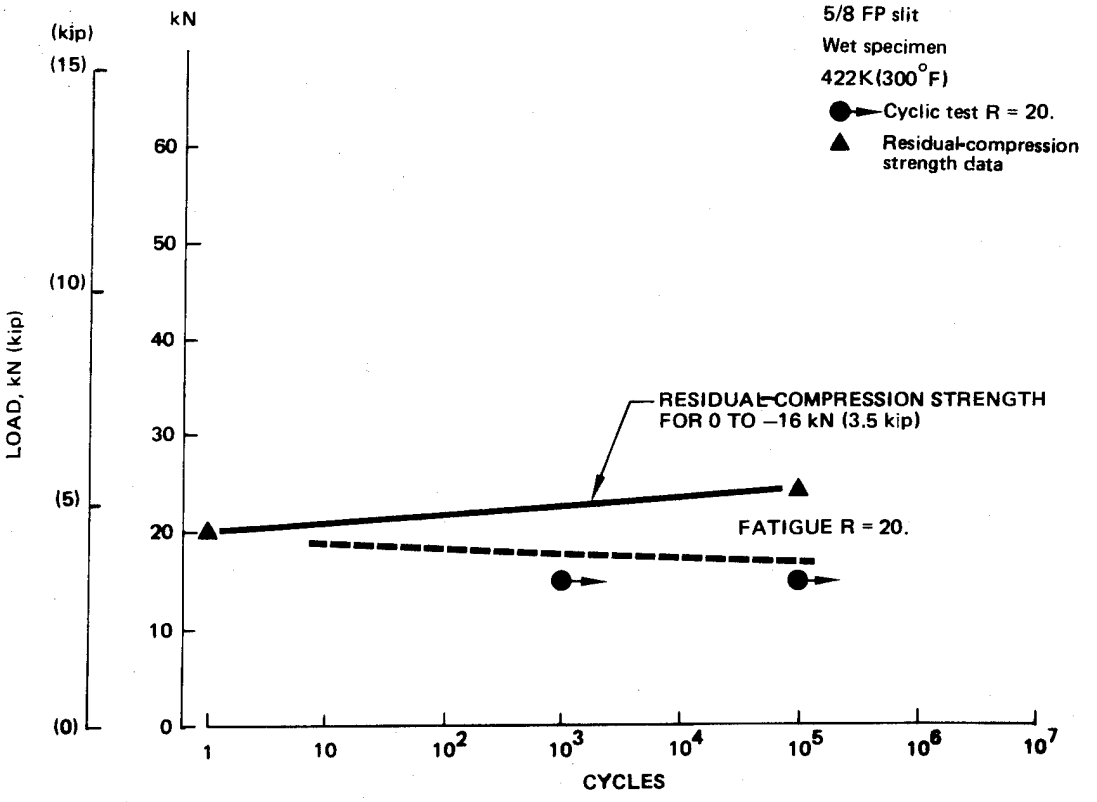

Figure 30. 422K (300°F) Wet-Specimen Residual-Strength Test Data

REFERENCES

1. Porter, T.R.: "Evaluation of Flawed Composite Structural Components Under Static and Cyclic Loading," NASA CR-135403, prepared under Boeing Contract NAS3-19709 with NASA-Lewis Research Center, February, 1979.

2. Porter, T.R.: "Environmental Effects on Defect Growth in Composite Materials," NASA CR-165213 prepared under Boeing Contract NAS3-20405 with NASA-Lewis Research Center, January 1981.

APPENDIX A

STATIC AND CYCLIC TEST DATA

This appendix contains the static and cyclic test data for all specimens. The reported data include specimen geometry, loads, and test parameters. The gross section stresses have been reported for all the critical test conditions.

DRY SPECIMEN STATIC COMPRESSION DATA

SPEC. NO.	LAYUP	THICKNESS mm (INCH)	WIDTH mm (INCH)	FLAW TYPE	FLAW LENGTH FRONT mm (INCH)	FLAW LENGTH BACK mm (INCH)	FLAW DEPTH mm (INCH)	TEST TYPE	TEST TEMP. °K (°F)	PRELOAD LOAD N (LB)	PRELOAD STRESS MN/m² (KSI)	CYCLIC LOADING MAX LOAD N (LB)	CYCLIC LOADING MAX STRESS MN/m² (KSI)	CYCLIC LOADING R	CYCLIC LOADING CYCLES	RESIDUAL STATIC LOAD N (LB)	RESIDUAL STATIC STRESS MN/m² (KSI)	REMARKS
L1-34	L1 [1]	2.63 (.1036)	12.7 (.5001)	NONE	—	—	—	DRY	ROOM	—	—	—	—	—	—	-25710 (-5780)	-758 (-110)	
1-C1		2.73 (.1075)	76.2 (2.999)	1/8 FP SLIT	3.12 (.1228)	3.06 (.1204)	THRU			—	—	—	—	—	—	-82730 (-18600)	-398 (-57.7)	TAB FAILURE RETEST TO 17925 LB
-2		2.74 (.1080)	76.2 (2.999)	3/8 FP SLIT	9.59 (.3777)	9.48 (.3731)				—	—	—	—	—	—	-66270 (-14900)	-317 (-46.0)	
-7		2.77 (.1091)	76.2 (2.999)	5/8 FP SLIT	16.0 (.6302)	15.86 (.6245)				—	—	—	—	—	—	-59600 (-13400)	-282 (-40.9)	
-10		2.65 (.1043)	12.7 (.5001)	NONE	—	—			394 (250)	—	—	—	—	—	—	-20280 (-4560)	-600 (-87.0)	
1-C2		2.70 (.1063)	76.1 (2.998)	1/8 FP SLIT	3.12 (.1230)	3.06 (.1205)				—	—	—	—	—	—	-64500 (-14500)	-313 (-45.5)	TAB FAILURE RETEST TO 10750 LB
-3		2.68 (.1054)	76.2 (2.999)	3/8 FP SLIT	9.62 (.3788)	9.51 (.3747)				—	—	—	—	—	—	-52710 (-11850)	-257 (-37.3)	
-8		2.70 (.1064)	76.1 (2.996)	5/8 FP SLIT	16.0 (.6309)	15.88 (.6253)				—	—	—	—	—	—	-46260 (-10400)	-225 (-32.6)	
-11		2.67 (.1052)	12.7 (.5004)	NONE	—	—			422 (300)	—	—	—	—	—	—	-17170 (-3860)	-503 (-73.0)	
1-C3		2.77 (.1089)	76.1 (2.996)	1/8 FP SLIT	3.15 (.1242)	3.09 (.1215)				—	—	—	—	—	—	-69390 (-15600)	-329 (-47.8)	
-13		2.77 (.1092)	76.2 (3.001)	3/8 FP SLIT	9.58 (.3770)	9.44 (.3715)				—	—	—	—	—	—	-48930 (-11000)	-231 (-33.5)	
-9		2.70 (.1065)	76.1 (2.998)	5/8 FP SLIT	15.95 (.6279)	15.83 (.6234)				—	—	—	—	—	—	-36380 (-8180)	-176 (-25.6)	
-12		2.72 (.1070)	76.1 (2.995)	5/8 HP SLIT	16.41 (.6460)	—	1.5 (.06)		ROOM	—	—	—	—	—	—	-80510 (-18100)	-389 (-56.5)	
-25		2.65 (.1044)	76.2 (3.000)		16.33 (.6433)	—	1.5 (.06)		394 (250)	—	—	—	—	—	—	-60940 (-13700)	-301 (-43.7)	
-26		2.80 (.1104)	76.0 (2.994)		16.40 (.6455)	—	1.5 (.06)		422 (300)	—	—	—	—	—	—	-61160 (-13750)	-286 (-41.6)	
-27																		

[1] $((0/\pm 45/0/90)_S)_2$

DRY SPECIMEN STATIC COMPRESSION DATA

SPEC. NO.	LAYUP	THICKNESS mm (INCH)	WIDTH mm (INCH)	FLAW TYPE	FLAW LENGTH FRONT mm (INCH)	FLAW LENGTH BACK mm (INCH)	FLAW DEPTH mm (INCH)	TEST TYPE	TEST TEMP. °K (°F)	PRELOAD LOAD N (LB)	PRELOAD STRESS MN/m² (KSI)	CYCLIC LOADING MAX LOAD N (LB)	CYCLIC LOADING MAX STRESS MN/m² (KSI)	CYCLIC LOADING R	CYCLIC LOADING CYCLES	RESIDUAL STATIC LOAD N (LB)	RESIDUAL STATIC STRESS MN/m² (KSI)	REMARKS
L3-22B 1-C1	L3 [3]	2.71 (.1068)	12.7 (.5003)	NONE	—	—	—	DRY	ROOM	—	—	—	—	—	—	-32760 (-7365)	-943 (-137.4)	
-2		2.68 (.1056)	76.1 (2.996)	1/8 FP SLIT	15.87 (.6248)	15.93 (.6275)	THRU			—	—	—	—	—	—	-60050 (-13500)	-294 (-42.7)	
-3		2.73 (.1077)	76.1 (2.997)	5/8 FP SLIT	3.10 (.1220)	3.04 (.1199)	THRU			—	—	—	—	—	—	-81840 (-18400)	-393 (-57.0)	TAB FAILURE RETEST 22350 LB
-4		2.70 (.1063)	76.2 (3.000)	5/8 HP SLIT	16.19 (.6373)	—	1.5 (.06)			—	—	—	—	—	—	-79620 (-17900)	-386 (-56.1)	TAB FAILURE RETEST 17725

[3] $((0/+30/0/-30/0)_2)_S$

WET SPECIMEN STATIC COMPRESSION DATA

SPEC. NO.	LAYUP	THICKNESS mm (INCH)	WIDTH mm (INCH)	FLAW TYPE	FLAW LENGTH FRONT mm (INCH)	FLAW LENGTH BACK mm (INCH)	FLAW DEPTH mm (INCH)	TEST TYPE	TEST TEMP. °K (°F)	PRELOAD LOAD N (LB)	PRELOAD STRESS MN/m² (KSI)	CYCLIC LOADING MAX LOAD N (LB)	CYCLIC LOADING MAX STRESS MN/m² (KSI)	CYCLIC LOADING R	CYCLIC LOADING CYCLES	RESIDUAL STATIC LOAD N (LB)	RESIDUAL STATIC STRESS MN/m² (KSI)	REMARKS
LI-34 -C4	LI [1]	2.71 (.1068)	12.7 (.5004)	NONE	—	—	—	WET	ROOM	—	—	—	—	—	—	-29220 (-6570)	-847 (-122.9)	
-14		2.74 (.1079)	76.1 (2.998)	1/8 FP SLIT	3.14 (.1235)	3.04 (.1197)	THRU			—	—	—	—	—	—	-80060 (-18000)	-383 (-55.6)	TAB FAILURE RETEST TO 18850 LB
-19		2.66 (.1048)	76.2 (3.001)	3/8 FP SLIT	9.63 (.3790)	9.51 (.3745)				—	—	—	—	—	—	-62050 (-13950)	-305 (-44.3)	
-22		2.67 (.1052)	76.2 (3.000)	5/8 FP SLIT	15.86 (.6246)	15.86 (.6248)				—	—	—	—	—	—	-50480 (-11350)	-248 (-36.0)	
-C5		2.72 (.1072)	12.7 (.5004)	NONE	—	—			394 (250)	—	—	—	—	—	—	-9920 (-2230)	-287 (-41.6)	
-15		2.72 (.1070)	76.2 (3.000)	1/8 FP SLIT	3.14 (.1237)	3.05 (.1200)				—	—	—	—	—	—	-52820 (-11875)	-255 (-37.0)	
-20		2.67 (.1051)	76.1 (2.997)	3/8 FP SLIT	9.60 (.3779)	8.86 (.3489)				—	—	—	—	—	—	-32690 (-7350)	-161 (-23.3)	TAB FAILURE RETEST TO 9125 LB
-23		2.76 (.1086)	76.2 (3.001)	5/8 FP SLIT	15.87 (.6249)	15.86 (.6245)				—	—	—	—	—	—	-27800 (-6250)	-132 (-19.2)	
-C6		2.71 (.1069)	12.7 (.5002)	NONE	—	—			422 (300)	—	—	—	—	—	—	-4890 (-1100)	-141 (-20.6)	
-37		2.58 (.1015)	76.3 (3.003)	1/8 FP SLIT	3.14 (.1235)	3.04 (.1199)				—	—	—	—	—	—	-27020 (-6075)	-137 (-19.9)	
-21		2.73 (.1074)	76.2 (3.000)	3/8 FP SLIT	9.55 (.3760)	9.45 (.3722)				—	—	—	—	—	—	-24460 (-5500)	-118 (-17.1)	
-24		2.76 (.1088)	76.2 (3.000)	5/8 FP SLIT	15.83 (.6233)	15.84 (.6235)				—	—	—	—	—	—	-20240 (-4550)	-96 (-13.9)	
-28		2.78 (.1093)	76.1 (2.996)	5/8 HP SLIT	16.21 (.6382)	0	1.5 (.06)		ROOM	—	—	—	—	—	—	-76730 (-17250)	-363 (-52.7)	
-29		2.73 (.1076)	76.1 (2.998)		15.89 (.6257)	0	1.5 (.06)		394 (250)	—	—	—	—	—	—	-41030 (-9225)	-197 (-28.6)	
-30		2.65 (.1043)	76.2 (3.001)		15.99 (.6295)	0	1.5 (.06)		422 (300)	—	—	—	—	—	—	-21240 (-4775)	-105 (-15.3)	

[1] $((0/\pm45/0/90)_S)_2$

TENSION) COMPRESSION) FATIGUE TESTS

SPEC. NO.	LAYUP	THICKNESS mm (INCH)	WIDTH mm (INCH)	FLAW TYPE	FLAW LENGTH FRONT mm (INCH)	FLAW LENGTH BACK mm (INCH)	FLAW DEPTH mm (INCH)	TEST TYPE	TEST TEMP. °K (°F)	PRELOAD LOAD N (LB)	PRELOAD STRESS MN/m² (KSI)	CYCLIC LOADING MAX LOAD N (LB)	CYCLIC LOADING MAX STRESS MN/m² (KSI)	CYCLIC LOADING R	CYCLIC LOADING CYCLES	RESIDUAL STATIC LOAD N (LB)	RESIDUAL STATIC STRESS MN/m² (KSI)	REMARKS
L1-35	L1 [1]	2.76 (.1086)	73.8 (2.907)	IMPACT	—	—	—	DRY FATIGUE	Room	—	—	40 030 (9000)	196 (28.5)	-1.0	1.5×10^6			
-19																		SUBSEQUENT CYCLED ±11000 lb FOR 1.0 x 10⁶ CYCLES. ±13000 lb FOR 180 000 CYCLES (FAILED)
-20		2.89 (.1138)	76.2 (3.001)		—	—	—			—	—	40 030 (9000)	182 (26.4)	-1.0	1.51×10^6	—	—	
-21		2.90 (.1140)	76.1 (2.997)	5/8 FP SLIT	15.78 (.6214)	15.79 (.6217)	THRU		394 (250)	—	—	40 030 (9000)	181 (26.3)	-1.0	7270	—	—	FATIGUE FAILURE
-22		2.92 (.1148)	76.0 (2.994)		15.70 (.6181)	15.71 (.6187)				—	—	35 580 (8000)	161 (23.3)	-1.0	83 700	—	—	FATIGUE FAILURE
-23		2.85 (.1122)	76.1 (2.997)		15.83 (.6236)	15.79 (.6215)				—	—	33 360 (7500)	154 (22.3)	-1.0	1.0×10^6			±7000 lb FOR 500 000 ADDITIONAL CYCLES
-24		2.92 (.1148)	76.2 (3.001)		15.85 (.6241)	15.77 (.6211)				—	—	33 360 (7500)	150 (21.8)	-1.0	447, 100	—	—	FATIGUE FAILURE
-25		2.91 (.1144)	76.3 (3.002)		15.84 (.6237)	15.75 (.6199)				—	—	37 810 (8500)	171 (24.8)	-1.0	1790	—	—	FATIGUE FAILURE
-26		2.92 (.1150)	76.2 (3.001)	IMPACT	—	—	—		422 (300)	—	—	40 030 (9000)	180 (26.1)	-1.0	1.51×10^6	—	—	SUBSEQUENT CYCLED ±11.000 lb FOR 235010 CYC
-27		2.81 (.1107)	76.2 (3.000)		—	—	—	DRY FATIGUE		—	—	53 380 (12000)	249 (36.1)	-1.0	52 630	—	—	FATIGUE FAILURE
-28		2.89 (.1139)	76.2 (3.001)		—	—	—	WET FATIGUE	Room	—	—	57 820 (13000)	262 (38.0)	-1.0	131 500	—	—	FATIGUE FAILURE
-29		2.92 (.1149)	76.3 (3.002)		—	—	—			—	—	62 270 (14000)	280 (40.6)	-1.0	8150	—	—	FATIGUE FAILURE
-30		2.89 (.1140)	76.3 (3.002)	5/8 FP SLIT	15.91 (.6266)	15.86 (.6244)	THRU		394 (250)	—	—	22 240 (5000)	101 (14.6)	-1.0	1.5×10^6	-52 750 (11 860)	-238 (-34.6)	
-31		2.82 (.1112)	76.3 (3.005)		15.91 (.6263)	15.80 (.6220)				—	—	31 140 (7000)	144 (20.9)	-1.0	50800	—	—	FATIGUE FAILURE
-32		2.90 (.1141)	76.2 (3.000)		15.92 (.6269)	15.81 (.6225)				—	—	26 690 (6000)	121 (17.5)	-1.0	1 467 800	—	—	FATIGUE FAILURE
-33		2.89 (.1138)	76.2 (2.999)		15.92 (.6266)	15.84 (.6235)				—	—	28 910 (6500)	131 (19.0)	-1.0	1.5×10^6	-39 990 (-8990)	-181 (-26.3)	
-34		2.90 (.1142)	76.2 (3.000)		15.91 (.6263)	15.80 (.6222)		WET FATIGUE		—	—	30 020 (6750)	136 (19.7)	-1.0	124 100	—	—	FATIGUE FAILURE

[1] $((0/\pm 45/0/90)_S)_2$

TENSION COMPRESSION FATIGUE TESTS

SPEC. NO.	LAYUP	THICKNESS mm (INCH)	WIDTH mm (INCH)	FLAW TYPE	FLAW LENGTH FRONT mm (INCH)	FLAW LENGTH BACK mm (INCH)	FLAW DEPTH mm (INCH)	TEST TYPE	TEST TEMP. °K (°F)	PRELOAD LOAD N (LB)	PRELOAD STRESS MN/m² (KSI)	CYCLIC LOADING MAX LOAD N (LB)	CYCLIC LOADING MAX STRESS MN/m² (KSI)	CYCLIC LOADING R	CYCLIC LOADING CYCLES	RESIDUAL STATIC LOAD N (LB)	RESIDUAL STATIC STRESS MN/m² (KSI)	REMARKS
11-35	L1 [1]	2.84 (.1119)	76.2 (3.001)	IMPACT	–	–	–	WET FATIGUE	422 (300)	–	–	–	–	–	–	-31940 (-7180)	-147 (-21.4)	FIRST CYCLE COMPRESSION FAILURE
-35																		
-36		2.87 (.1131)	76.2 (3.001)		–	–	–			–	–	–	–	–	–	-28160 (-6330)	-128 (-18.6)	FIRST CYCLE COMPRESSION FAILURE
-1		2.90 (.1143)	76.3 (3.002)	5/8 HP SLIT	16.3 (.6425)	–	1.5 (.06)	DRY FATIGUE	ROOM	–	–	62270 (14000)	281 (40.8)	-1.0	9	-65830 (-14800)	-297 (-43.1)	
-2		2.87 (.1132)	76.3 (3.002)		16.4 (.6450)	–				–	–	57820 (13000)	263 (38.2)	-1.0	11800	–	–	FATIGUE FAILURE
-3		2.87 (.1130)	76.3 (3.002)		16.3 (.6434)	–			422 (300)	–	–	53380 (12000)	244 (35.4)	-1.0	378	–	–	FATIGUE FAILURE
-4		2.86 (.1125)	76.2 (3.000)		16.3 (.6399)	–				–	–	44480 (10000)	204 (29.6)	-1.0	3190	–	–	FATIGUE FAILURE
-5		2.89 (.1139)	76.3 (3.002)		16.3 (.6415)	–		WET FATIGUE	ROOM	–	–	48930 (11000)	222 (32.2)	-1.0	32130	–	–	FATIGUE FAILURE
-6		2.89 (.1139)	76.3 (3.002)		16.4 (.6446)	–				–	–	44480 (10000)	201 (29.2)	-1.0	53900	–	–	FATIGUE FAILURE
-7		2.87 (.1131)	76.3 (3.002)		17.1 (.6717)	–			422 (300)	–	–	–	–	–	–	-30910 (-6950)	-141 (-20.5)	FIRST CYCLE COMPRESSION FAILURE
-8		2.82 (.1112)	76.2 (3.000)		16.3 (.6432)	–				–	–	24460 (5500)	114 (16.5)	-1.0	8	–	–	FATIGUE FAILURE

[1] $((0/\pm45/0/90)_5)_2$

RESIDUAL COMPRESSION STRENGTH TESTS

SPEC. NO.	LAYUP	THICKNESS mm (INCH)	WIDTH mm (INCH)	FLAW TYPE	FLAW LENGTH FRONT mm (INCH)	FLAW LENGTH BACK mm (INCH)	FLAW DEPTH mm (INCH)	TEST TYPE	TEST TEMP. °K (°F)	PRELOAD LOAD N (LB)	PRELOAD STRESS MN/m² (KSI)	CYCLIC LOADING MAX LOAD N (LB)	CYCLIC LOADING MAX STRESS MN/m² (KSI)	CYCLIC LOADING R	CYCLIC LOADING CYCLES	RESIDUAL STATIC LOAD N (LB)	RESIDUAL STATIC STRESS MN/m² (KSI)	REMARKS
LI-21	[1]																	
-1		2.68 (.1057)	76.1 (2.997)	5/8 FP SLIT	15.72 (.6188)	15.57 (.6130)	THRU	DRY	ROOM	—	—	35600 (8000)	173 (25.2)	-1.0	1	-53930 (-12125)	264 (38.3)	
-2		2.71 (.1067)	76.1 (2.998)		15.75 (.6203)	15.63 (.6157)				—	—	35600 (8000)	172 (25.0)		10	-55040 (-12375)	-266 (-38.7)	
-3		2.71 (.1068)	76.1 (2.995)		15.76 (.6206)	15.63 (.6157)				—	—	35600 (8000)	172 (25.0)		1000	-56380 (-12675)	-273 (-39.6)	
-4		2.64 (.1041)	76.1 (2.997)		15.79 (.6216)	15.65 (.6160)				—	—	35600 (8000)	176 (25.6)		10^5	-46590 (-10475)	-231 (-33.6)	
-5		2.67 (.1054)	76.1 (2.995)		15.79 (.6219)	15.68 (.6174)				—	—	35600 (8000)	174 (25.3)		391550	—	—	FATIGUE FAILURE
-6		2.67 (.1054)	76.1 (2.998)		15.87 (.6247)	15.68 (.6175)		WET		—	—	31100 (7000)	152 (22.1)	-1.0	1	-49480 (-11125)	-243 (-35.2)	
-7		2.70 (.1064)	76.1 (2.998)		15.86 (.6244)	15.70 (.6182)				—	—	31100 (7000)	151 (21.9)		10	-52040 (-11700)	-253 (-36.7)	
-8		2.68 (.1057)	76.1 (2.998)		15.90 (.6261)	15.72 (.6190)				—	—	31100 (7000)	152 (22.1)		1000	-51600 (-11600)	-252 (-36.6)	
-9		2.72 (.1070)	76.2 (2.999)		15.92 (.6268)	15.74 (.6198)				—	—	31100 (7000)	150 (21.8)		10^5	-51480 (-11575)	-249 (-36.1)	
-10		2.67 (.1054)	76.2 (2.999)		15.93 (.6270)	15.74 (.6197)				—	—	31100 (7000)	153 (22.2)		725570	—	—	FATIGUE FAILURE
LI-35 -9		2.89 (.1139)	76.3 (3.003)		15.88 (.6251)	15.77 (.6208)				—	—	-31100 (-7000)	141 (20.5)	20	1	-52260 (-11750)	-237 (-34.4)	
-10		2.90 (.1141)	76.1 (2.998)		15.92 (.6268)	15.80 (.6219)				—	—	-31100 (-7000)	141 (20.5)		10	-54260 (-12200)	-246 (-35.7)	
-11		2.86 (.1125)	76.2 (3.001)		15.94 (.6279)	15.80 (.6222)				—	—	-31100 (-7000)	143 (20.7)		10^3	-50930 (-11450)	-234 (-33.9)	
-12		2.87 (.1129)	76.2 (3.000)		15.98 (.6293)	15.86 (.6243)				—	—	-31100 (-7000)	143 (20.7)		10^5	-52040 (-11700)	-238 (-34.5)	
-13		2.94 (.1156)	76.2 (3.001)		15.97 (.6293)	15.86 (.6245)	THRU			—	—	-31100 (-7000)	139 (20.2)		10^6	-52380 (-11775)	-234 (-33.9)	

[1] $((0/\pm45/0/90)_S)_2$

RESIDUAL COMPRESSION STRENGTH TESTS

SPEC. NO.	LAYUP	THICKNESS mm (INCH)	WIDTH mm (INCH)	FLAW TYPE	FLAW LENGTH FRONT mm (INCH)	FLAW LENGTH BACK mm (INCH)	FLAW DEPTH mm (INCH)	TEST TYPE	TEST TEMP. [4] °K (°F)	PRELOAD LOAD N (LB)	PRELOAD STRESS MN/m² (KSI)	CYCLIC LOADING MAX LOAD N (LB)	CYCLIC LOADING MAX STRESS MN/m² (KSI)	CYCLIC LOADING R	CYCLIC LOADING CYCLES	RESIDUAL STATIC LOAD N (LB)	RESIDUAL STATIC STRESS MN/m² (KSI)	REMARKS
L1-34	L1 [1]	2.73 (.107)	76.1 (2.997)	5/8 FP SLIT	15.92 (.6267)	15.81 (.6224)	THRU	DRY	422 (300)	—	—	26690 (6000)	128 (18.6)	-1.0	10	-35580 (-8000)	-171 (-24.8)	
-31		2.77 (.1092)	76.2 (2.999)		15.96 (.6285)	15.78 (.6213)				—	—	26690 (6000)	126 (18.3)	—	3	—	—	GRIP FAILURE
-32		2.73 (.107)	76.2 (3.000)		15.94 (.6277)	15.78 (.6212)				—	—	26690 (6000)	128 (18.6)	—	1	—	—	GRIP FAILURE
-33		2.64 (.1041)	76.2 (2.999)		15.88 (.6251)	15.74 (.6198)		WET		—	—	-15570 (-3500)	77 (11.2)	20	10^3	220 (+50)	1 (+.2)	
-34		2.73 (.1074)	76.2 (2.999)		15.83 (.6232)	15.69 (.6177)				—	—	-15570 (-3500)	75 (10.9)	-1.0	1000	-19350 (-4350)	-93 (-13.5)	
-35		2.69 (.1061)	76.2 (2.999)		15.84 (.6239)	15.73 (.6193)				—	—	-15570 (-3500)	76 (11.0)	-1.0	10^5	-20020 (-4500)	-97 (-14.1)	
-36		2.90 (.1141)	76.3 (3.002)		15.98 (.6293)	15.89 (.6255)				—	—	—	—	—	0	-26100 (-5870)	-117 (-17.1)	FAILED DURING FIRST CYCLE
L1-35		2.88 (.1133)	76.2 (3.001)		15.97 (.6290)	15.90 (.6260)				—	—	—	—	—	0	-28910 (-6500)	-131 (-19.1)	FAILED DURING FIRST CYCLE
-14		2.87 (.1130)	76.2 (3.001)		15.97 (.6286)	15.82 (.6227)	THRU			—	—	-15570 (-3500)	71 (10.3)	20	10^5	-25580 (-5750)	-117 (-17.0)	
-17																		
-16																		

[1] $((0/\pm45/0/90)_S)_2$

[4] TEMPERATURE DURING CYCLING - STATIC TEST AT ROOM TEMP

APPENDIX B

ULTRASONIC INSPECTION DATA

This appendix contains copies of the ultrasonic C-scan records that were developed for the test specimens. The records are identified by the test specimen number, the defect code and a brief description of the point in the test sequence at which the inspection was made. For many of the test specimens, ultrasonic inspection was performed several times during the test showing the progressive development of the damage.

1/8 slit

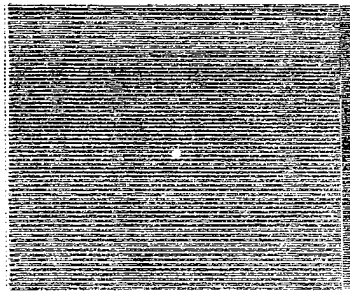

L1-34-2

3/8 slit

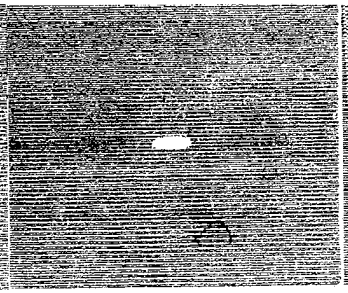

L1-34-7

5/8 slit

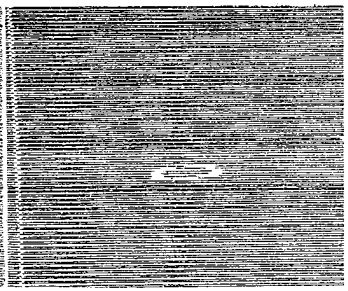

L1-34-10

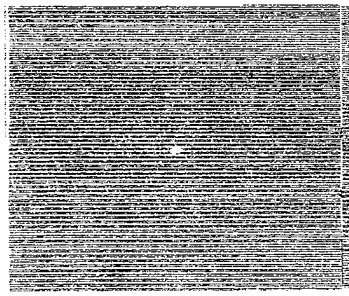

L1-34-3

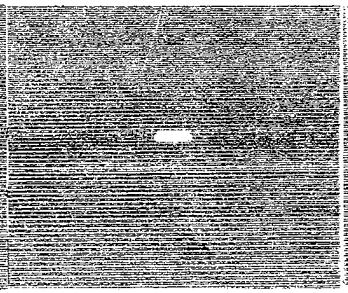

L1-34-8

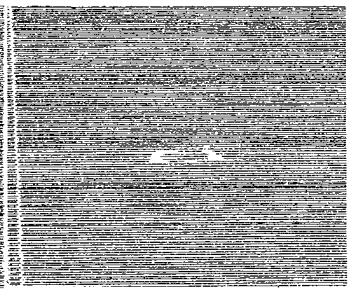

L1-34-11

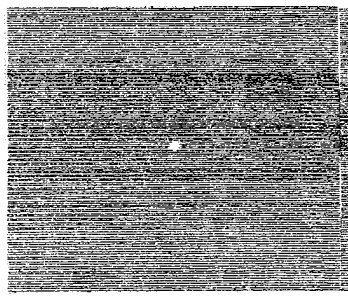

L1-34-13

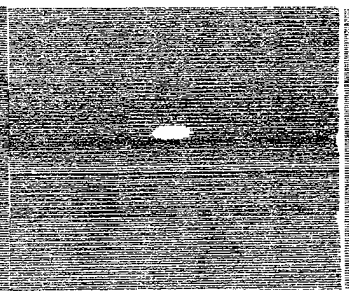

L1-34-9

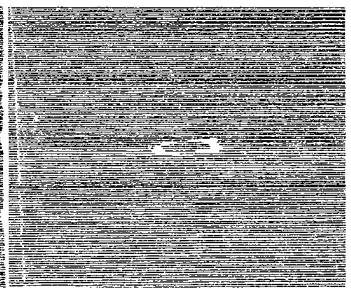

L1-34-12

BEFORE TEST

1/8 slit | 3/8 slit | 5/8 slit

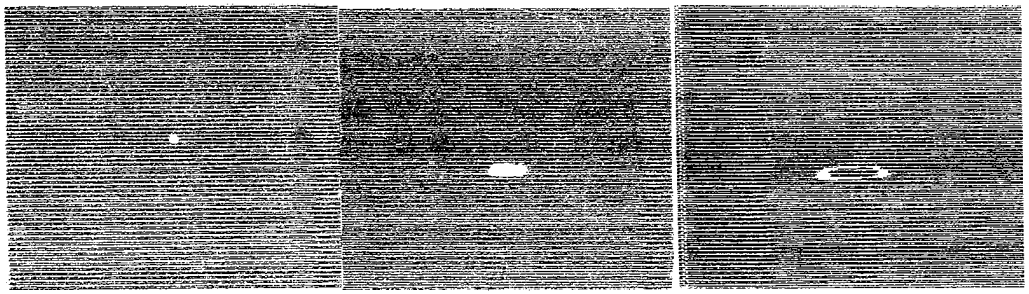

L1-34-14 | L1-34-19 | L1-34-22

AFTER MOISTURE EXPOSURE

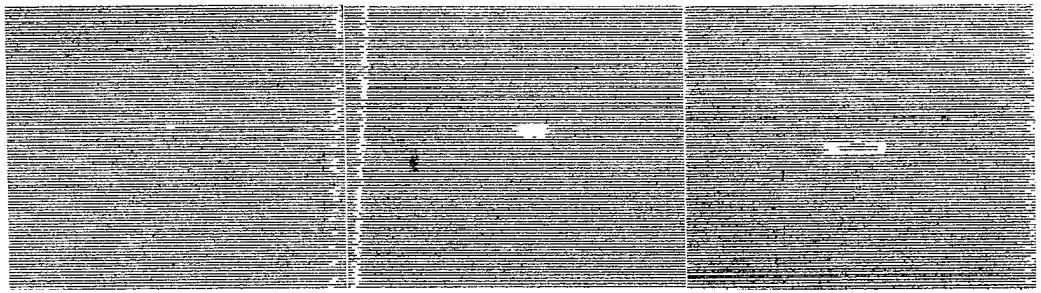

L1-34-14 | L1-34-19 | L1-34-22

BEFORE TEST

1/8 slit | 3/8 slit | 5/8 slit

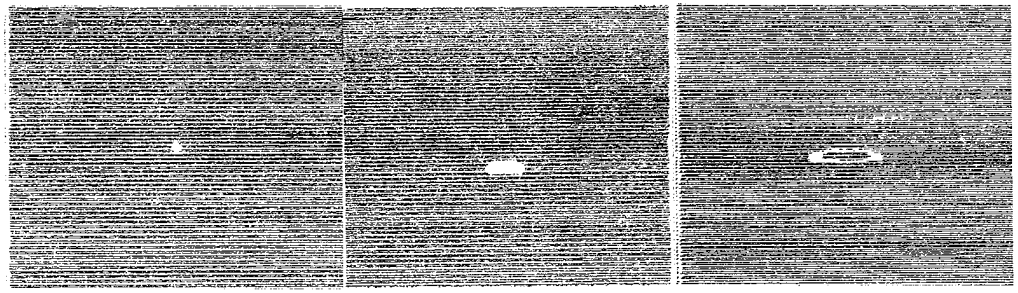

L1-34-15 | L1-34-20 | L1-34-23

AFTER MOISTURE EXPOSURE

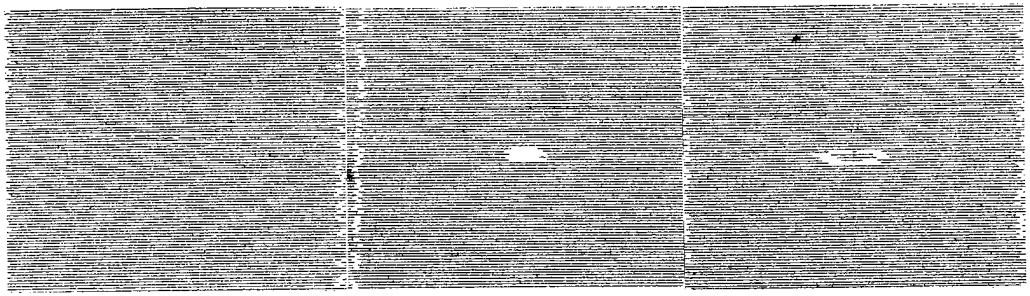

L1-34-15 | L1-34-20 | L1-34-23

BEFORE TEST

1/8 slit | 3/8 slit | 5/8 slit

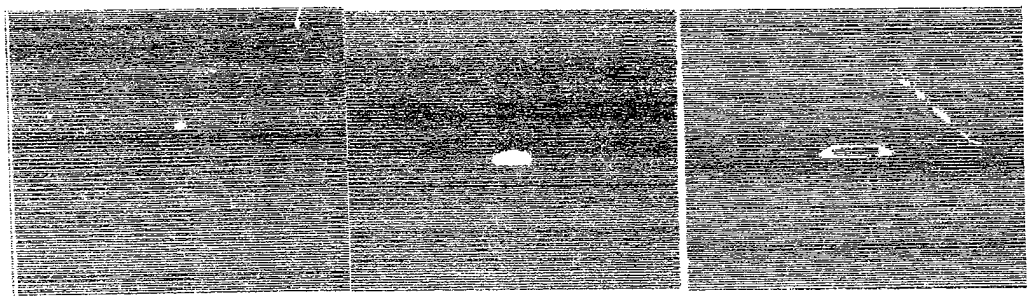

L1-34-37 | L1-34-21 | L1-34-24

AFTER MOISTURE EXPOSURE

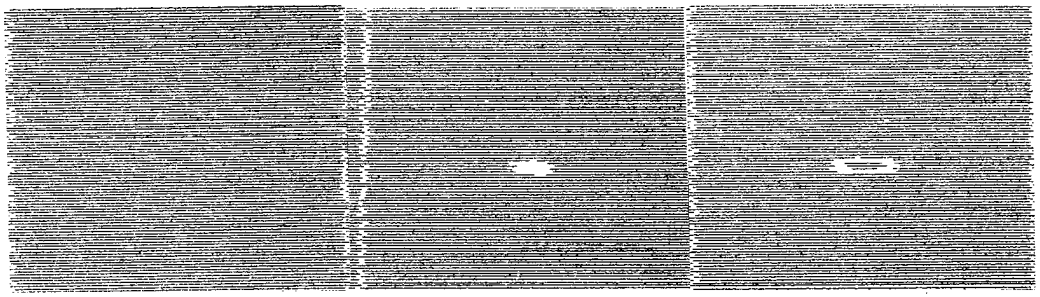

L1-34-27 | L1-34-21 | L1-34-24

5/8 HP slit | 5/8 HP slit | 5/8 HP slit

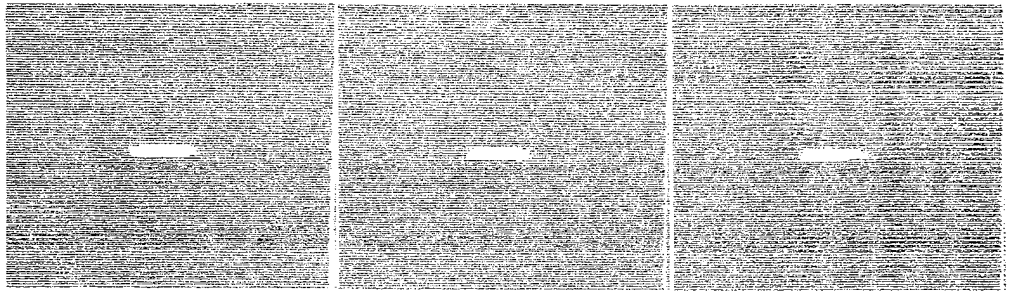

L1-34-25 | L1-34-26 | L1-34-27

BEFORE TEST

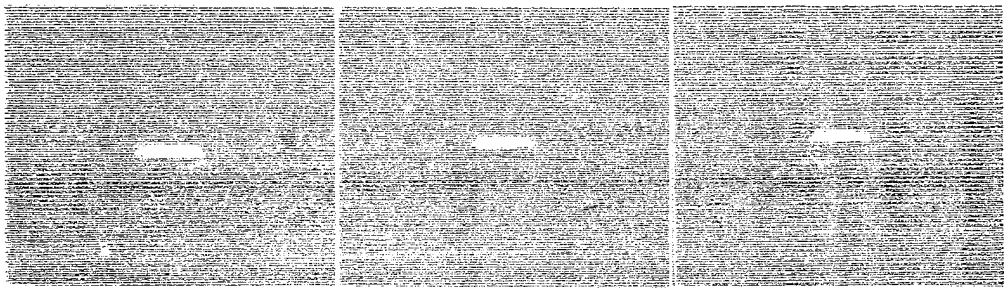

L1-34-28 | L1-34-29 | L1-34-30

AFTER MOISTURE EXPOSURE

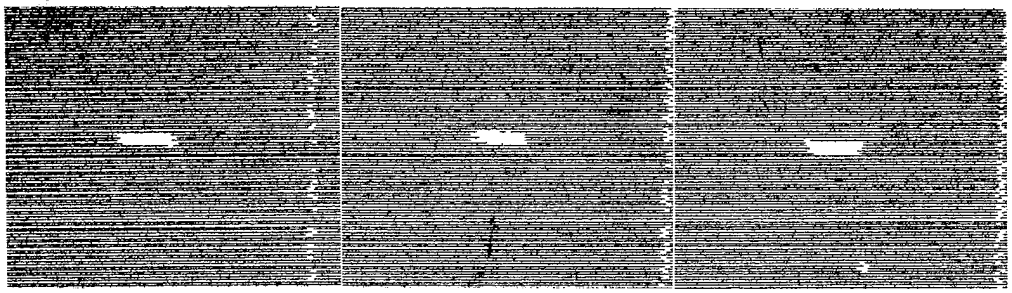

L1-34-28 | L1-34-29 | L1-34-30

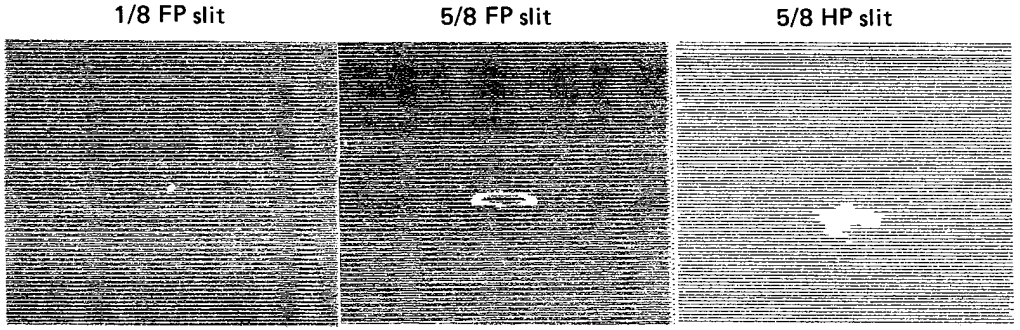
1/8 FP slit
5/8 FP slit
5/8 HP slit
L3-22B-3
L3-22B-2
L3-22B-4

5/8 FP SLIT

BEFORE CYCLIC LOADING

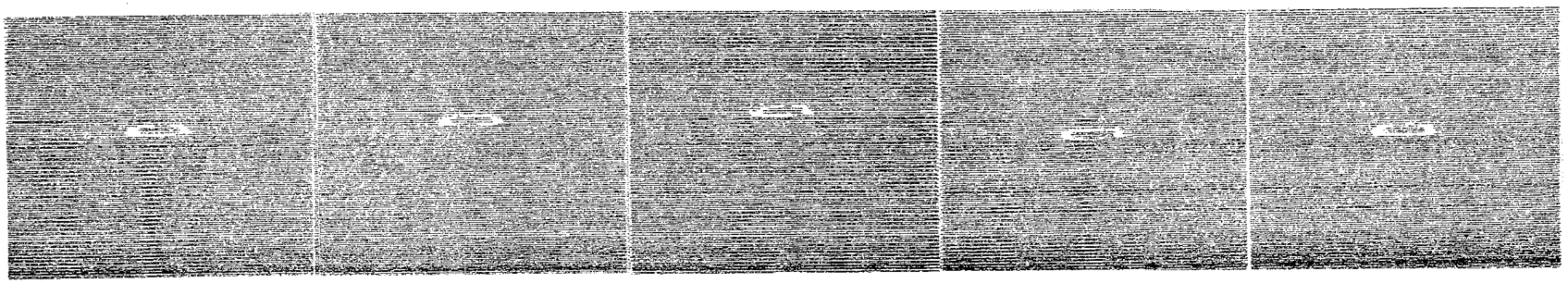

L1-21-1 L1-21-2 L1-21-3 L1-21-4 L1-21-5

AFTER CYCLIC TEST

1 cycle 10 cycles 1,000 cycles 100,000 cycles 391,340 cycles

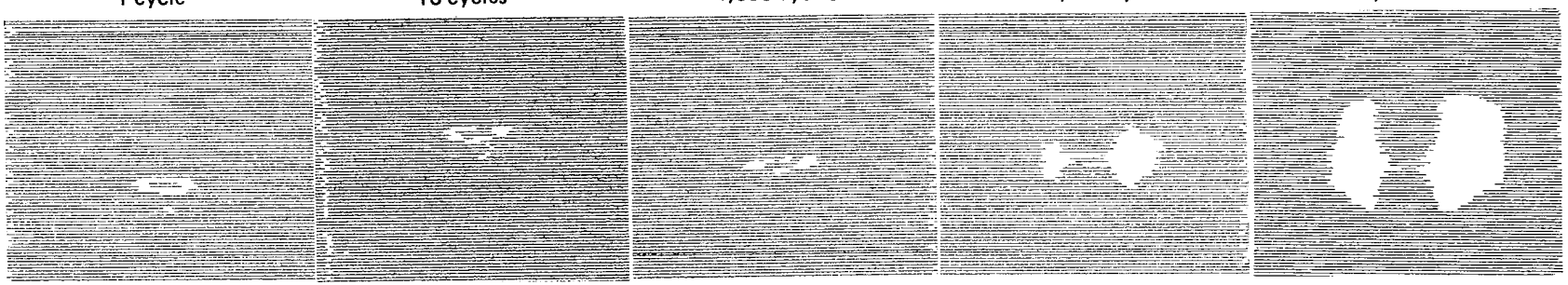

L1-21-1 L1-21-2 L1-21-3 L1-21-4 L1-21-5

5/8 FP Slit

BEFORE TEST

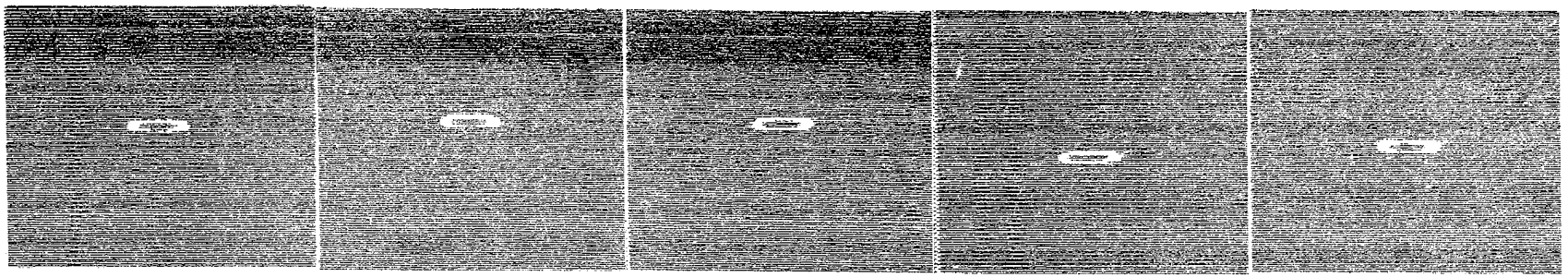

L1-35-9 L1-35-10 L1-35-11 L1-35-12 L1-35-13

AFTER MOISTURE EXPOSURE

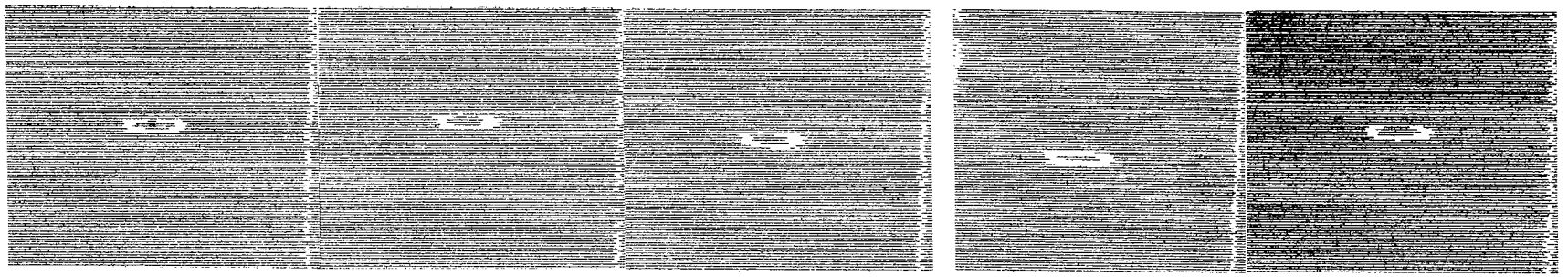

L1-35-9 L1-35-10 L1-34-11 L1-35-12 L1-35-13

AFTER CYCLIC TEST

1 cycle 10 cycles 1,000 cycles 100,000 cycles 10^6 cycles

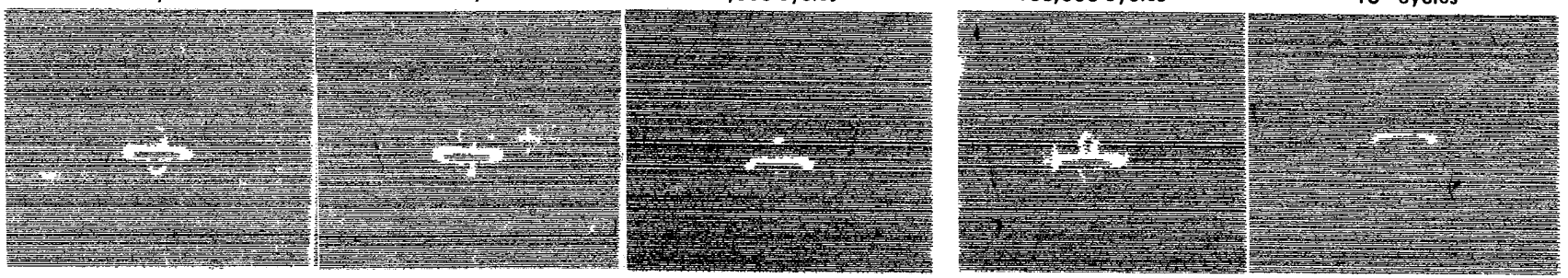

L1-35-9 L1-35-10 L1-35-11 L1-35-12 L1-35-13

5/8 FP Slit

BEFORE TEST

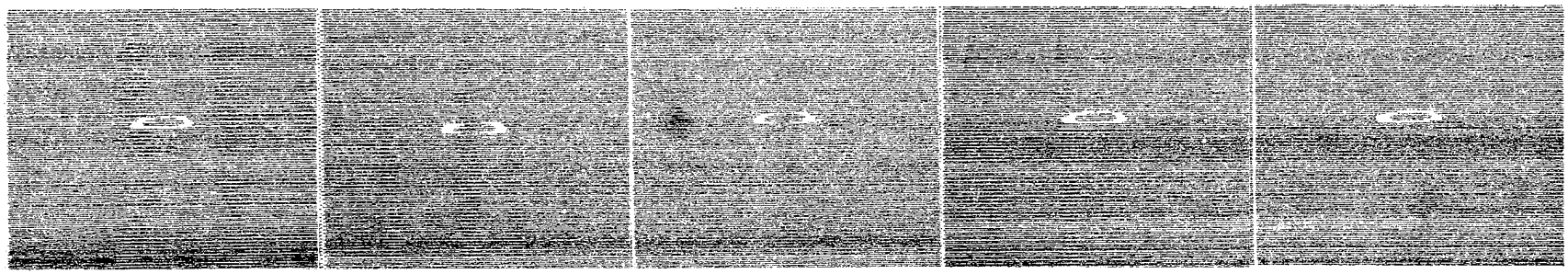

L1-21-6 L1-21-7 L1-21-8 L1-21-9 L1-21-10

AFTER MOISTURE EXPOSURE

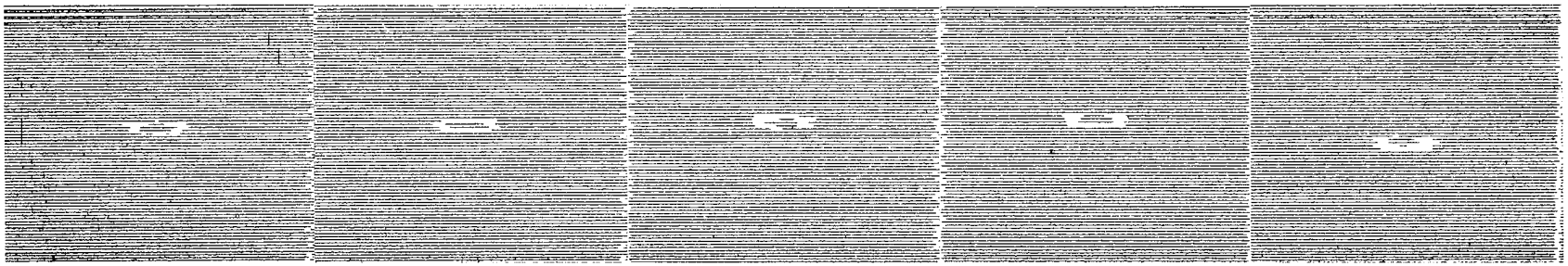

L1-21-6 L1-21-7 L1-21-8 L1-21-9 L1-21-10

AFTER CYCLIC TEST

1 cycle 10 cycles 1,000 cycles 100,000 cycles

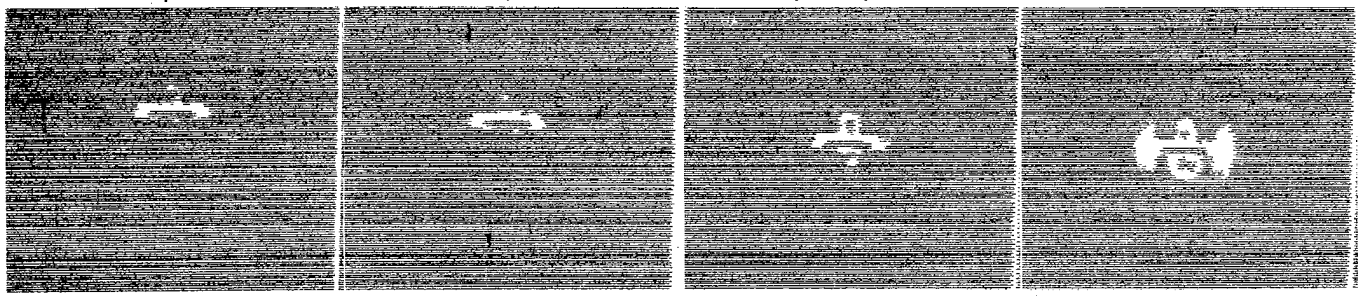

L1-21-6 L1-21-7 L1-21-8 L1-21-9

Fatigue failure at
725,570 cycles

L1-21-10

5/8 FP Slit

BEFORE TEST

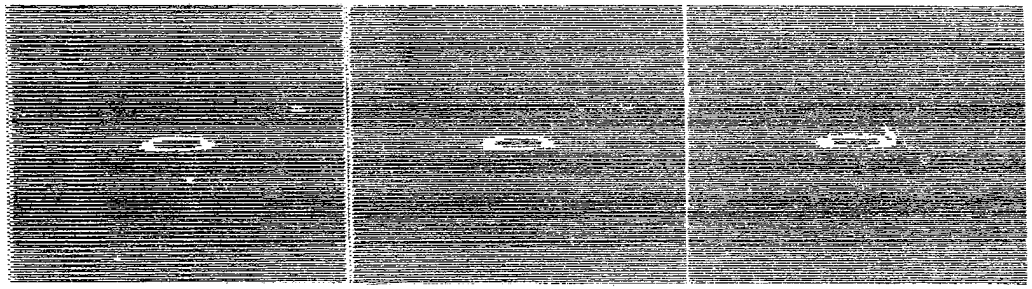

L1-34-31 L1-34-32 L1-34-33

AFTER CYCLIC TEST

10 cycles

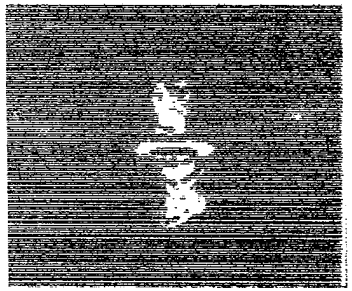

L1-34-31

Fatigue Failure

Fatigue Failure

5/8 FP Slit

BEFORE TEST

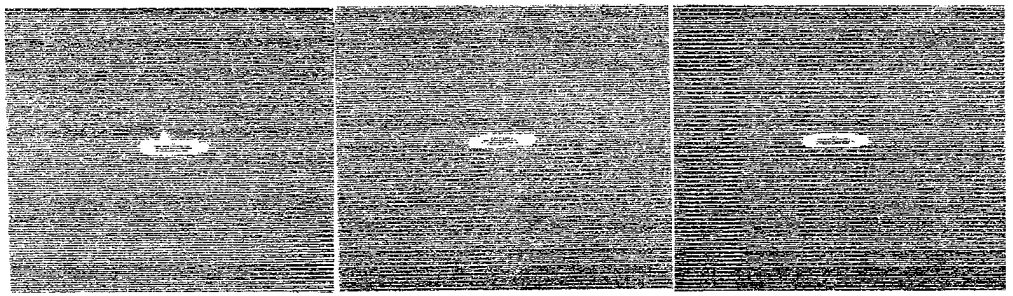

L1-35-14 L1-35-17 L1-35-16

AFTER MOISTURE EXPOSURE

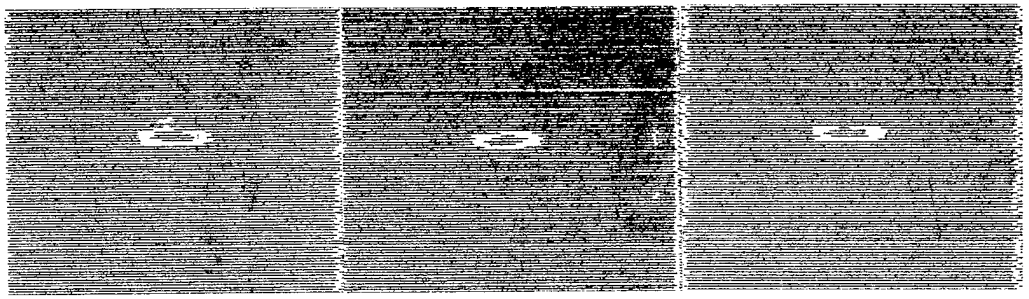

L1-35-14 L1-35-17 L1-35-16

AFTER CYCLIC TEST

100,000 cycles

Fatigue Failure

Fatigue Failure

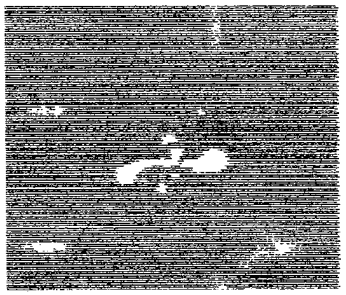

L1-35-16

5/8 FP Slit

BEFORE TEST

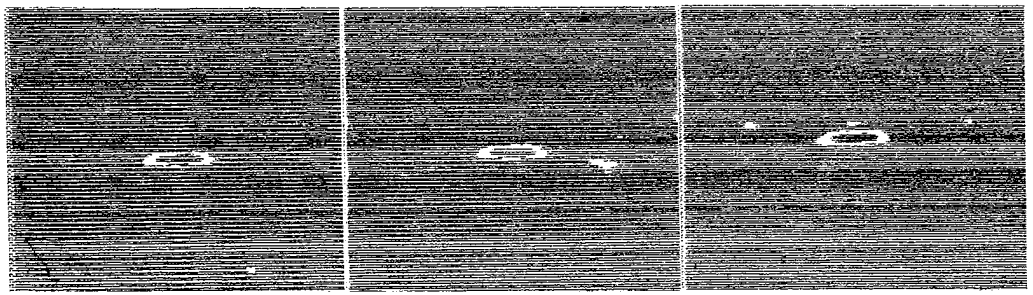

L1-34-34 L1-34-35 L1-34-36

AFTER MOISTURE EXPOSURE

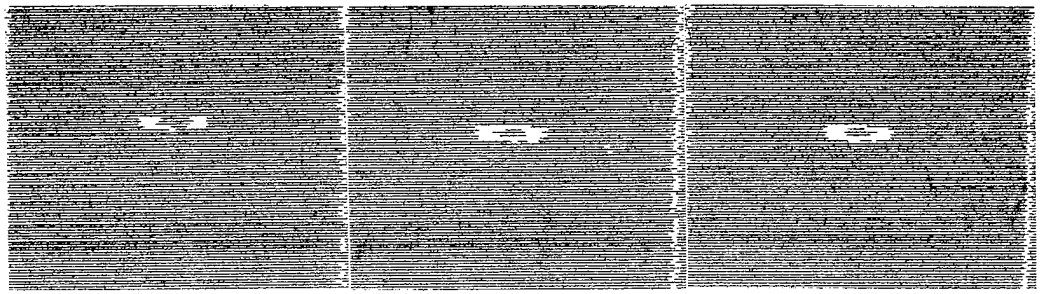

L1-34-34 L1-34-35 L1-34-36

AFTER CYCLIC TEST

1,000 cycles 100,000 cycles

Fatigue Failure

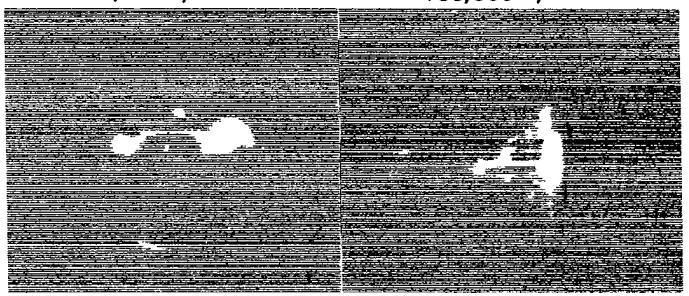

L1-34-34 L1-34-35 L1-34-36

IMPACT DELAMINATION

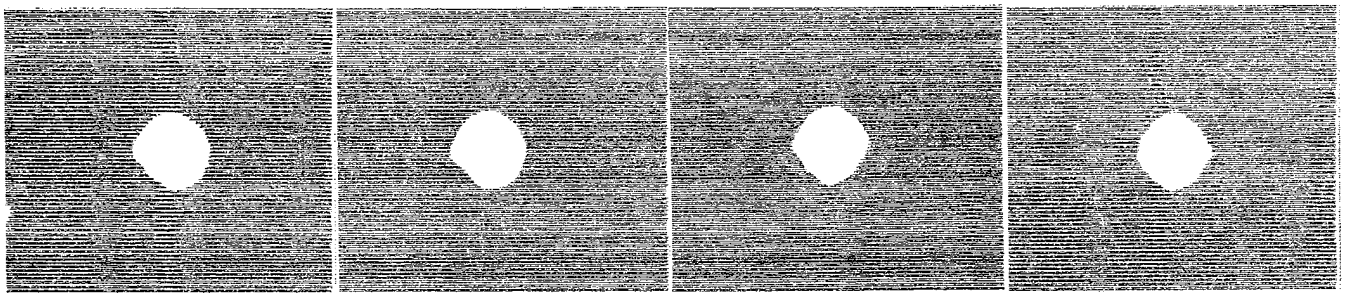

L1-35-19 L1-35-20 L1-35-26 L1-35-27

BEFORE TEST

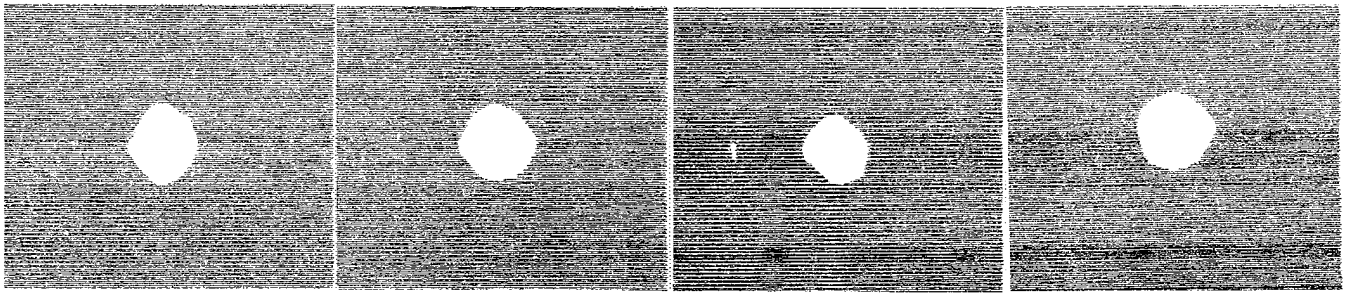

L1-35-28 L1-35-29 L1-35-35 L1-35-36

AFTER MOISTURE EXPOSURE

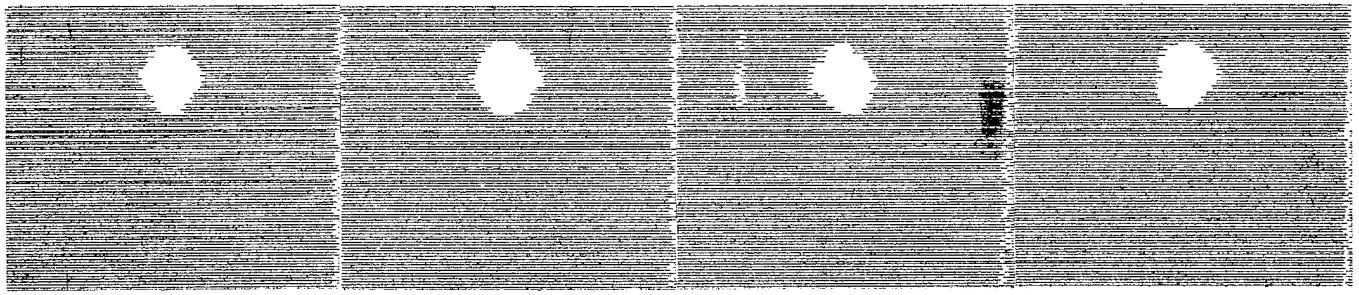

L1-35-28 L1-35-29 L1-35-35 L1-35-36

5/8 FP Slit

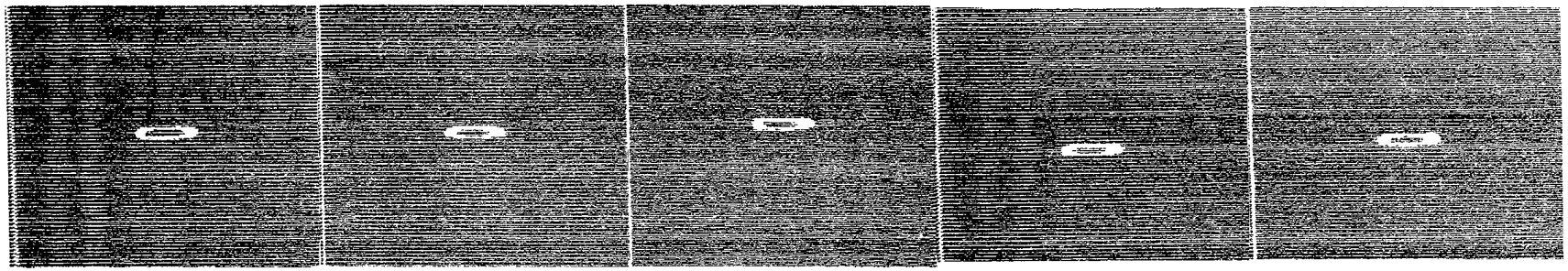

L1-35-21 L1-35-22 L1-35-23 L1-35-24 L1-35-25

BEFORE TEST

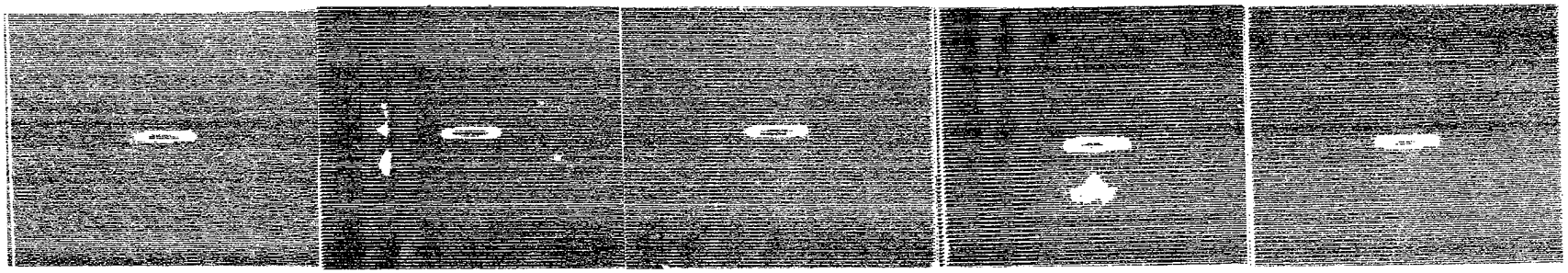

L1-35-30 L1-35-31 L1-35-32 L1-35-33 L1-35-34

AFTER MOISTURE EXPOSURE

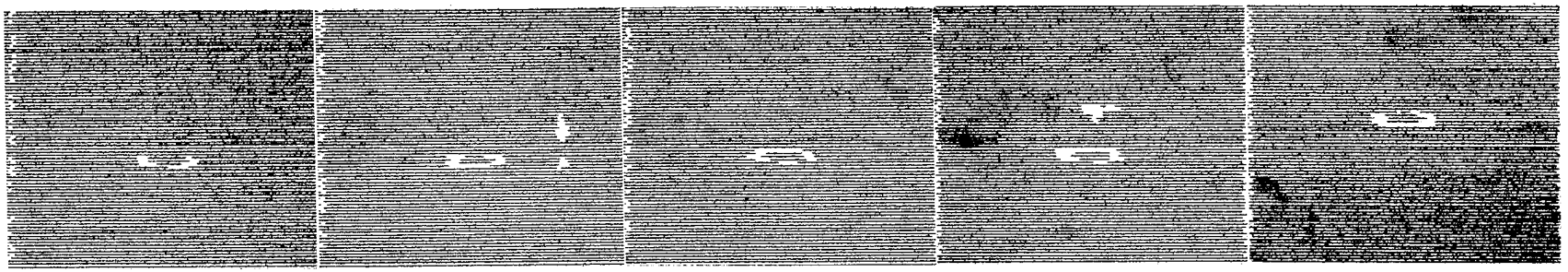

L1-35-30 L1-35-31 L1-35-32 L1-35-33 L1-35-34

5/8 HP Slit

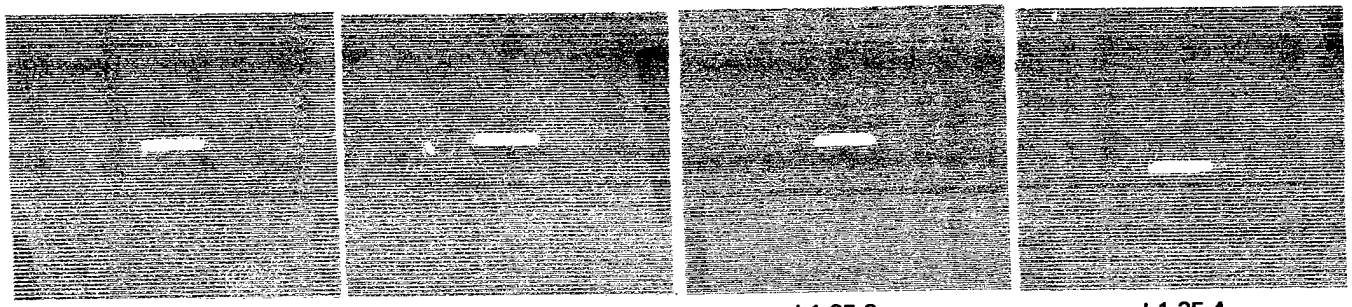

L1-35-1 L1-35-2 L1-35-3 L1-35-4

BEFORE TEST

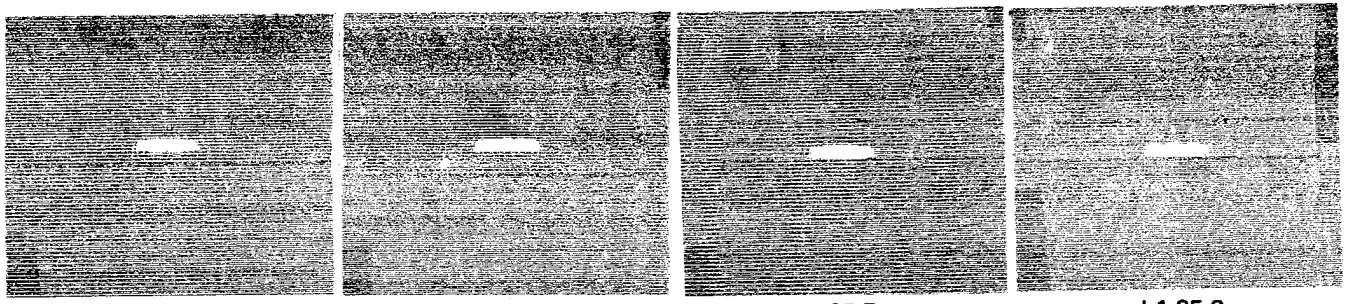

L1-35-5 L1-35-6 L1-35-7 L1-35-8

AFTER MOISTURE EXPOSURE

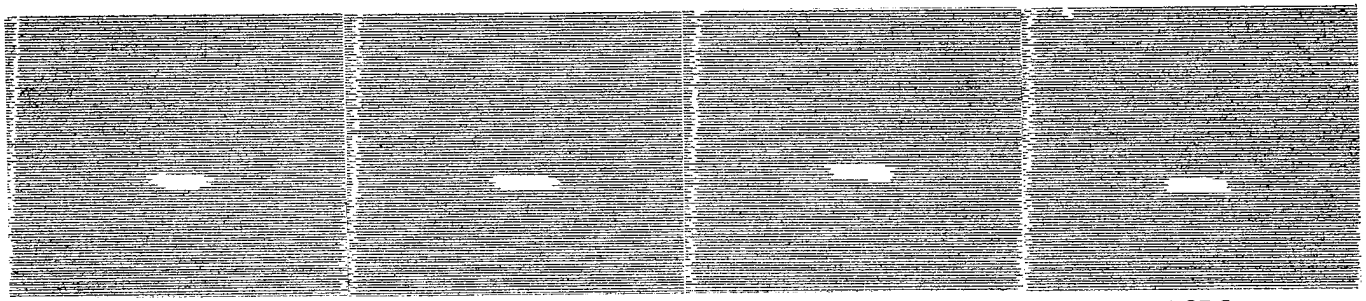

L1-35-5 L1-35-6 L1-35-7 L1-35-8

APPENDIX C

WEIGHT GAIN DATA

The tabulated weight-gain data for each test specimen is included in this appendix as recorded during the course of making the measurements.

Weeks / Specimen number	Weight (g)					Thickness (in)	
	0	2	4	6	8	0	8
L1-34-C4	4.0819	4.1182	4.1253	4.1299	4.1302	0 .1068	0 .1071
L1-34-C5	4.1054	4.1415	4.1486	4.1515	4.1526	0 .1072	0 .1074
L1-34-C6	4.0831	4.1198	4.1271	4.1298	4.1310	0 .1069	0 .1071
L1-34-14	176.8098	178.6516	179.0554	179.2915	179.3515	0 .1079	0 .1080
L1-34-15	174.5267	176.3645	176.7565	177.0001	177.0554	0 .1070	0 .1072
L1-34-37	168.5092	170.3476	170.6374	170.8402	170.8867	0 .1015	0 .1013
L1-34-19	173.2963	175.0298	175.4626	175.6400	175.7257	0 .1048	0 .1072
L1-34-20	173.3624	175.0975	175.5259	175.6970	175.7908	0 .1051	0 .1055
L1-34-21	173.7663	175.5032	175.9594	176.1357	176.2373	0 .1074	0 .1098
L1-34-22	170.6202	172.3768	172.8056	173.0408	173.1043	0 .1052	0 .1052
L1-34-23	175.8027	177.5674	178.0089	178.2517	178.3129	0 .1086	0 .1087
L1-34-24	175.8918	177.6491	178.0988	178.3483	178.4134	0 .1088	0 .1088
L1-34-28	176-2864	178.0486	178.5457	178.7624	178.8038	0 .1093	0 .1109
L1-34-29	174.9364	176.7163	177.1927	177.4117	177.4518	0 .1076	0 .1092
L1-34-30	171.0282	172.7823	173.2717	173.4928	173.5165	0 .1043	0 .1063
A1	24.7716	24.9781	25.0352	25.0615	25.0771	0 .1107	0 .1119
A2	25.0326	25.2311	25.2835	25.3148	25.3311	0 .1116	0 .1118
B1	25.2260	25.4295	25.4880	25.5160	25.5335	0 .1122	0 .1142
B2	25.0228	25.2280	25.2843	25.3161	25.3311	0 .1119	0 .1128
C1	25.0511	25.2552	25.3089	25.3397	25.3544	0 .1113	0 .1122
C2	24.8656	25.0707	25.1247	25.1569	25.1719	0 .1113	0 .1120

STATIC-COMPRESSION SPECIMENS

Weeks / Specimen number	Weight (g)					Thickness (in)	
	0	2	4	6	8	0	8
L1-21-6	174.1640	175.8480	176.3648	176.6680	176.8114	0.1054	0.1067
L1-21-7	174.7194	176.4282	176.9306	176.2361	177.3997	0.1064	0.1078
L1-21-8	171.0876	172.7849	173.2647	173.5513	173.6884	0.0157	0.1039
L1-21-9	175.1247	176.8358	177.3258	177.6415	177.7785	0.1070	0.1085
L1-21-10	174.3747	176.0785	176.5699	176.8836	177.0142	0.1053	0.1056
L1-34-34	170.6149	172.3510	172.8189	172.9913	173.0629	0.1041	0.1056
L1-34-35	174.1471	175.8721	176.3482	176.5202	176.6005	0.1074	0.1084
L1-34-36	172.9127	174.6087	175.0790	175.2602	175.3314	0.1061	0.1077
L1-35-9	183-5851	185.4614	185.9848	186.2226	186.3756	0.1139	0.1163
L1-35-10	182.5219	184.4428	184.9368	185.1493	185.3209	0.1141	0.1148
L1-35-11	181.8074	183.7338	184.2131	184.4102	184.5509	0.1125	0.1148
L1-35-12	180.5841	182.5288	183.0067	183.2194	183.3683	0.1129	0.1144
L1-35-13	184.1565	186.0603	186.5721	186.8189	186.9901	0.1156	0.1168
L1-35-14	183.5168	185.4366	185.9221	186.1547	186.3217	0.1141	0.1148
L1-35-16	182.1129	184.0405	184.5183	184.7268	184.8824	0.1130	0.1142
L1-35-17	182.0280	183.9748	184.4647	184.6929	184.8233	0.1132	0.1149

RESIDUAL COMPRESSION STRENGTH SPECIMENS

Weeks / Specimen number	Weight (g)					Thickness (in)	
	0	2	4	6	8	0	8
L1-35-28	183.8683	185.7637	186.2271	186.5000	186.5901	0.1139	0.1152
L1-35-29	183.4381	185.2234	185.8077	186.0798	186.1811	0.1149	0.1164
L1-35-30	183.9754	185.8558	186.3409	186.6033	186.7123	0.1140	0.1141
L1-35-31	180.3130	182.2224	182.6934	182.9269	183.0182	0.1112	0.1107
L1-35-32	184.0418	185.9354	186.4206	186.6815	186.7864	0.1141	0.1144
L1-35-33	182.9957	184.8947	185.3694	185.6382	185.7303	0.1138	0.1136
L1-35-34	184.1329	186.0184	186.4983	186.7702	186.8719	0.1142	0.1142
L1-35-35	180.3555	182.2828	182.7291	182.9892	183.0831	0.1119	0.1143
L1-35-36	183.4653	185.4109	185.8543	186.1184	186.1965	0.1131	0.1154
L1-35-5	183.7329	185.6283	186.0822	186.3559	186.4574	0.1139	0.1144
L1-35-6	182.7651	184.6872	185.1145	185.3976	185.4948	0.1139	0.1145
L1-35-7	180.2581	184.1776	184.6016	184.8769	184.9664	0.1131	0.1154
L1-35-8	180.9453	182.8548	183.3149	183.5808	183.6873	0.1112	0.1129

FATIGUE TEST SPECIMENS

APPENDIX D

STATIC TEST CRACK OPENING DISPLACEMENT RECORDS

This appendix contains copies of the machine records giving the crack opening displacement gage reading versus the static-test machine load. The curves are identified by specimen number. The value of the maximum test machine load as read from the test machine dial is also recorded on the record.

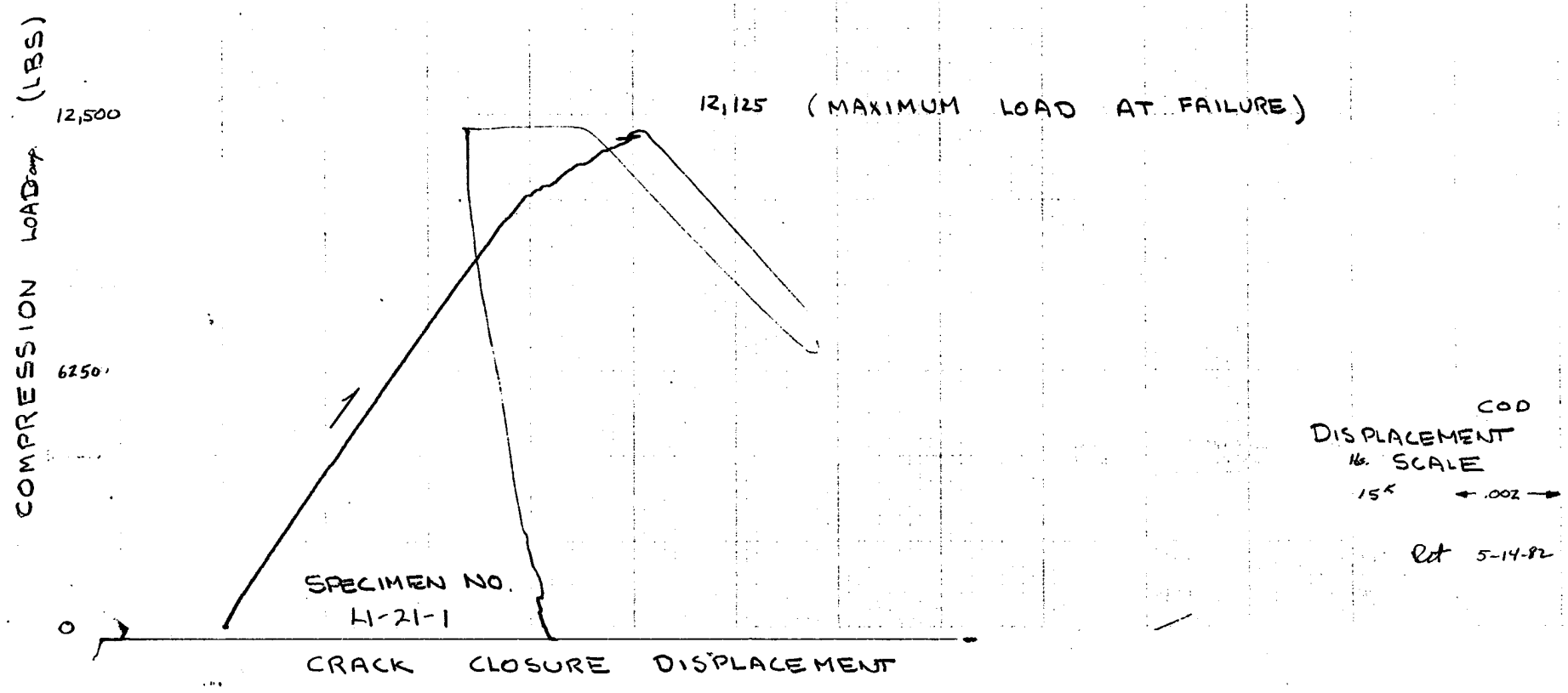
COMPRESSION LOAD (LBS)
12,500
6250
0
12,125 (MAXIMUM LOAD AT FAILURE)
SPECIMEN NO.
41-21-1
CRACK CLOSURE DISPLACEMENT
COD
DISPLACEMENT
16. SCALE
15K
.002
Rct 5-14-82

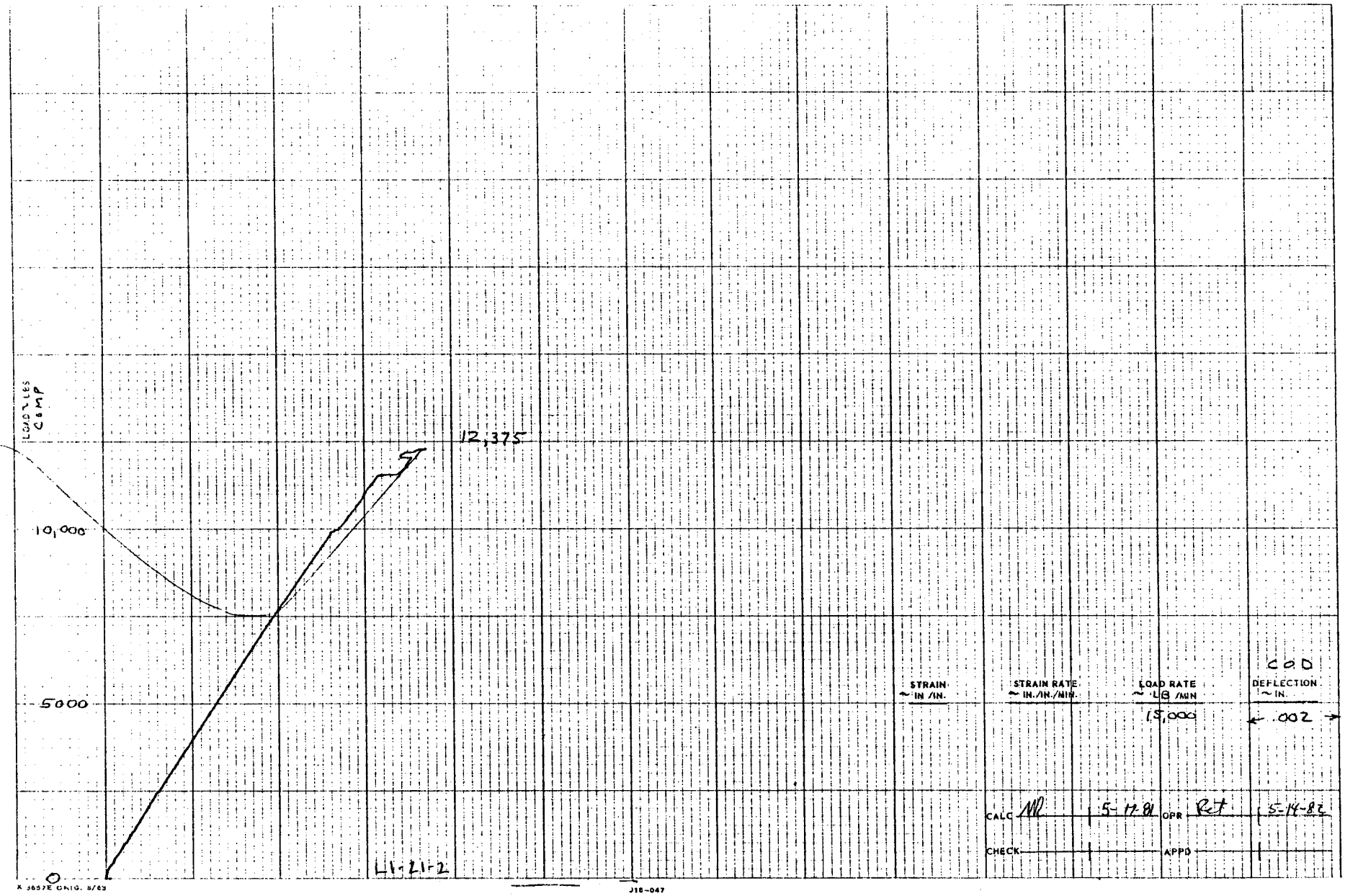
POUNDS COMP
12,375
10,000
5000
0
STRAIN ~ IN /IN.
STRAIN RATE ~ IN./IN./MIN.
LOAD RATE ~ LB /MIN
15,000
C O D
DEFLECTION ~ IN.
.002
CALC
5-17-81
OPR
RET
5-14-82
CHECK
APPD
LL-21-2
X 3657E ORIG. 8/69
J16-047

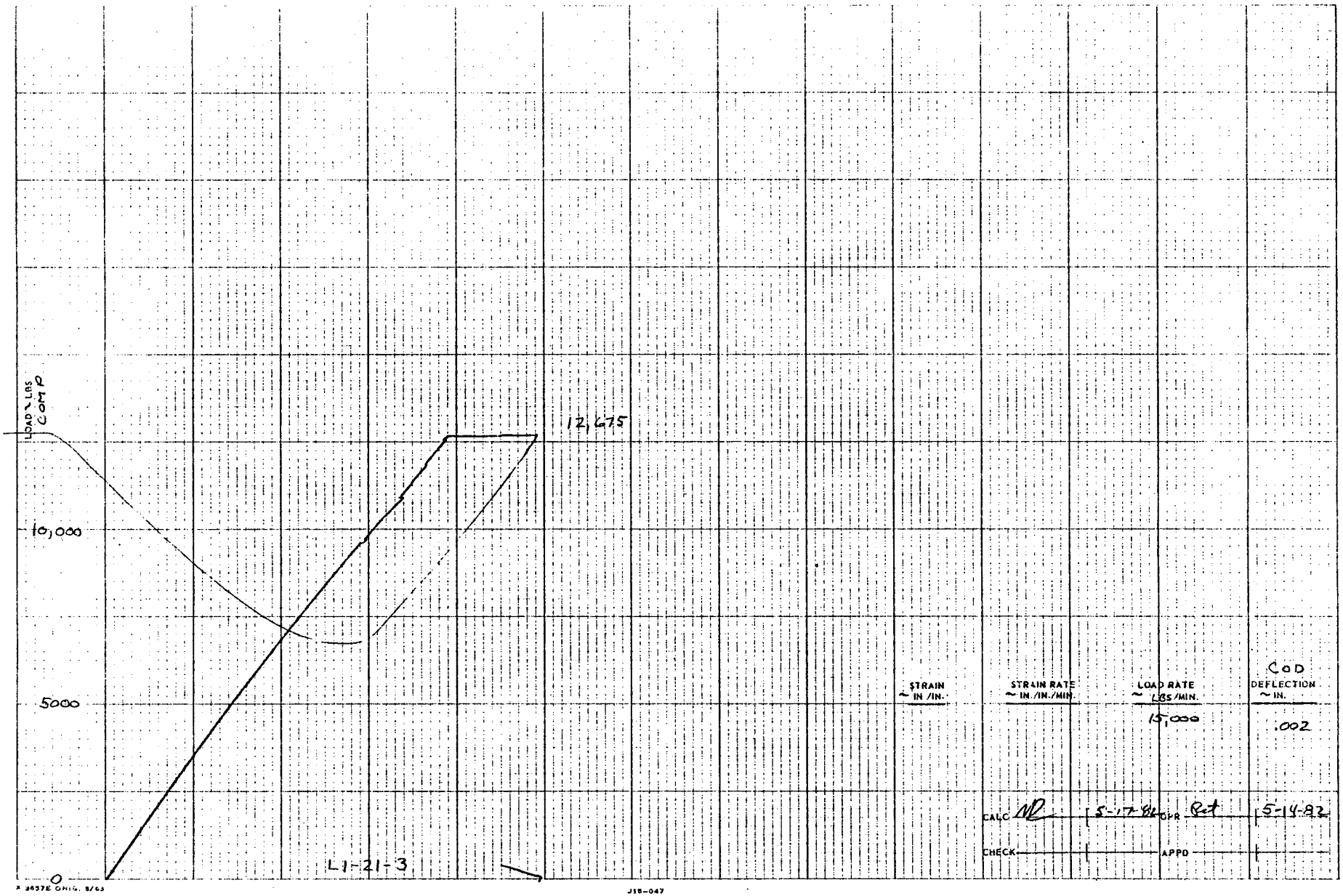
LOAD, LBS COMP
12,675
10,000
5000
0
L1-21-3
STRAIN ~ IN /IN.
STRAIN RATE ~ IN./IN./MIN.
LOAD RATE ~ LBS/MIN.
15,000
COD DEFLECTION ~ IN.
.002
CALC MD 5-17-82 CPR RET 5-14-82
CHECK APPD
X 3837E GNIG. 8/63
J18-047

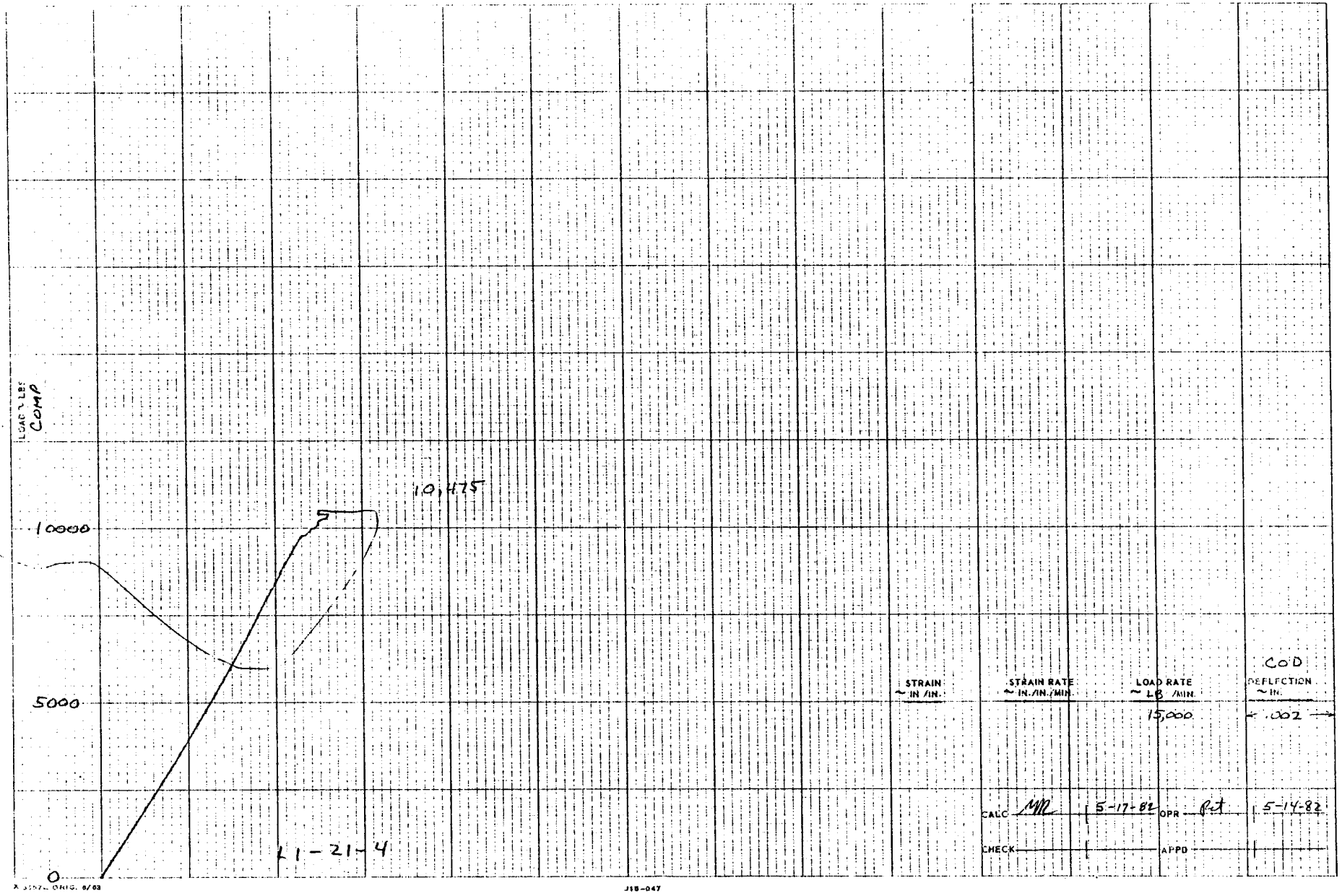
LOAD LBS
COMP
10000
5000
0
10,475
21-21-4
STRAIN
~ IN /IN.
STRAIN RATE
~ IN./IN./MIN.
LOAD RATE
~ LB /MIN.
15,000
C.O.D
DEFLECTION
~ IN.
.002
CALC
5-17-82
OPR
5-14-82
CHECK
APPD
A 10572 ORIG. 8/83
J15-047

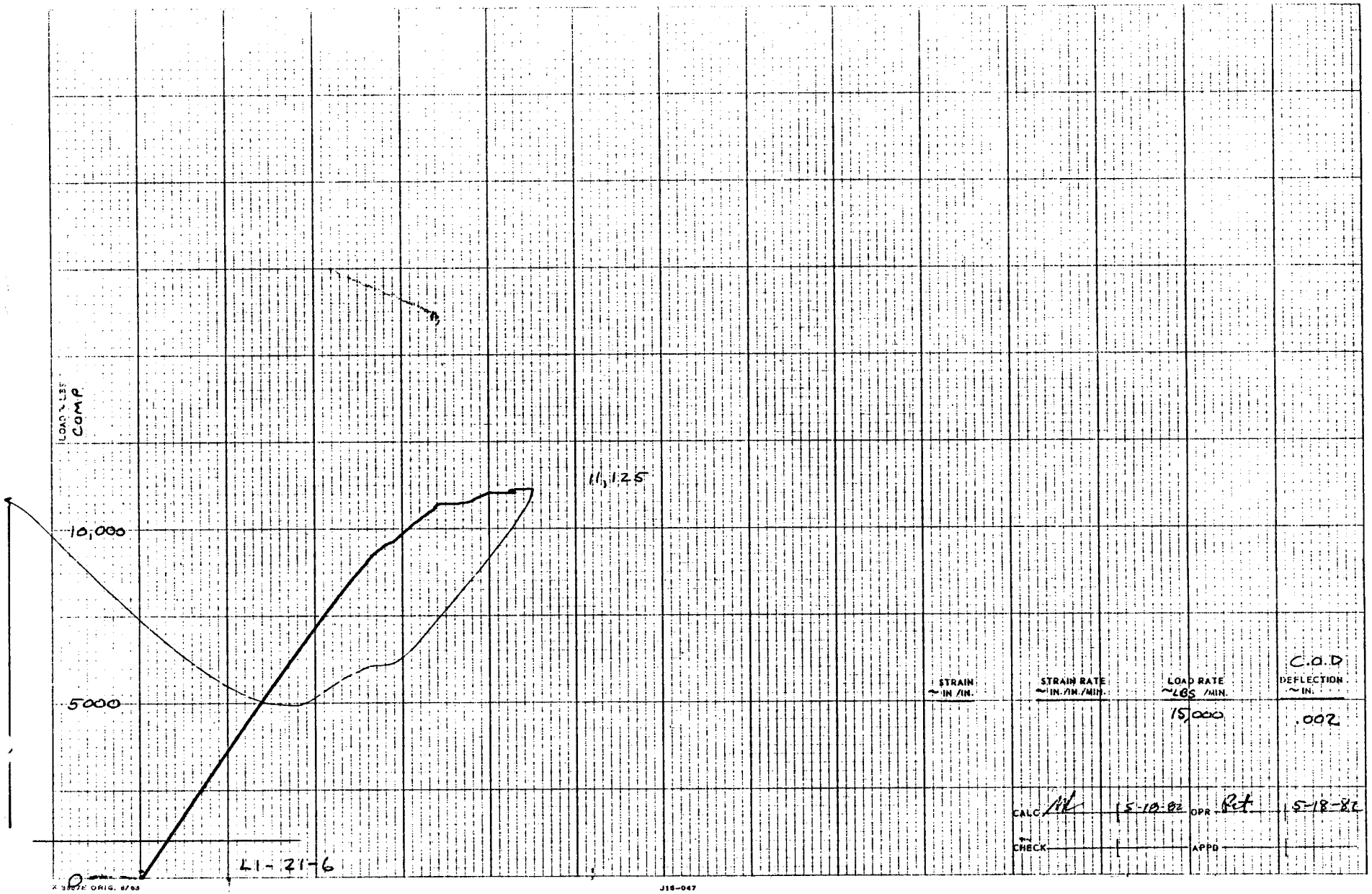
LOAD - LBS
COMP
11,125
10,000
5000
0
41-21-6
STRAIN
~IN /IN.
STRAIN RATE
~IN./IN./MIN.
LOAD RATE
~LBS /MIN.
15,000
C.O.D
DEFLECTION
~IN.
.002
CALC
5-10-82
OPR
5-18-82
CHECK
APPD

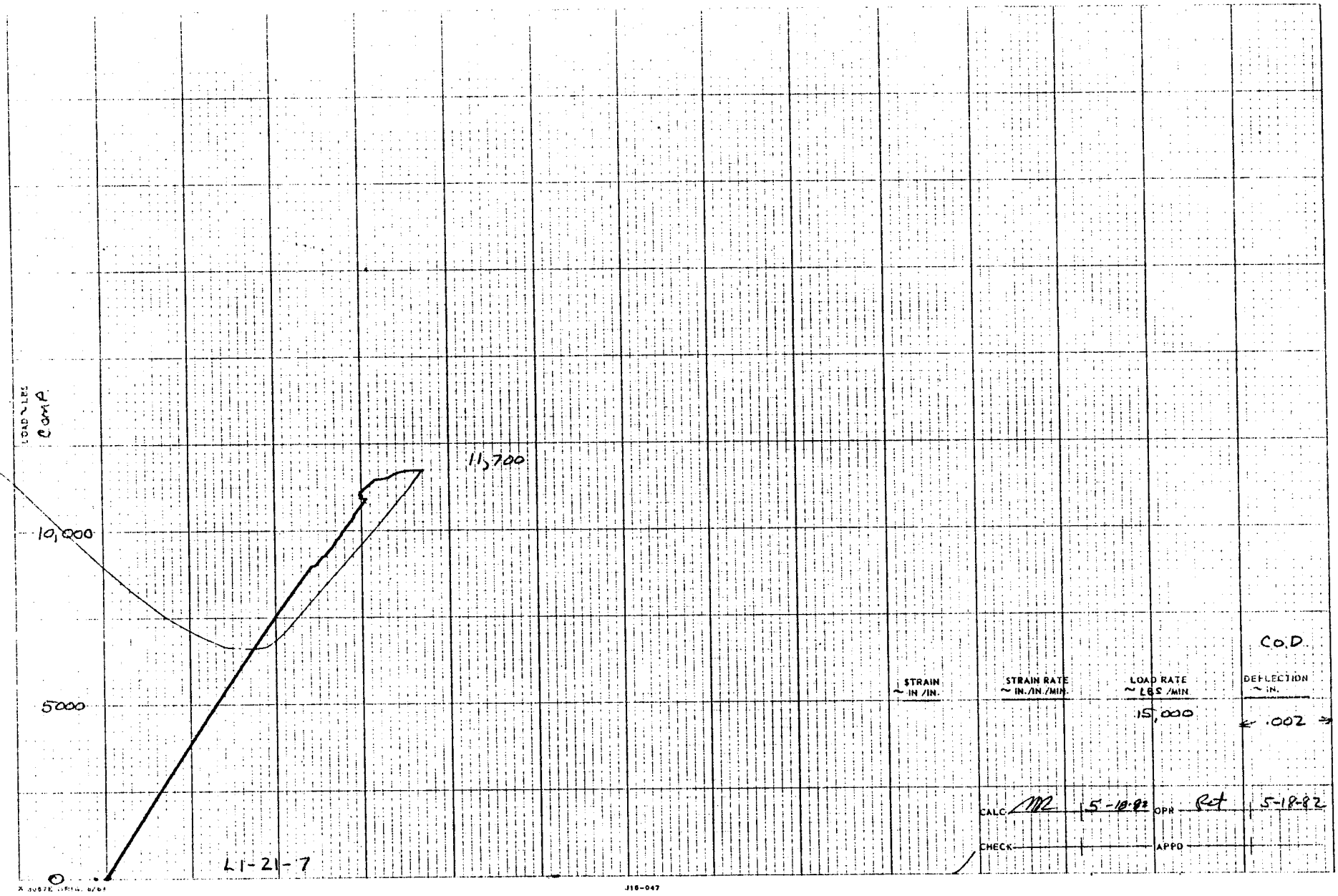
LOAD LBS
comp
11,700
10,000
5000
0
L1-21-7
~ STRAIN ~ IN /IN.
STRAIN RATE ~ IN./IN./MIN.
LOAD RATE ~ LBS /MIN
15,000
Co.D.
DEFLECTION ~ IN.
.002
CALC MM 5-18-92
OPR Ret 5-18-92
CHECK
APPD
J16-047

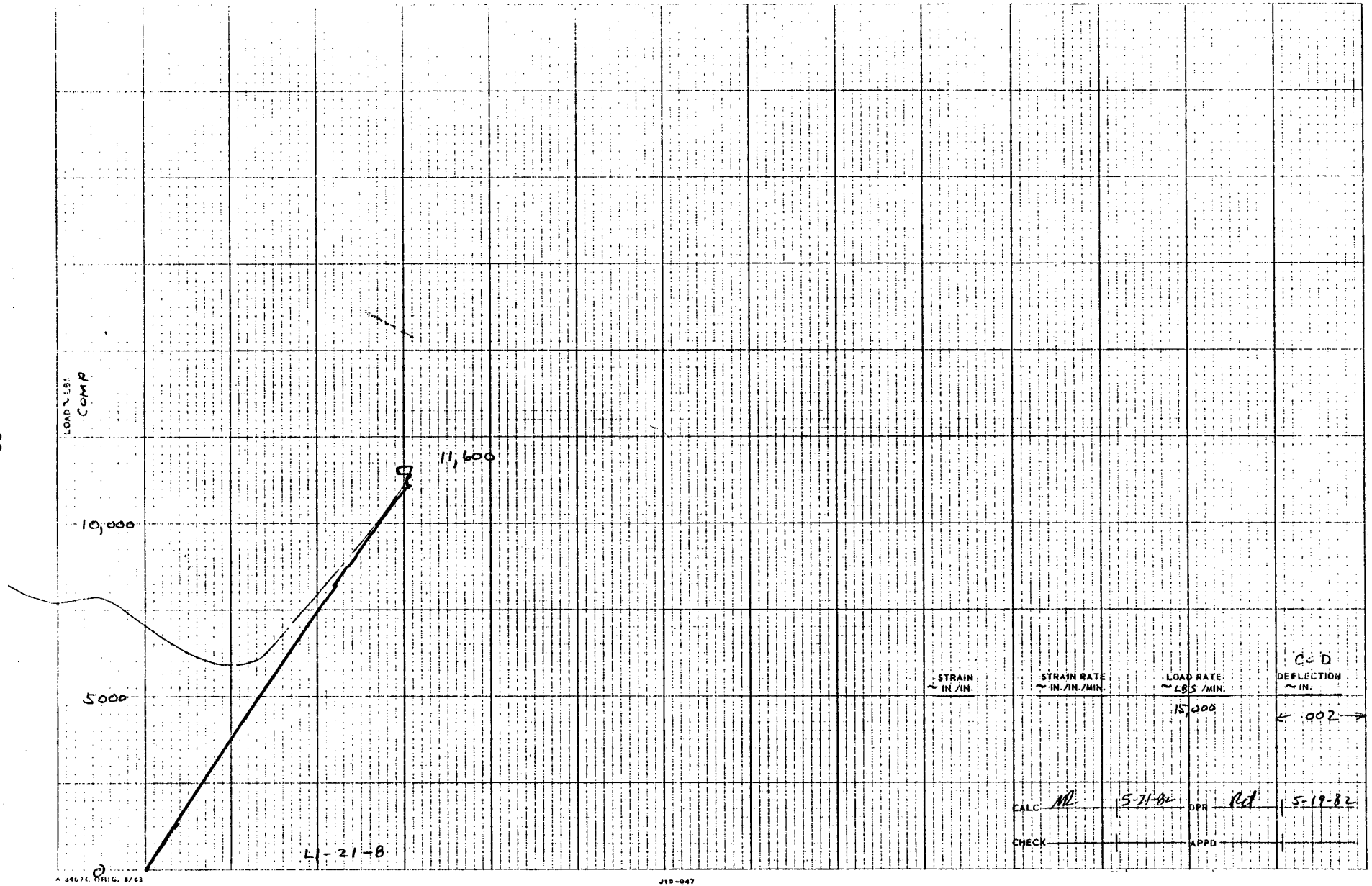
LOAD ~ LBS
COMP
11,600
10,000
5000
0
L-21-B
STRAIN ~ IN./IN.
STRAIN RATE ~ IN./IN./MIN.
LOAD RATE ~ LBS /MIN.
15,000
C-D DEFLECTION ~ IN.
.002
CALC MR 5-11-82
DPR RJ 5-19-82
CHECK
APPD

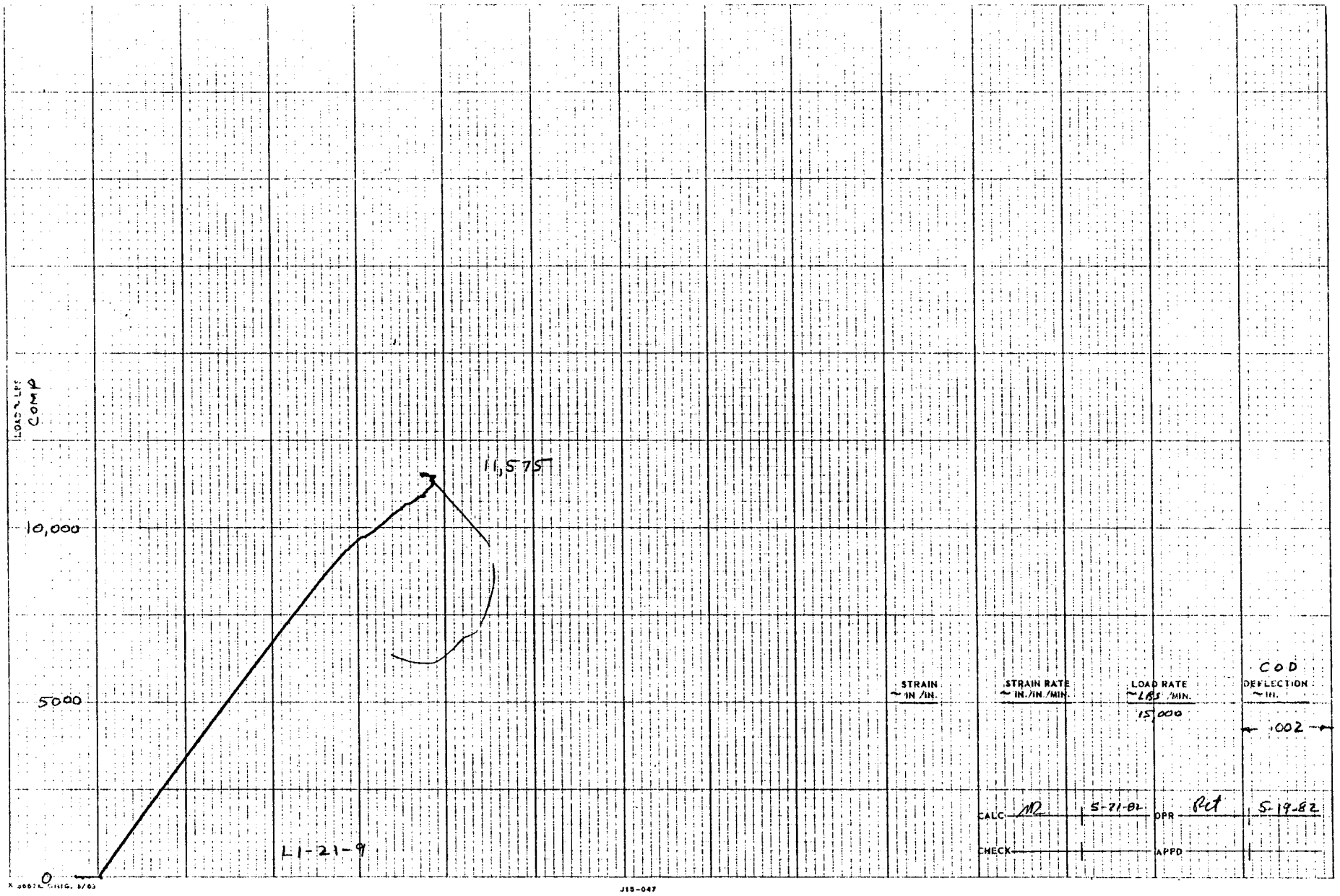
LOAD, LBS
COMP
11,575
10,000
5000
0
L1-21-9
STRAIN
~ IN /IN.
STRAIN RATE
~ IN./IN./MIN.
LOAD RATE
~LBS /MIN.
15,000
COD
DEFLECTION
~ IN.
.002
CALC
MR
5-21-82
DPR
Rct
5-19-82
CHECK
APPD
J15-047

06

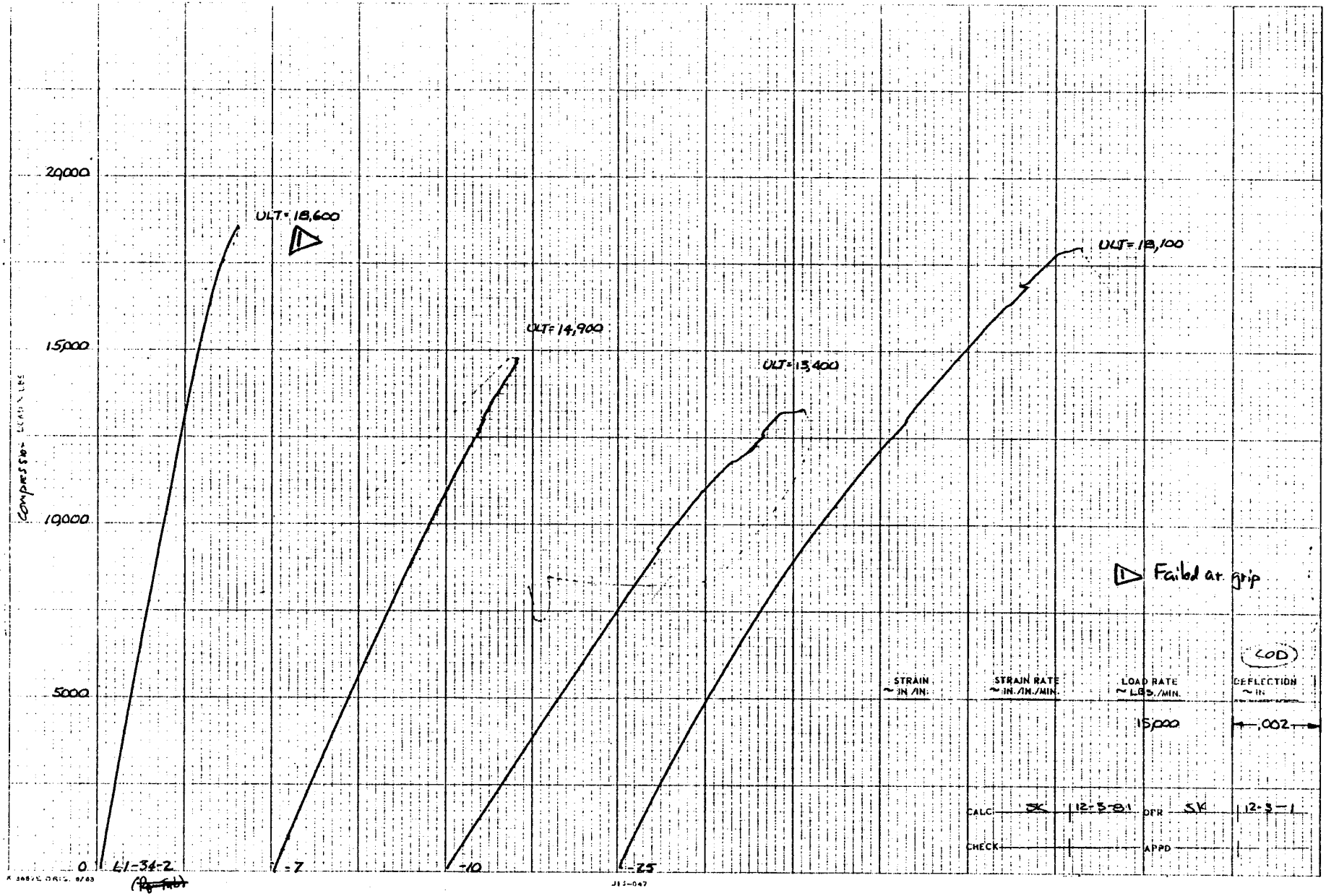
20000
15000
10000
5000
0
COMPRESSION - LBS.
ULT=18,600
ULT=14,900
ULT=13,400
ULT=18,100
Failed at grip
E1-34-2
-7
-10
-25
STRAIN ~ IN./IN.
STRAIN RATE ~ IN./IN./MIN.
LOAD RATE ~ LBS./MIN.
15000
DEFLECTION ~ IN.
.002
(OD)
CALC
CHECK
APPD
DFR
12-3-81
12-3-1

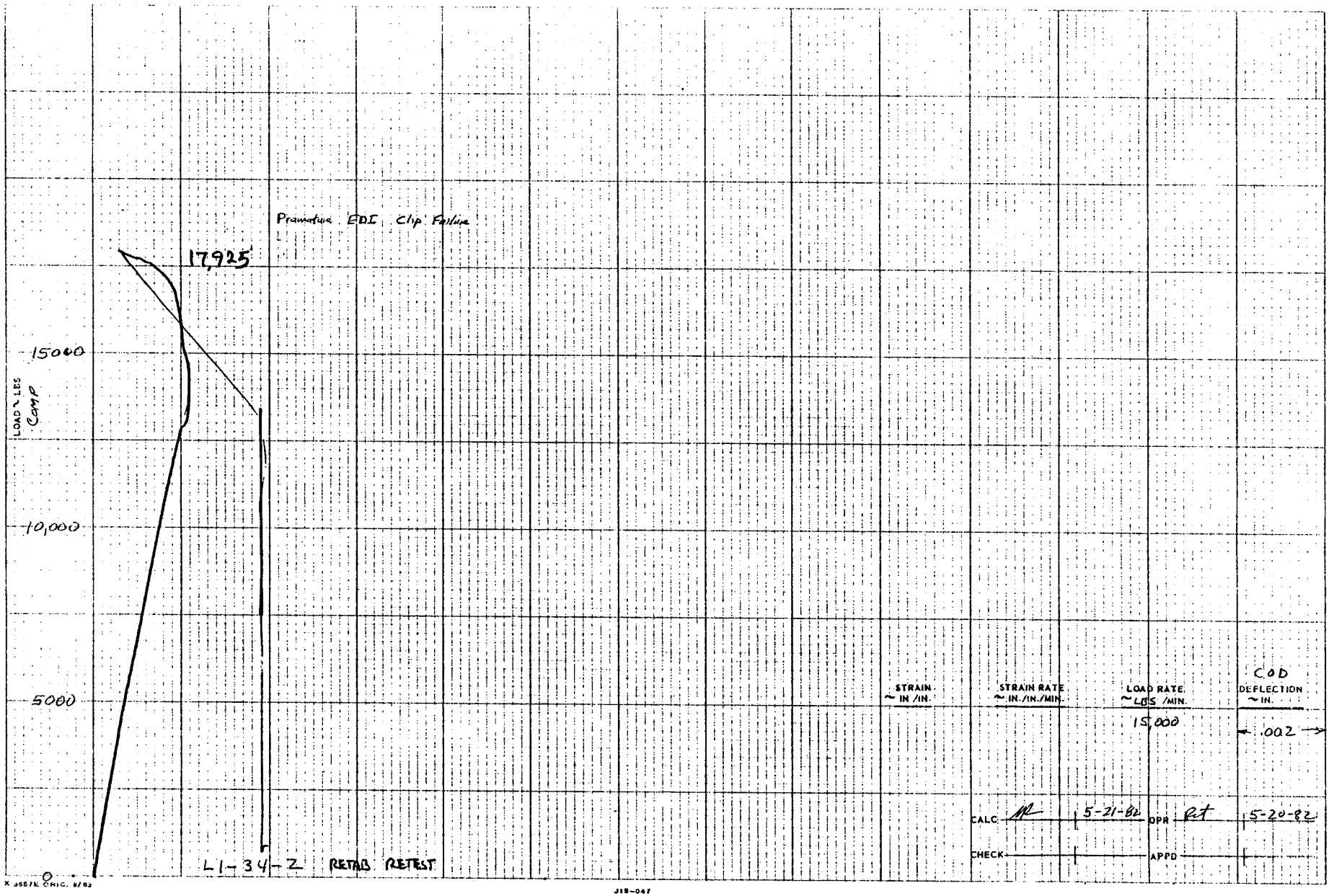

X 35571E CHIC. 8/83

J18-047

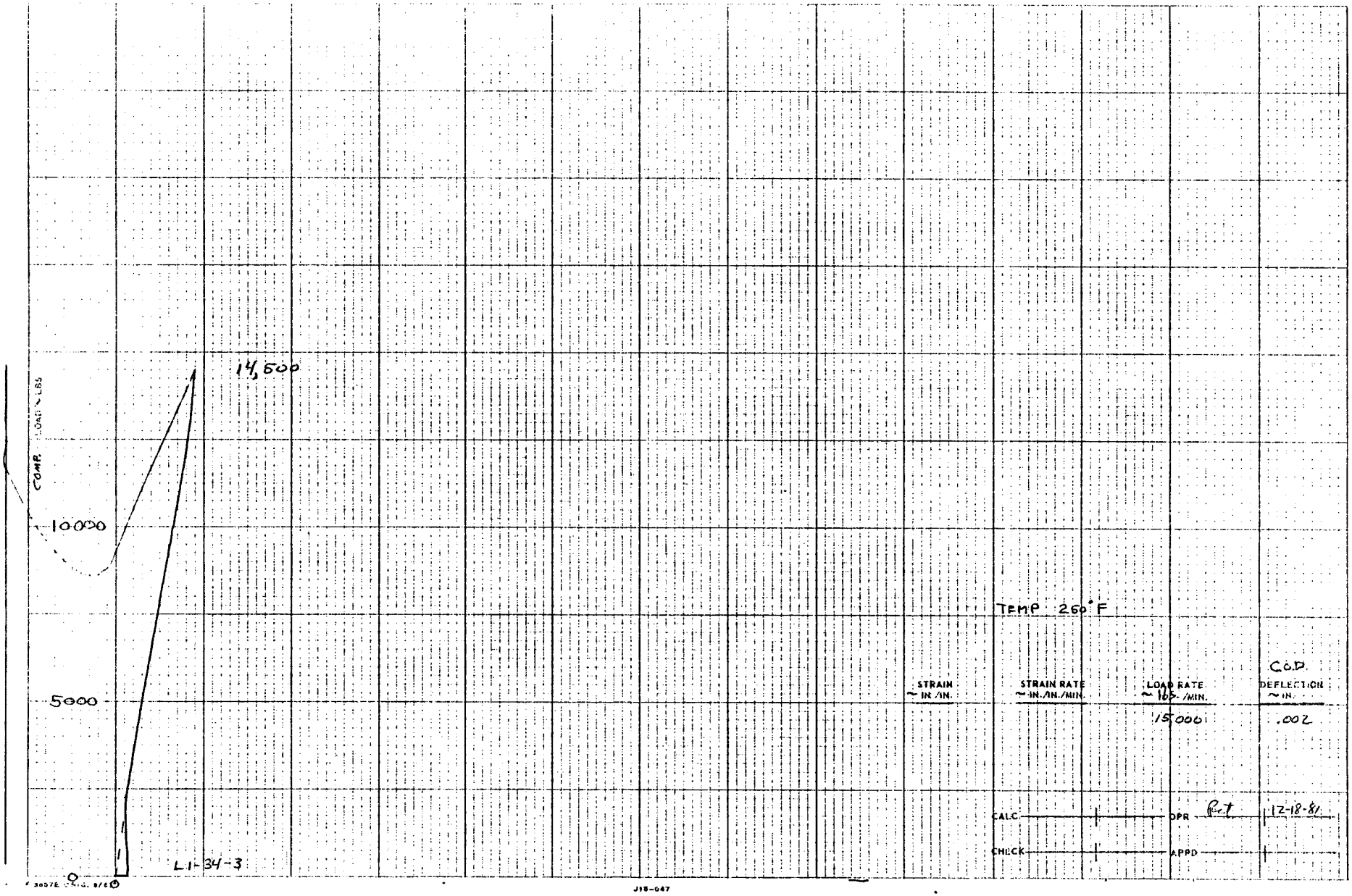
COMP. LOAD ~ LBS
14,500
10000
5000
0
L1-34-3
TEMP 260°F
STRAIN ~ IN./IN.
STRAIN RATE ~ IN./IN./MIN.
LOAD RATE ~ LBS./MIN.
15000
C.O.D. DEFLECTION ~ IN.
.002
CALC
OPR
R.T
12-18-81
CHECK
APPD
J18-047

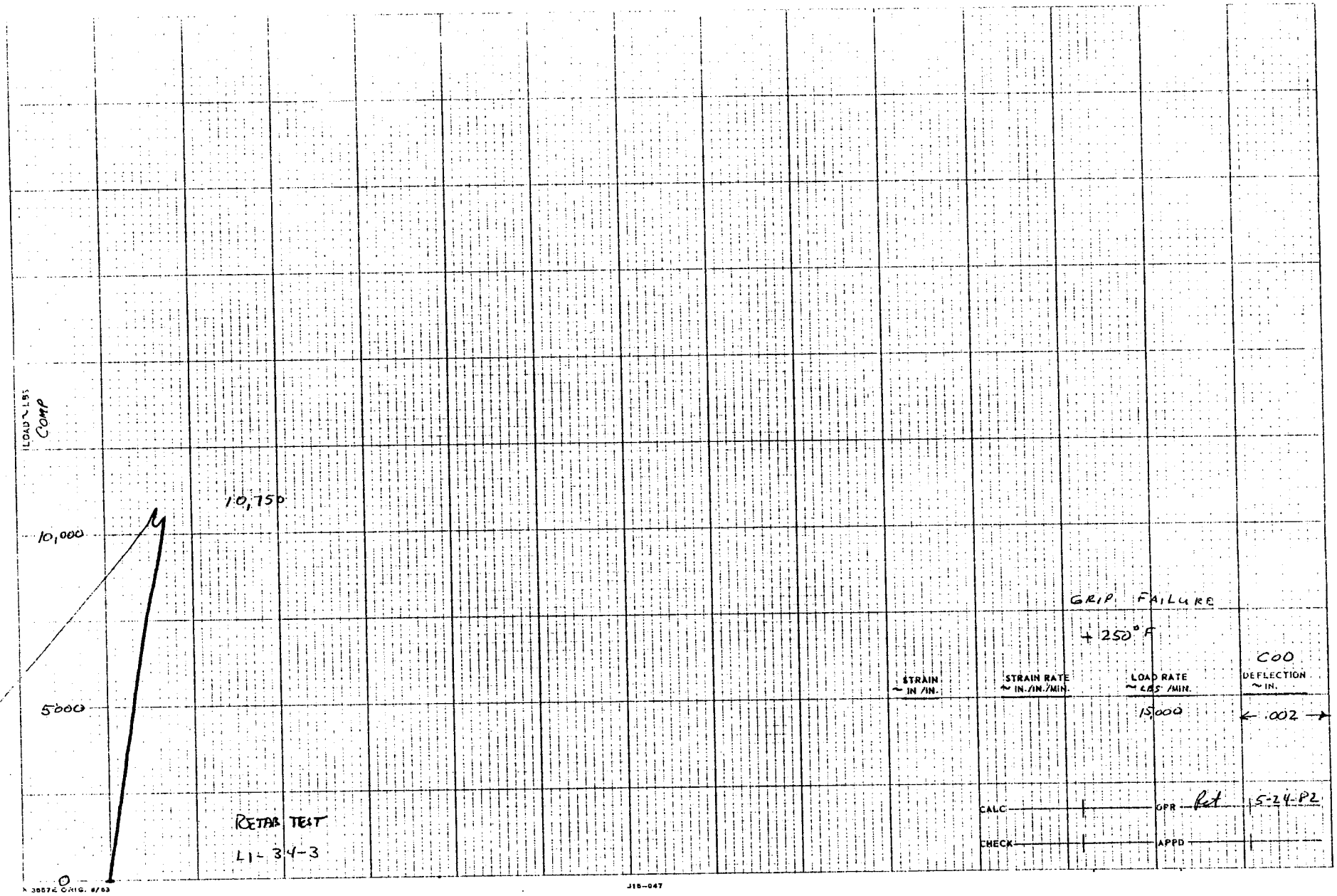
LOAD ~ LBS
COMP
10,750
10,000
5000
0
RETAB TEST
L1-3-4-3
GRIP FAILURE
+ 250°F
STRAIN ~ IN /IN.
STRAIN RATE ~ IN./IN./MIN.
LOAD RATE ~ LBS /MIN.
15,000
C00
DEFLECTION ~ IN.
.002
CALC
GPR
Ret
5-24-P2
CHECK
APPD
X 3857-E ORIG. 8/63
J15-047

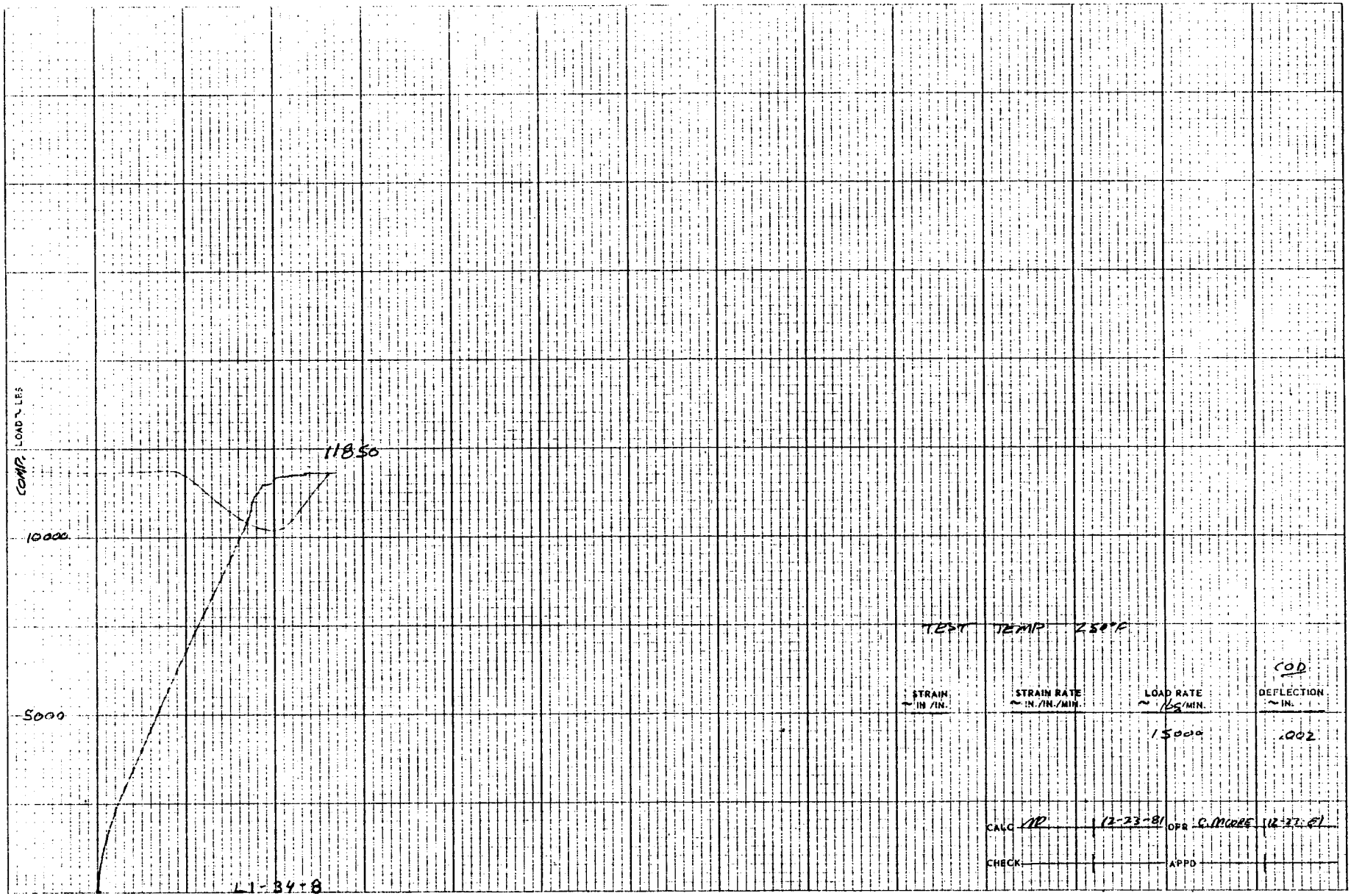

X 3657E ORIG. 8/68

J15-047

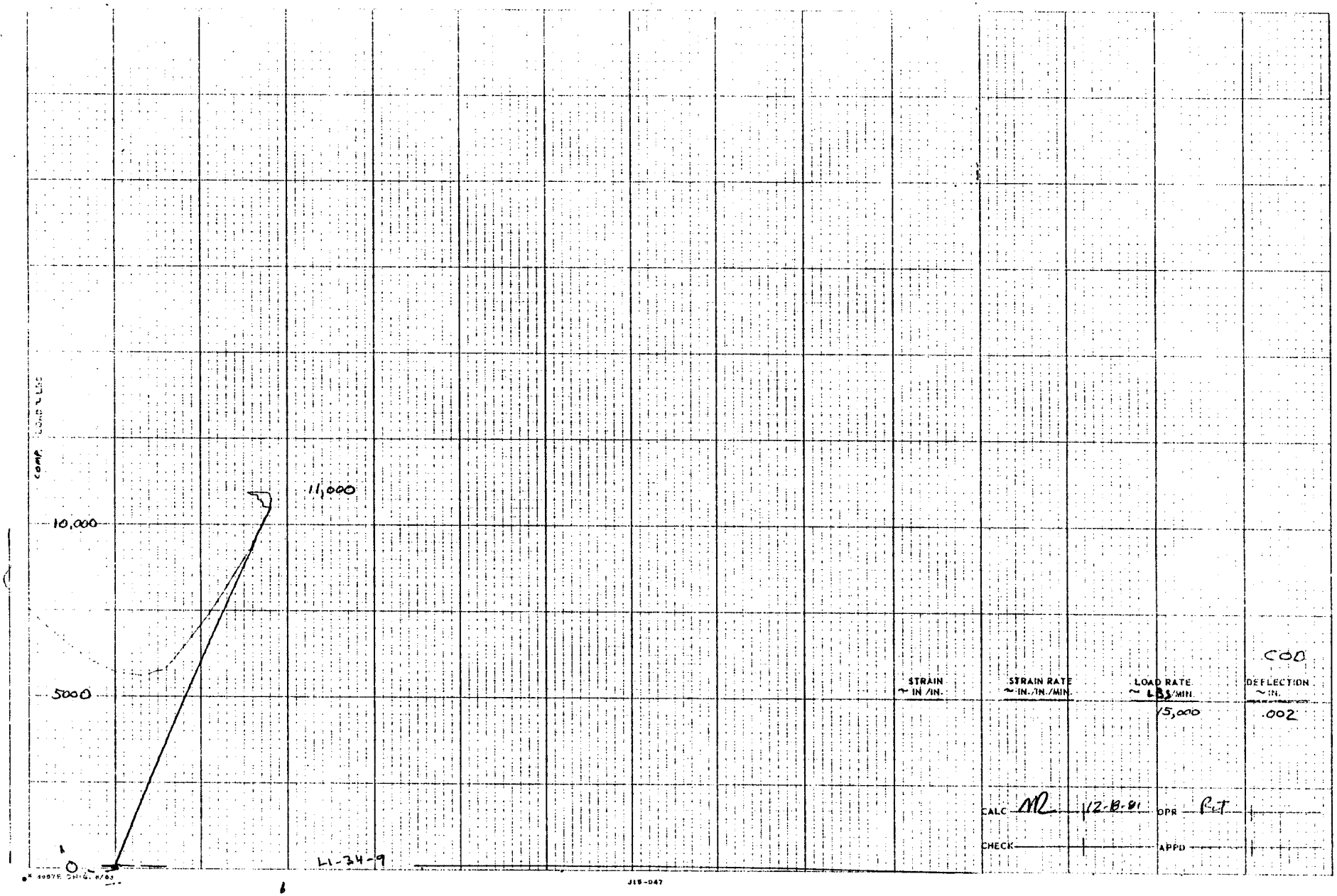
COMP. LOAD, LBS
11,000
10,000
5000
0
L1-34-9
STRAIN ~ IN /IN.
STRAIN RATE ~ IN./IN./MIN.
LOAD RATE ~ LBS/MIN.
15,000
DEFLECTION ~ IN.
.002
COD
CALC MR 12-18-81 OPR PT
CHECK APPD
J15-047

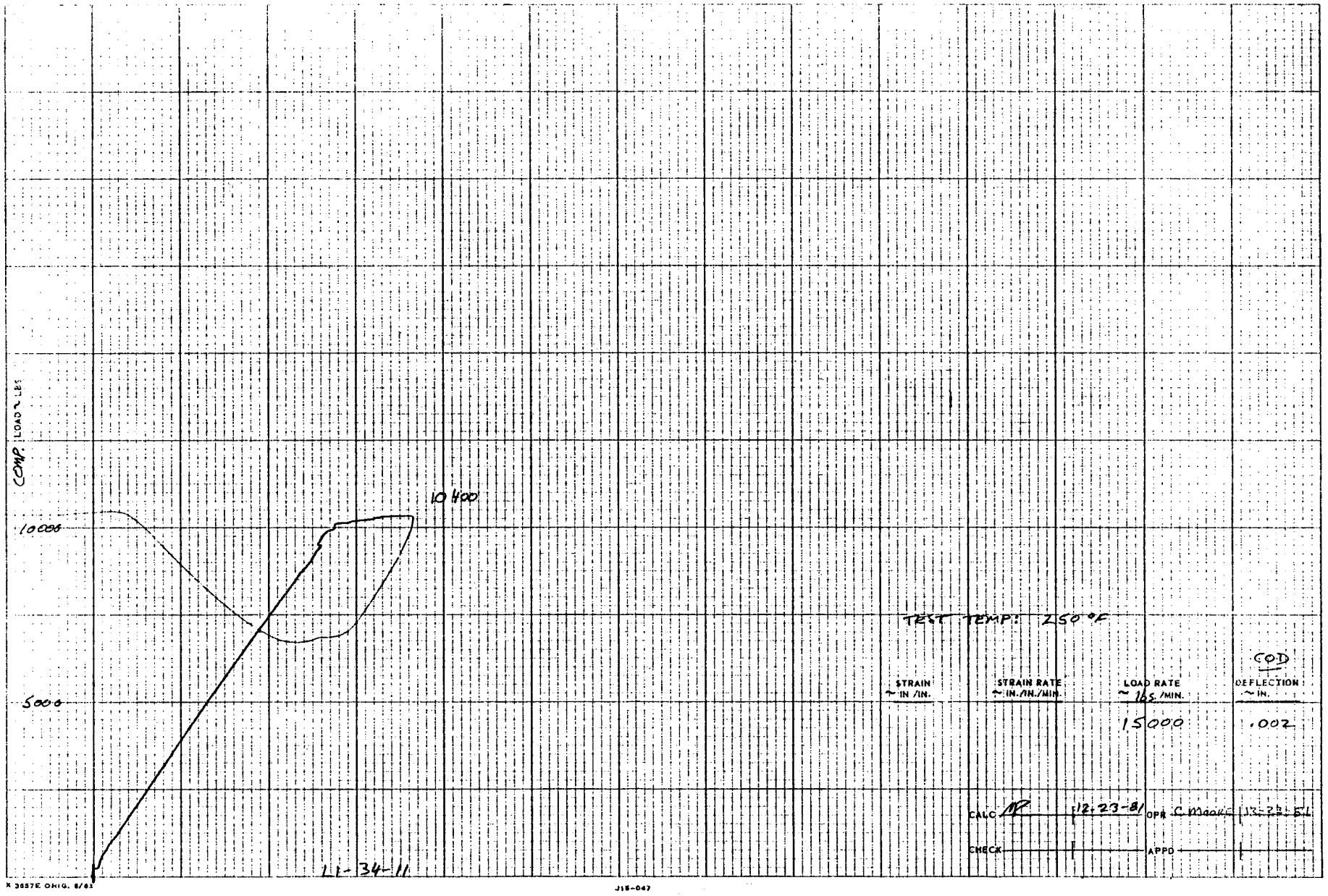

X 3857E ORIG. 8/63

J15-047

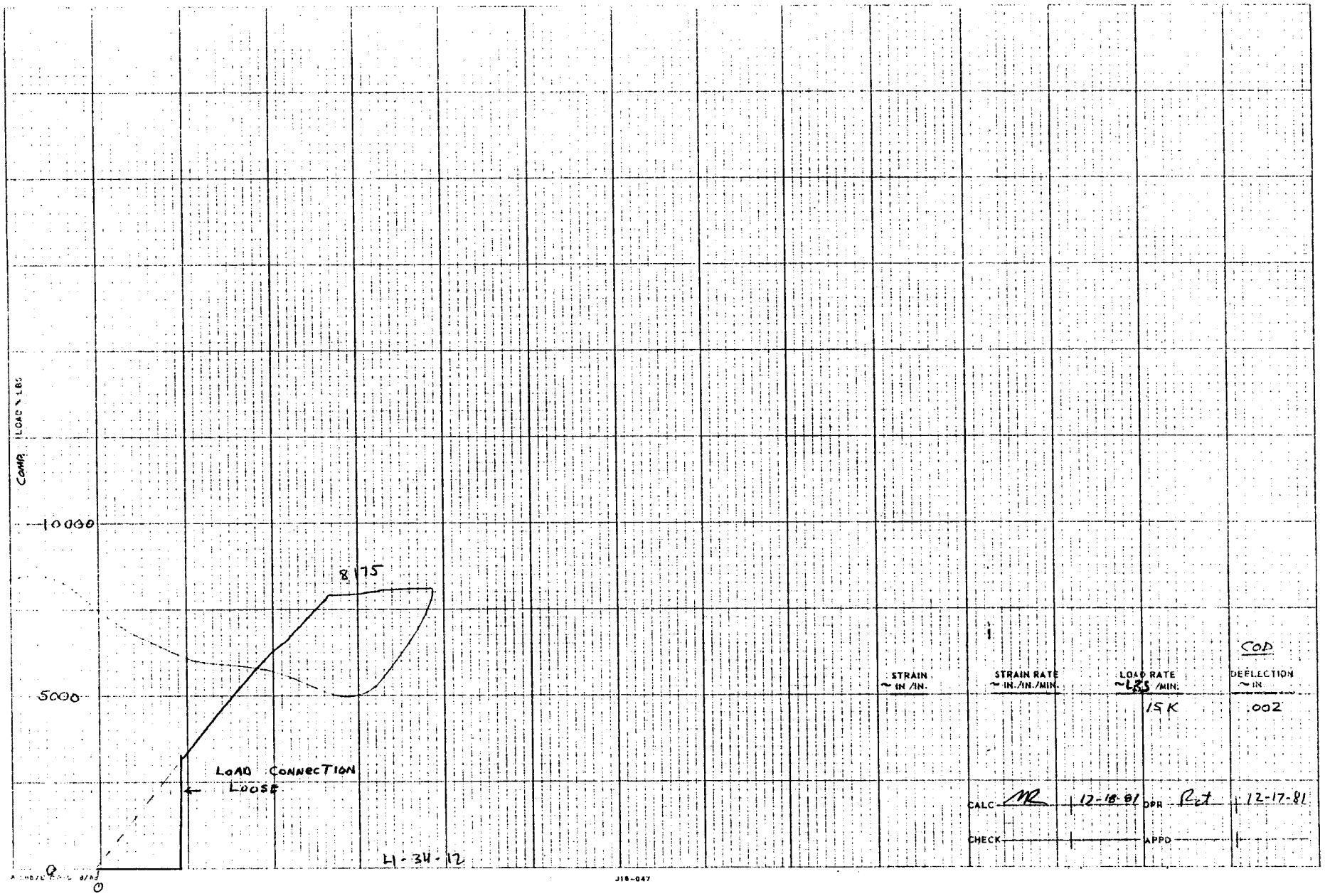

STRAIN ~ IN./IN.	STRAIN RATE ~ IN./IN./MIN.	LOAD RATE ~LBS /MIN.	COD DEFLECTION ~ IN
		15K	.002

CALC MR 12-18-81 DPR Rst 12-17-81

CHECK ——— APPD ———

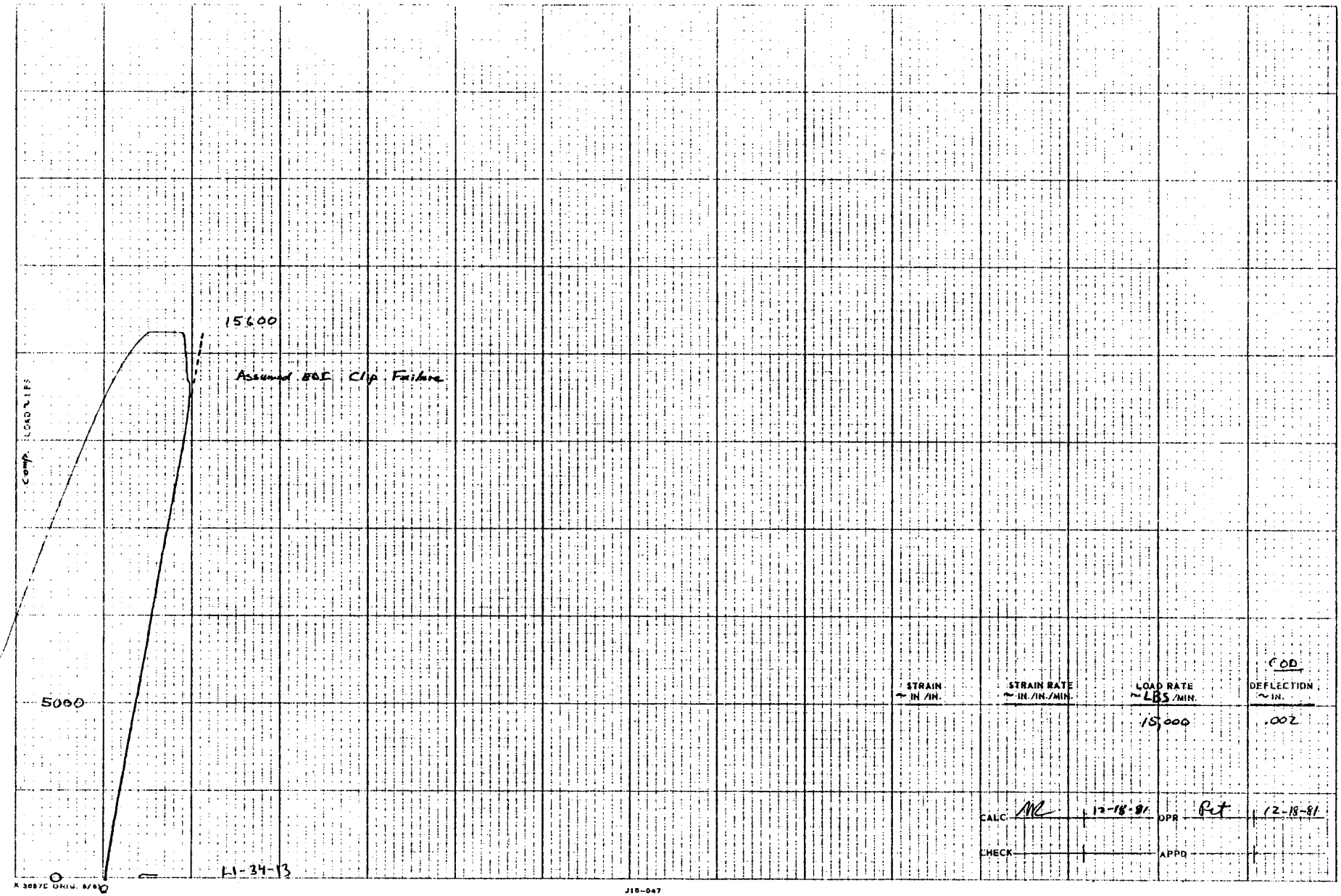

66

K 3087C ORIG. 8/81

J15-047

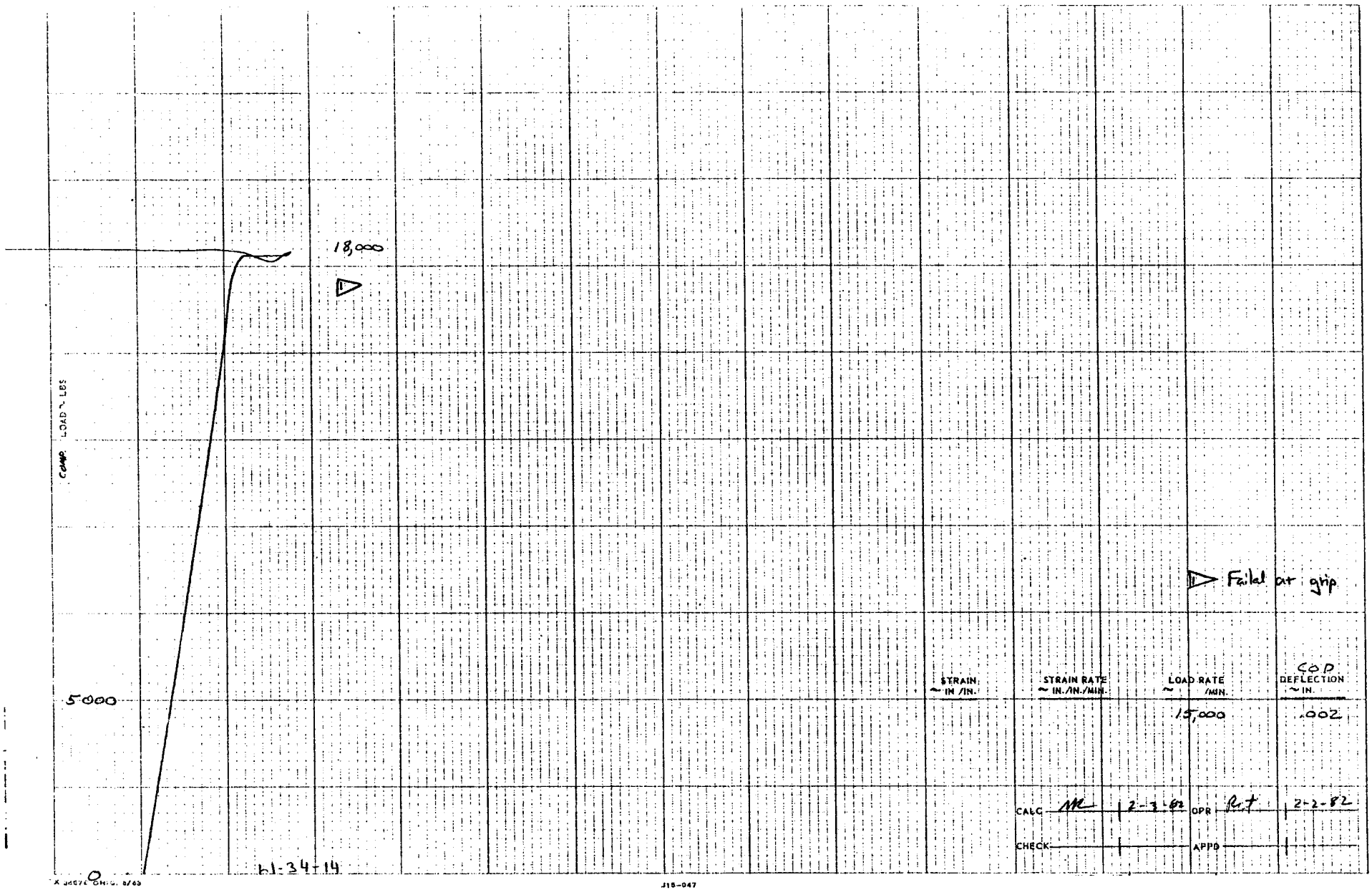
18,000
5000
0
COMP. LOAD ~ LBS
Failed at grip
~ STRAIN IN /IN.
STRAIN RATE ~ IN./IN./MIN.
LOAD RATE ~ /MIN.
15,000
COD DEFLECTION ~ IN.
.002
CALC
2-1-82
OPR
2-2-82
CHECK
APPD
61-34-14

100

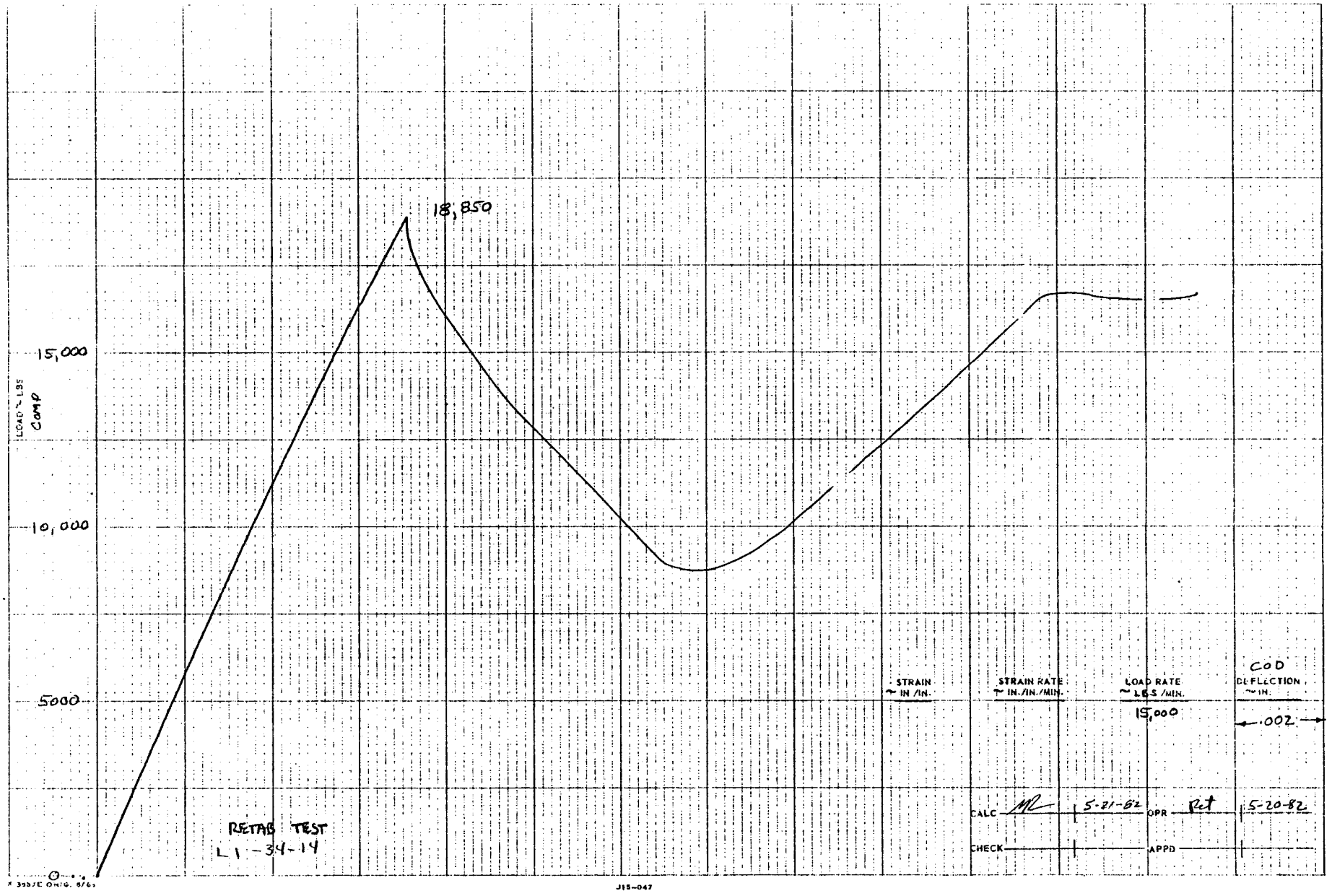
18,850
15,000
10,000
5000
0
LOAD ~ LBS
COMP
STRAIN ~ IN /IN.
STRAIN RATE ~ IN./IN./MIN.
LOAD RATE ~ LBS /MIN.
15,000
COD DEFLECTION ~ IN.
.002
RETAB TEST
L1-34-14
CALC MR 5-21-82
OPR Ret 5-20-82
CHECK
APPD
X 355/E ONIG. 8/65
J15-047

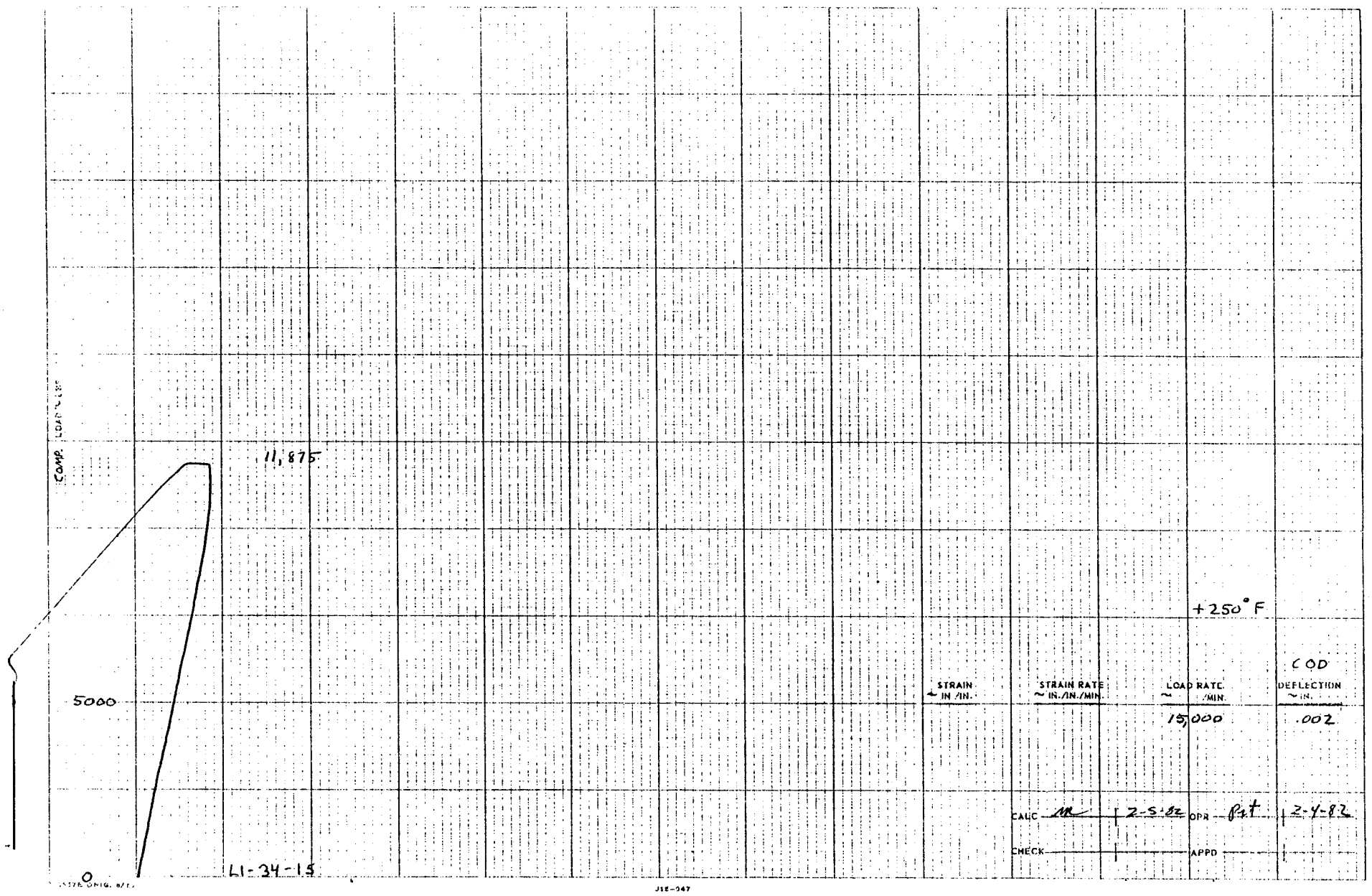
COMP. LOAD, LBS.
11,875
5000
0
L1-34-15
+250° F
STRAIN ~ IN./IN.
STRAIN RATE ~ IN./IN./MIN.
LOAD RATE ~ /MIN.
15,000
COD DEFLECTION ~ IN.
.002
CALC MR 2-5-82
OPR Pat 2-4-82
CHECK
APPD

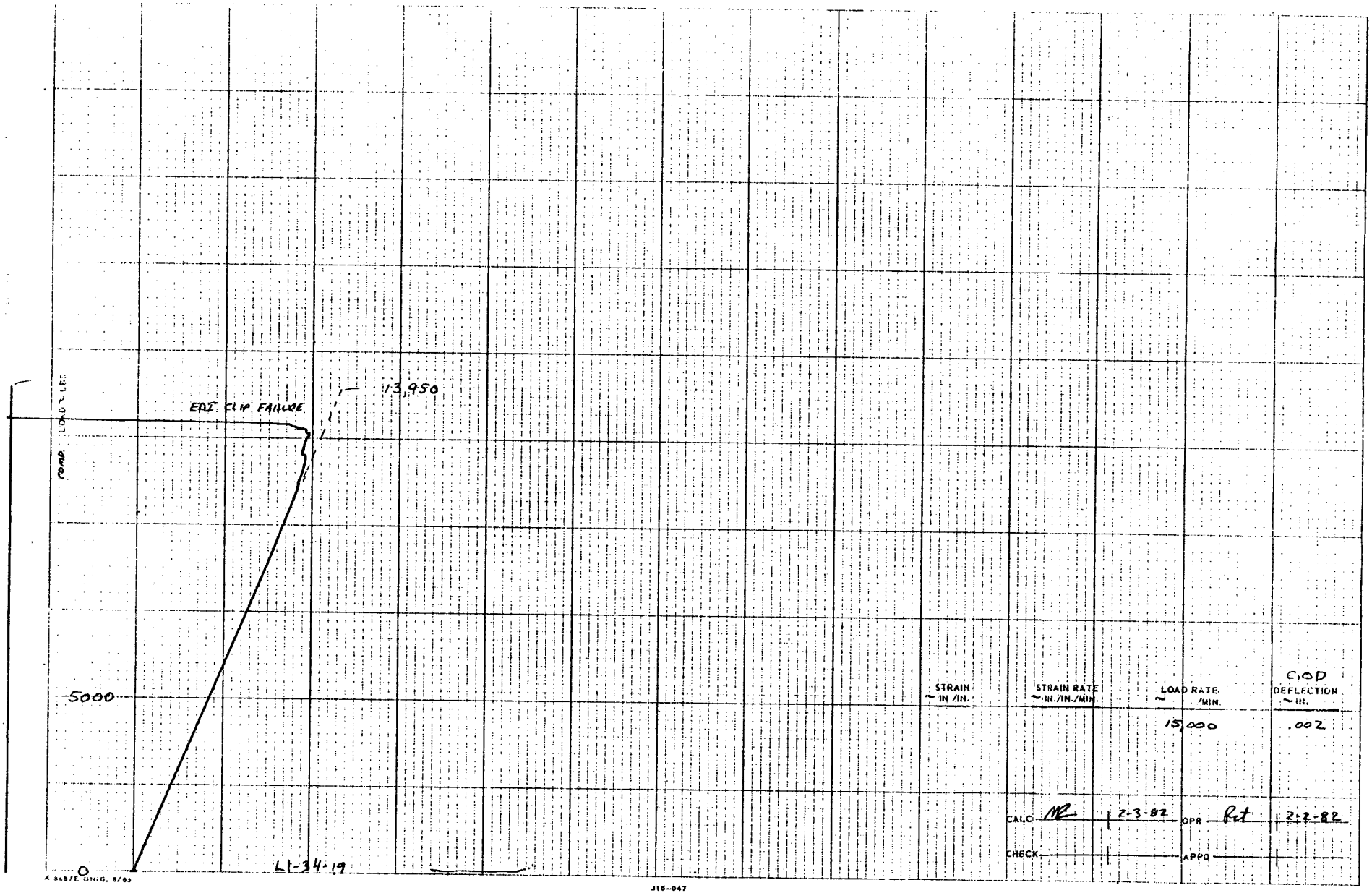

A SCOTE ORIG. 8/83

J15-047

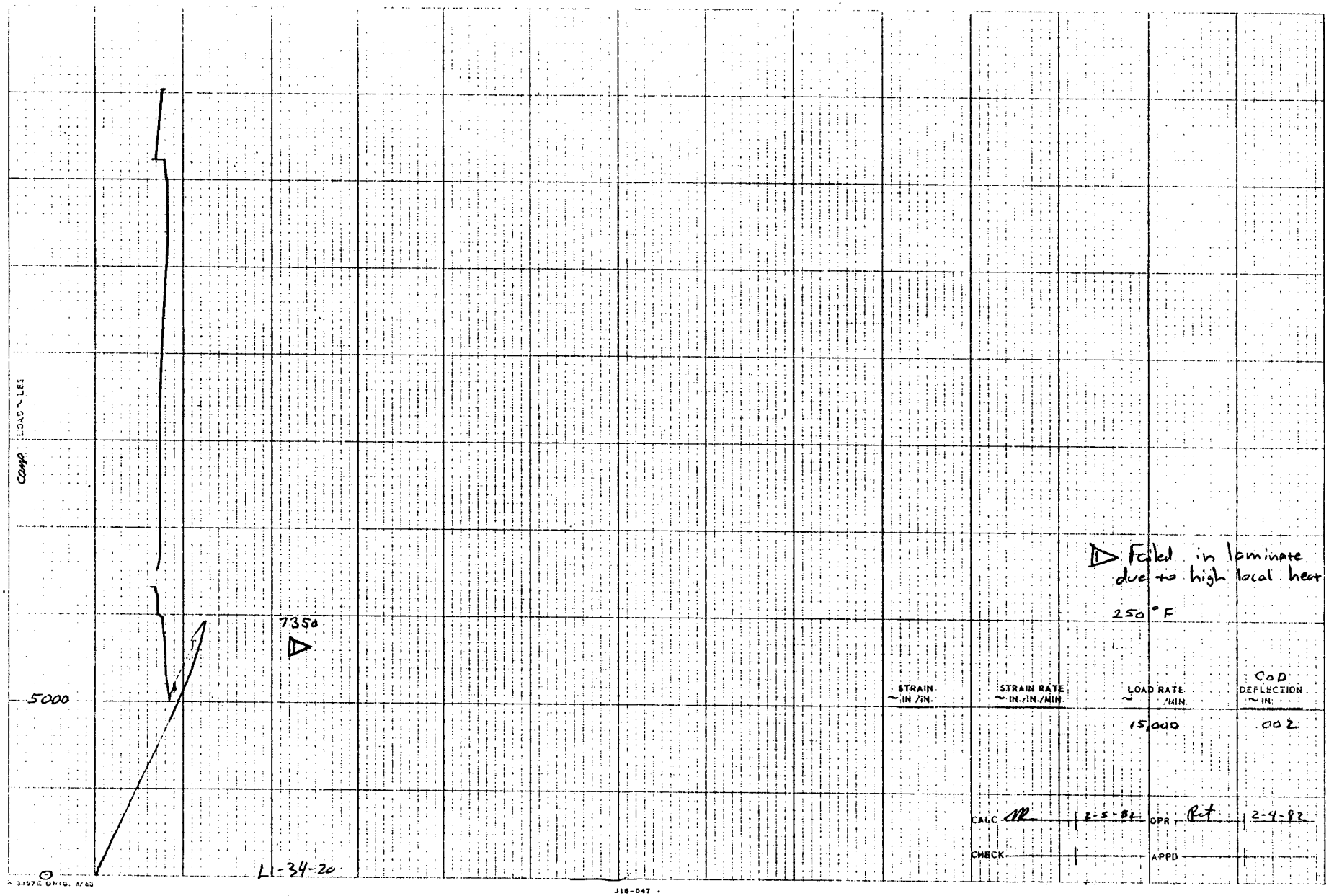
Comp LOADS - LBS
7350
5000
0
L1-34-20
Δ Failed in laminate due to high local heat
250 °F
STRAIN ~ IN /IN.
STRAIN RATE ~ IN./IN./MIN.
LOAD RATE ~ /MIN.
15,000
CoD DEFLECTION ~ IN.
.002
CALC
2-5-82
OPR
2-4-82
CHECK
APPD

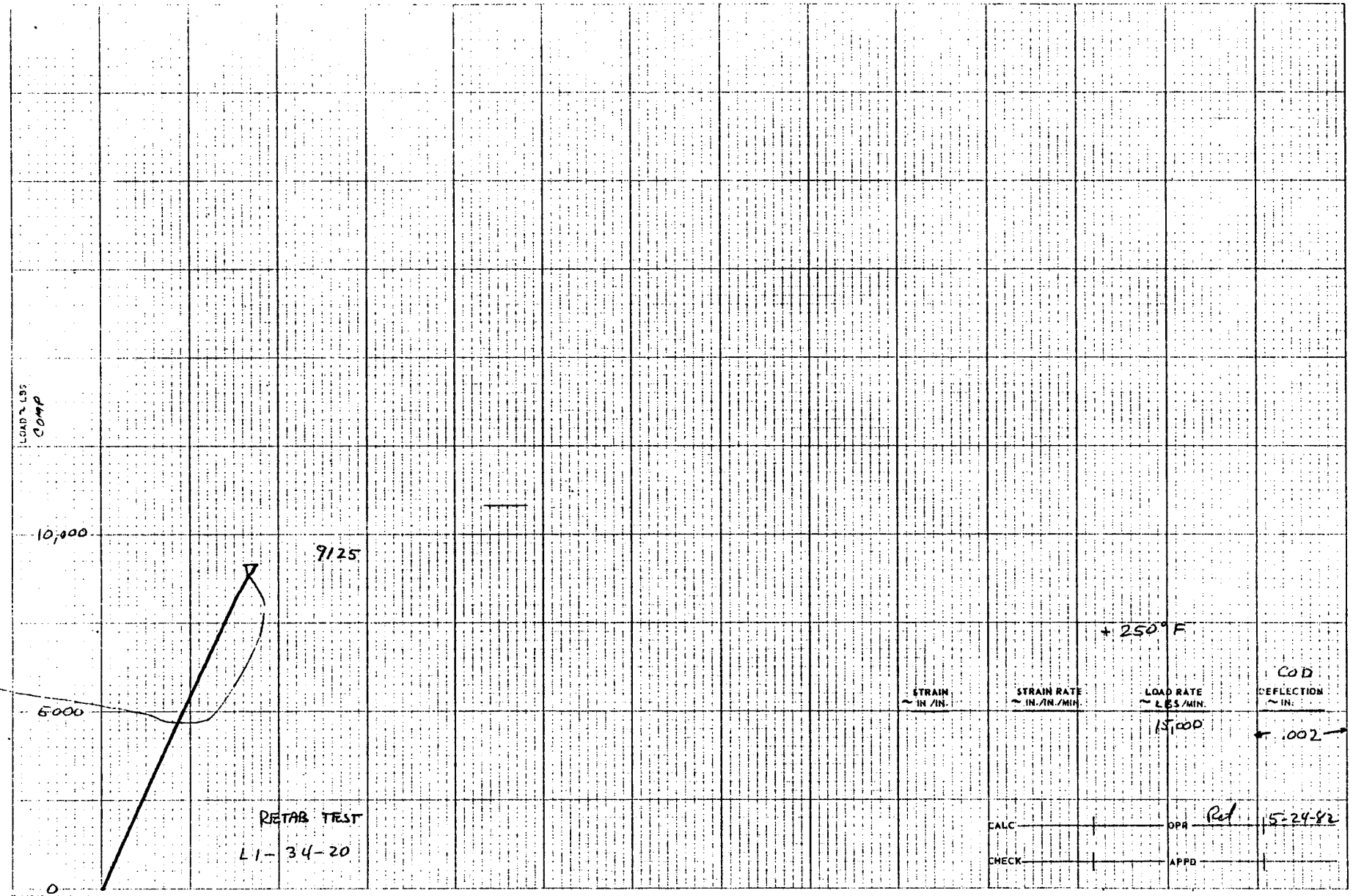
LOAD ~ LBS
Comp
10,000
9125
6000
0
+250° F
STRAIN ~ IN /IN.
STRAIN RATE ~ IN./IN./MIN.
LOAD RATE ~ LBS/MIN.
15000
COD DEFLECTION ~ IN.
.002
RETAB TEST
L1-34-20
CALC
OPR
Rel
5-24-82
CHECK
APPD
X 366/E ORIG. 6/83
J18-047

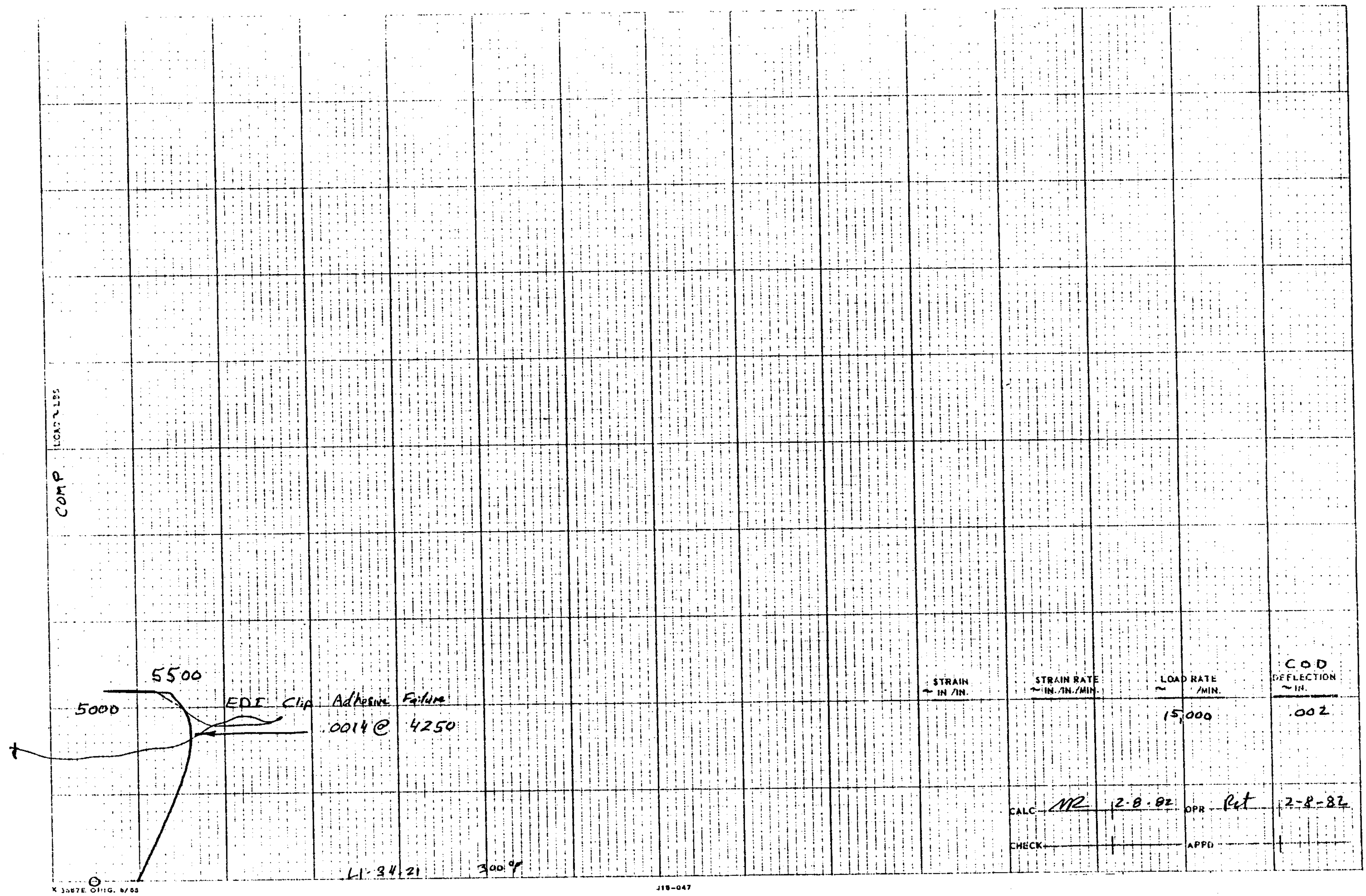
COMP
LOAD ~ LBS
5500
5000
EDI Clip Adhesive Failure
.0014 @ 4250
L1-34-21
300 °F
STRAIN ~ IN./IN.
STRAIN RATE ~ IN./IN./MIN.
LOAD RATE ~ /MIN.
15,000
COD DEFLECTION ~ IN.
.002
CALC
2-8-82
OPR
2-8-82
CHECK
APPD
X 3587E ORIG. 6/65
J18-047

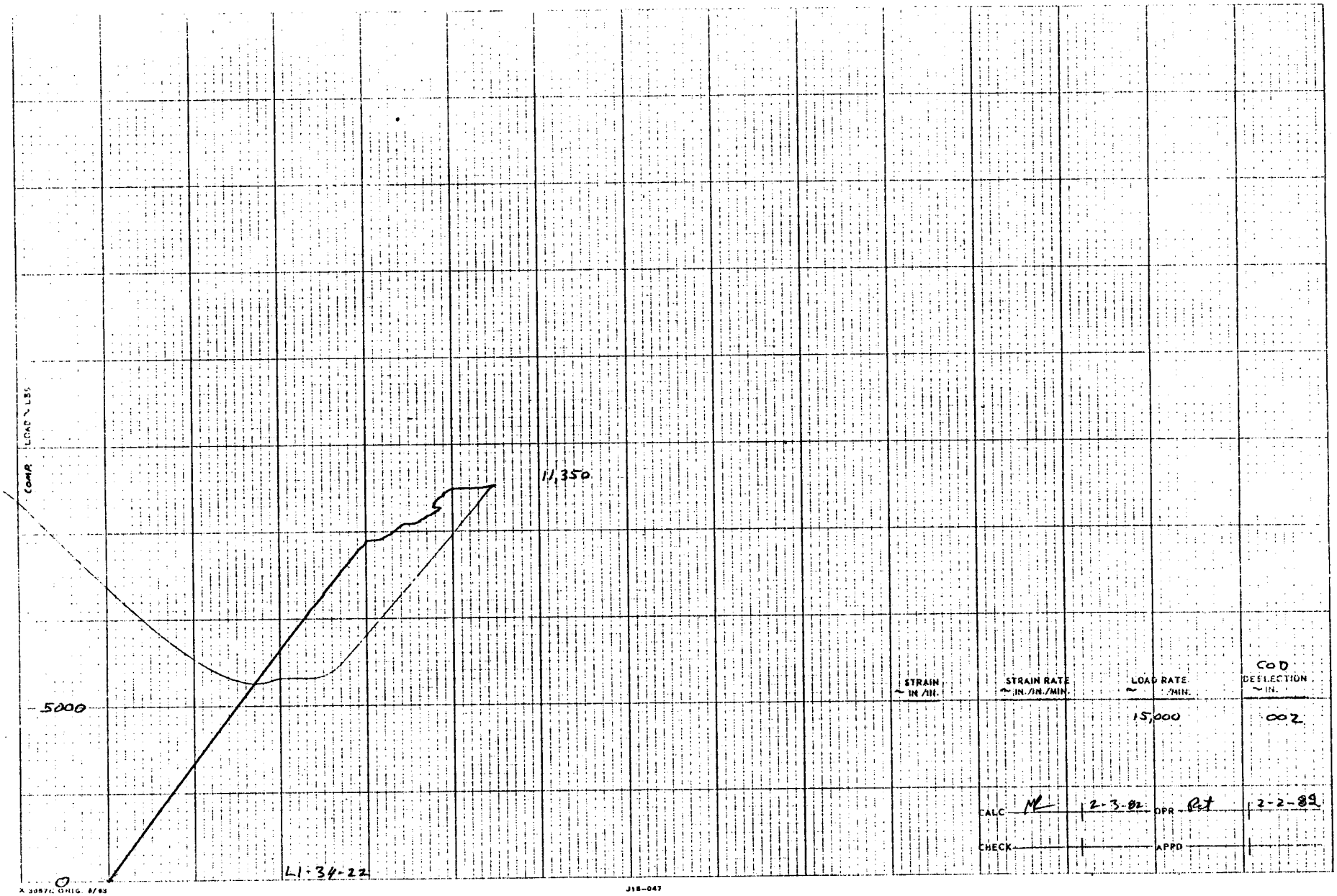
LOAD ~ LBS
COMP
11,350
5000
0
L1-34-22
STRAIN ~ IN./IN.
STRAIN RATE ~ IN./IN./MIN.
LOAD RATE ~ /MIN.
15,000
COD DEFLECTION ~ IN.
.002
CALC M 2-3-82 DPR Pst 2-2-82
CHECK APPD
X 3057L ORIG. 8/82
J18-047

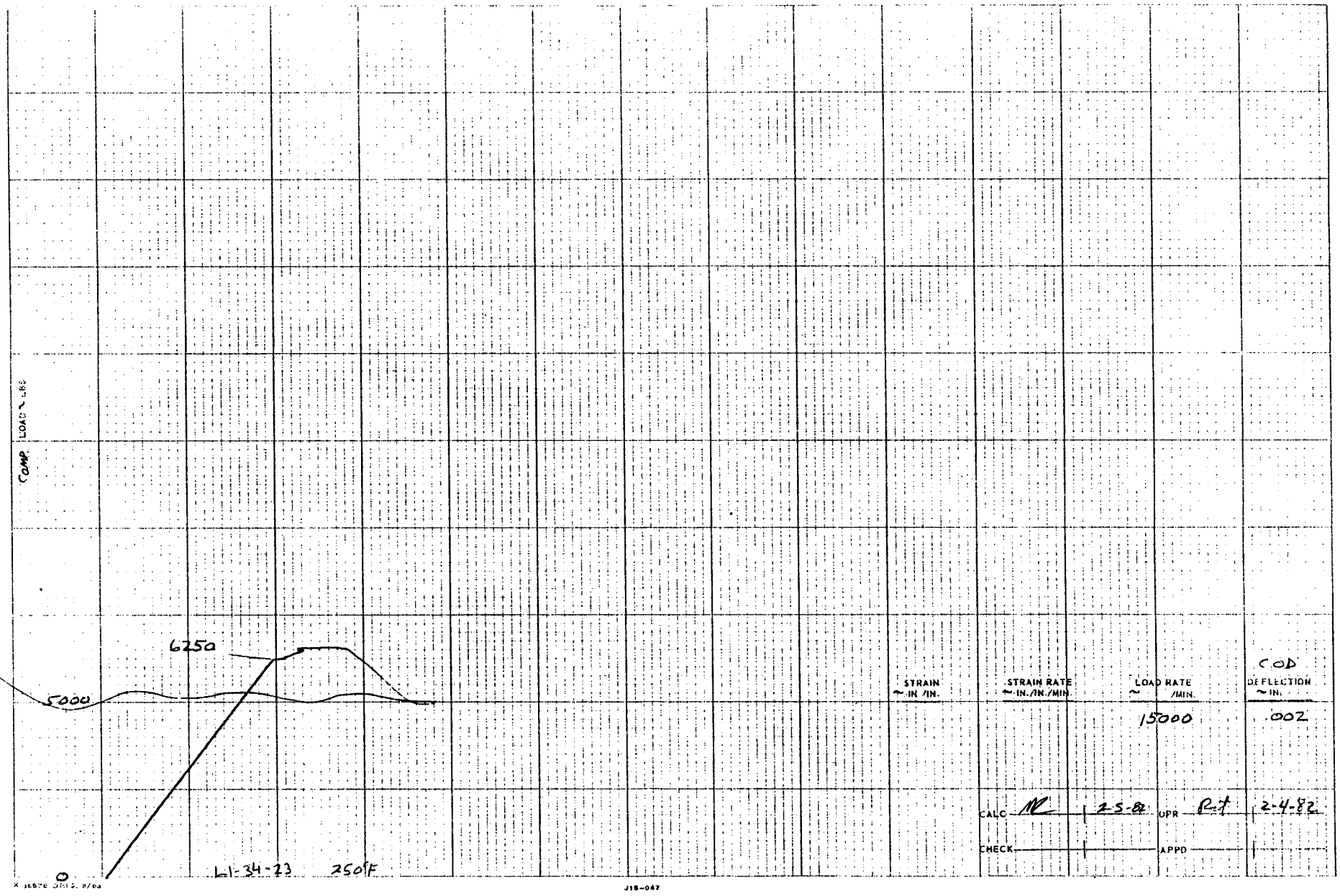
COMP. LOAD ~ LBS
5000
6250
0
L-34-73 250°F
STRAIN ~ IN./IN.
STRAIN RATE ~ IN./IN./MIN.
LOAD RATE ~ /MIN.
15000
COD DEFLECTION ~ IN.
.002
CALC NC 2-5-82
CHECK
APPD
UPR R-T 2-4-82

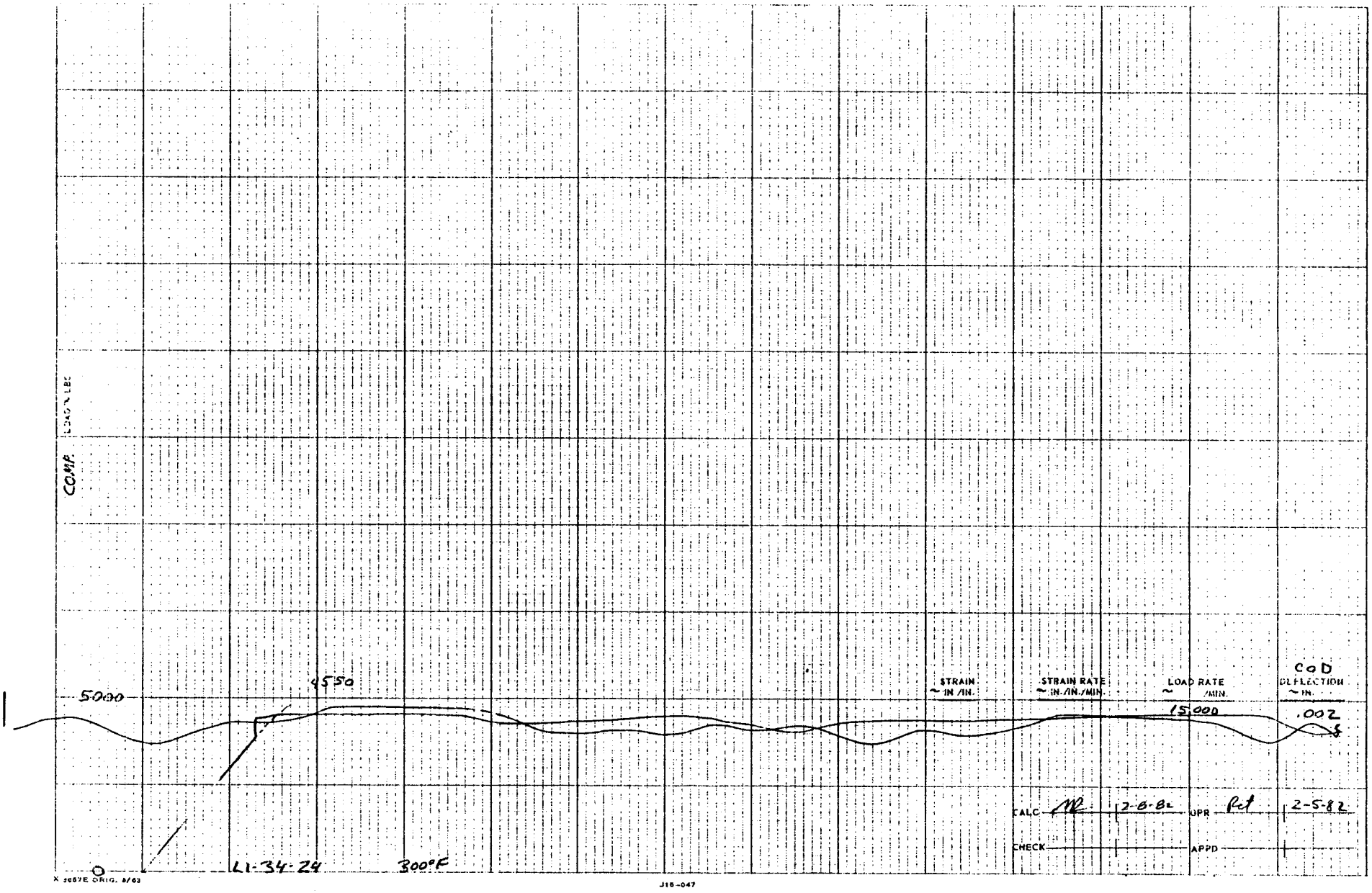
COMP.
5000
4550
STRAIN ~ IN /IN.
STRAIN RATE ~ IN./IN./MIN.
LOAD RATE ~ /MIN.
15,000
COD DEFLECTION ~ IN.
.002
CALC
2-8-82
APPD
CHECK
APPD
2-5-82
L1-34-24
300°F
X 2657E ORIG. 8/63
J18-047

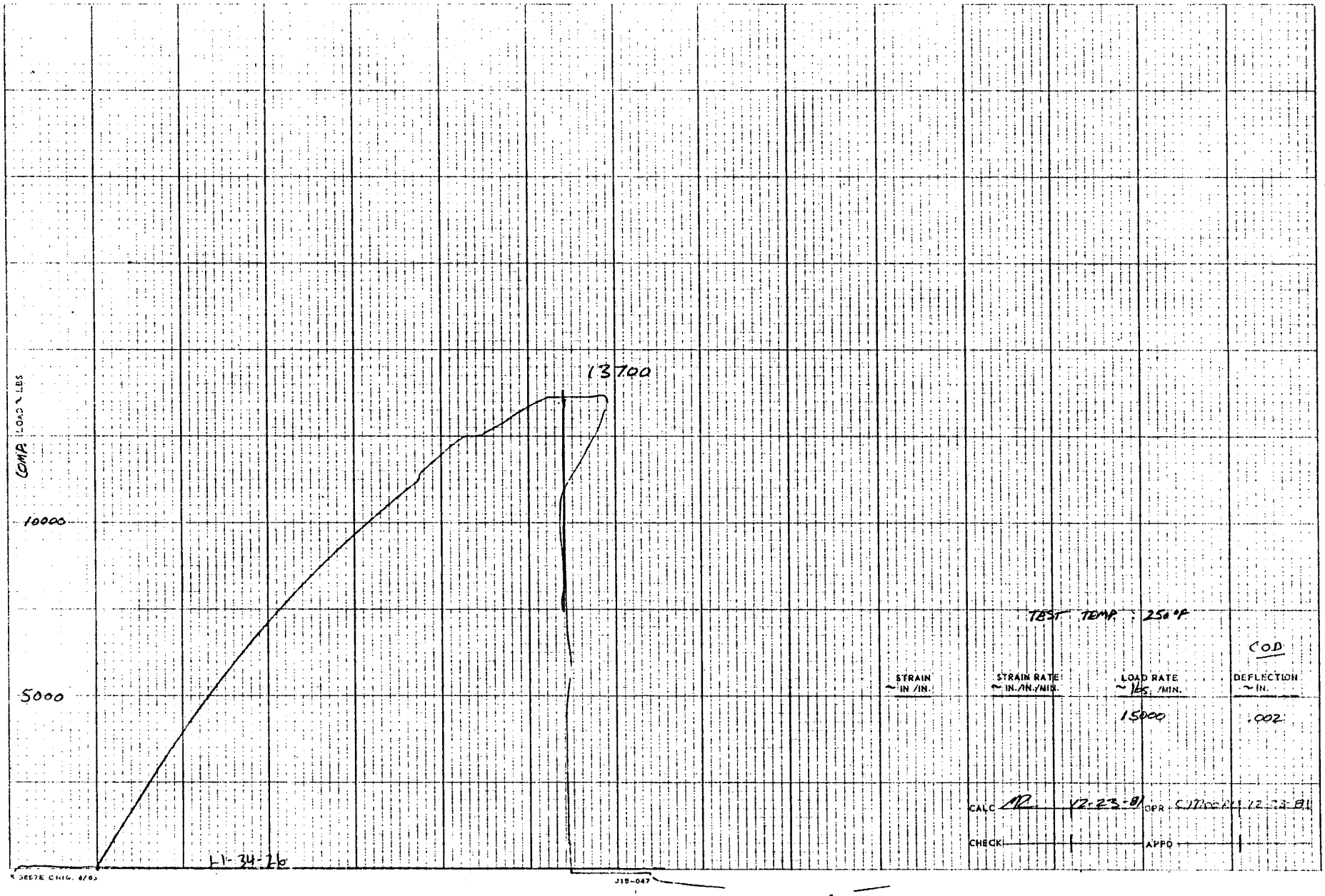
COMP LOAD ~ LBS
10000
5000
13700
TEST TEMP : 250°F
COD
STRAIN ~ IN /IN.
STRAIN RATE ~ IN./IN./MIN.
LOAD RATE ~ LBS. /MIN.
15000
DEFLECTION ~ IN.
.002
CALC 12-23-81
CHECK
APPD
L1-34-26
J15-047

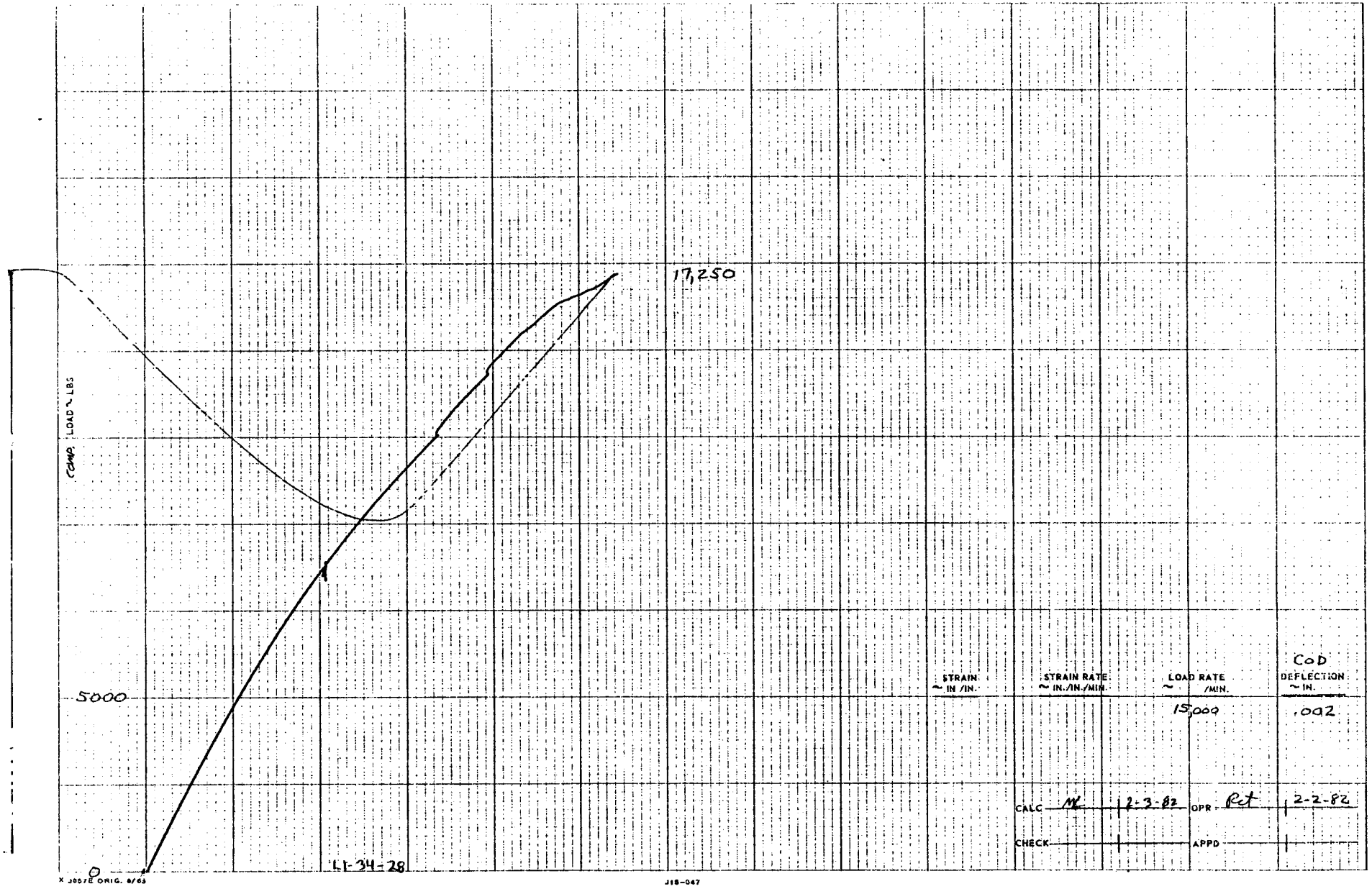
17,250
5000
0
LOAD ~ LBS
STRAIN ~ IN /IN.
STRAIN RATE ~ IN./IN./MIN.
LOAD RATE ~ /MIN.
15,000
CoD DEFLECTION ~ IN.
.002
CALC M 2-3-82
OPR Pat 2-2-82
CHECK
APPD
LL-34-28
X JOSTE ORIG. 8/63
J18-047

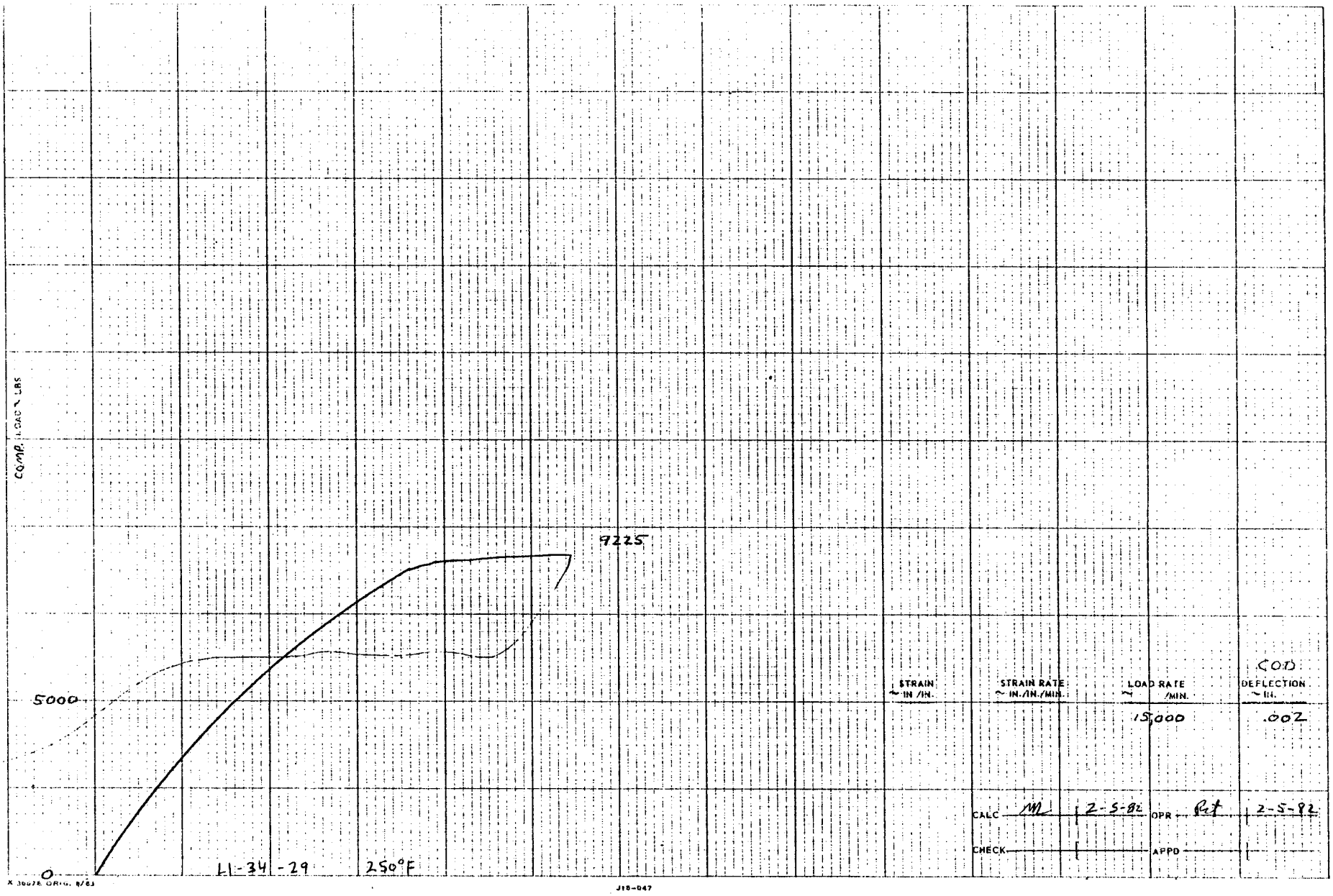
COMP. LOAD ~ LBS
9225
5000
0
LI-34-29
250°F
STRAIN ~ IN/IN.
STRAIN RATE ~ IN./IN./MIN.
LOAD RATE ~ /MIN.
15,000
COD DEFLECTION ~ IN.
.002
CALC M 2-5-82
OPR RJT 2-5-82
CHECK
APPD
X 30078 ORIG. 8/83
J18-047

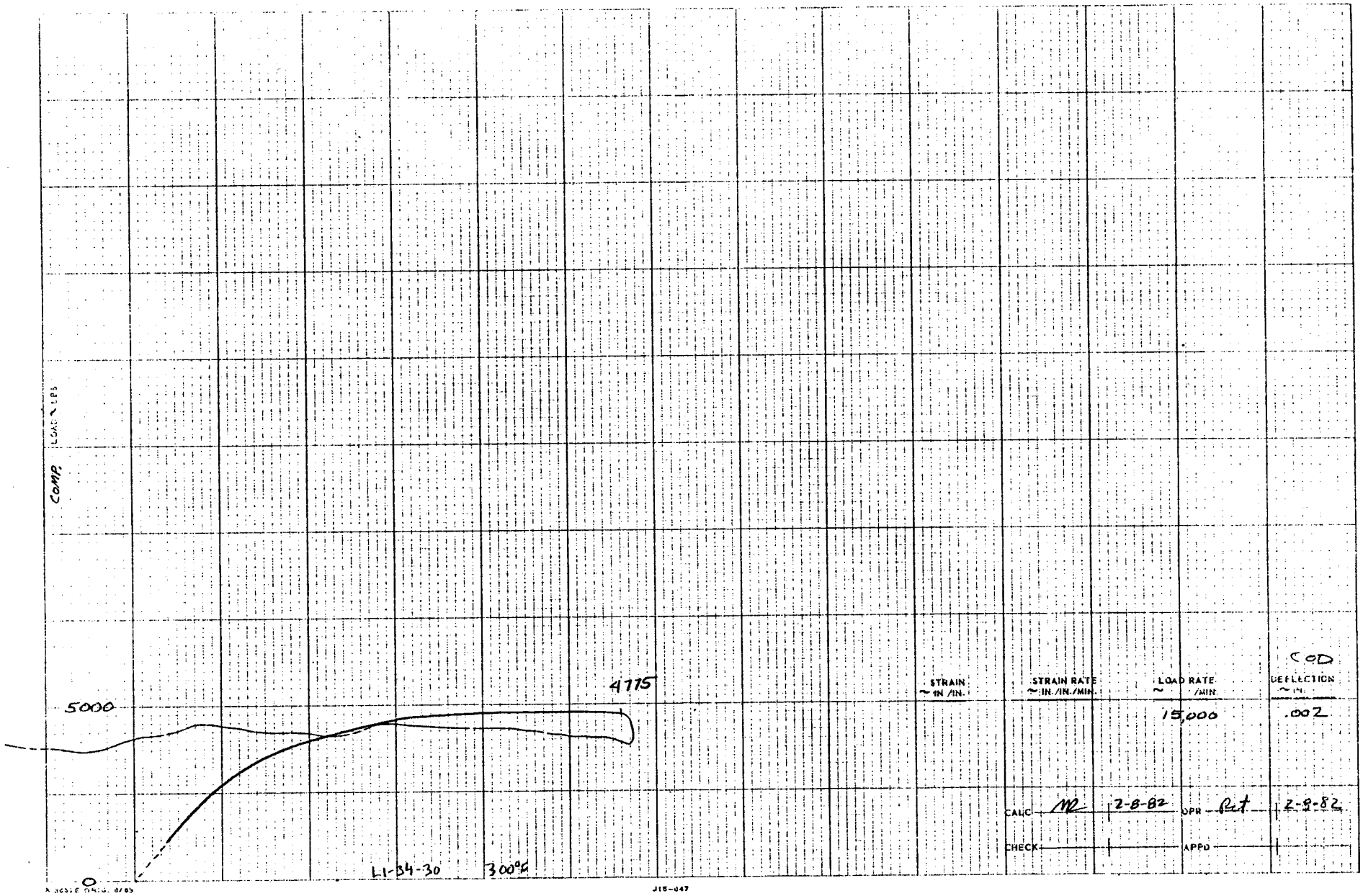
COMP. LOADS - LBS
5000
4775
0
L1-34-30
300°F
STRAIN ~IN/IN.
STRAIN RATE ~IN./IN./MIN.
LOAD RATE ~ /MIN
15,000
COD
DEFLECTION ~IN.
.002
CALC M 2-8-82
OPR Rat 2-9-82
CHECK
APPD
J15-047

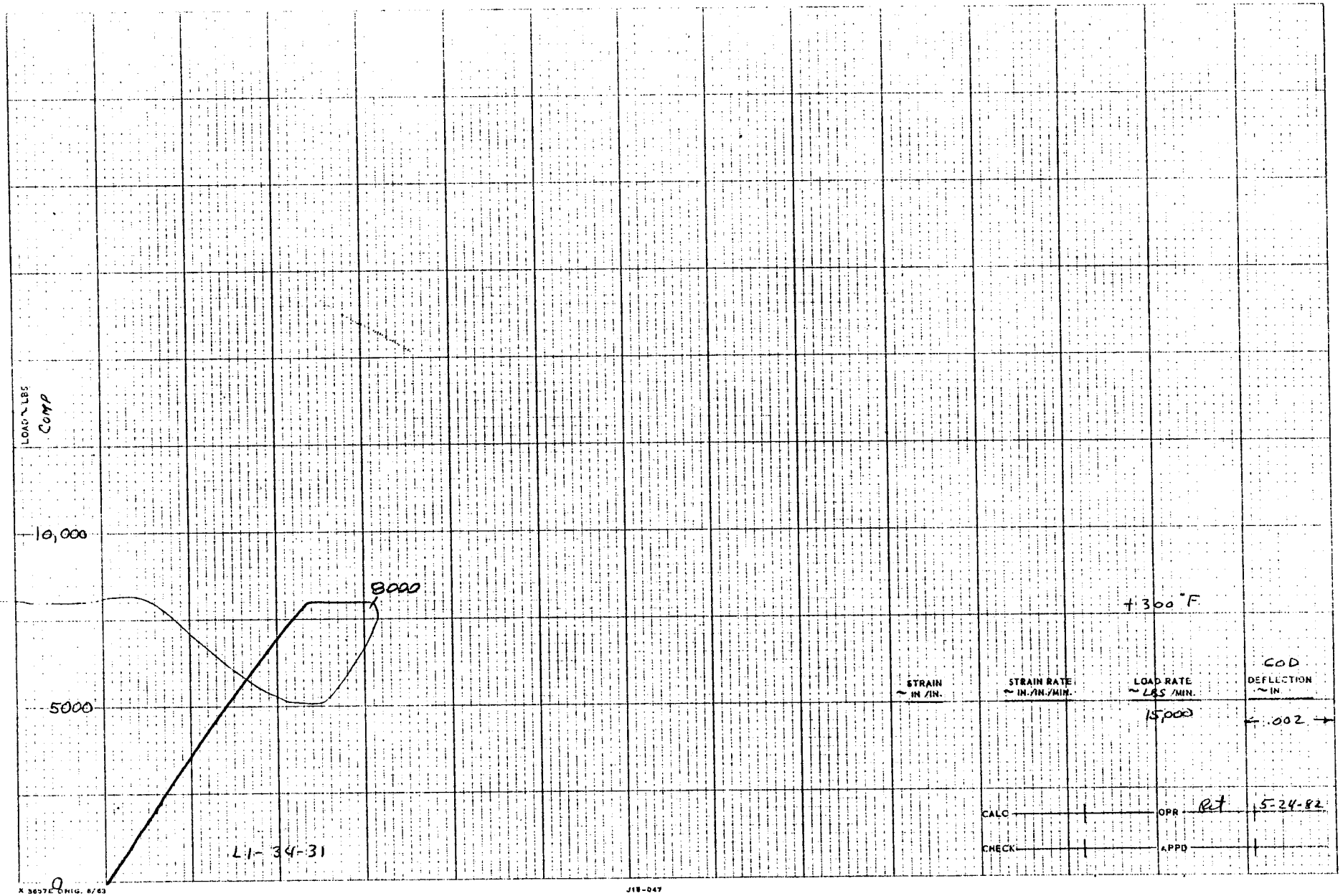
LOAD ~ LBS
Comp
10,000
5000
0
8000
+300 °F
STRAIN ~ IN /IN.
STRAIN RATE ~ IN./IN./MIN.
LOAD RATE ~ LBS /MIN.
15,000
COD DEFLECTION ~ IN
.002
CALC
OPR
Rt
5-24-82
CHECK
APPD
L1-34-31
X 36372 ORIG. 8/63
J18-047

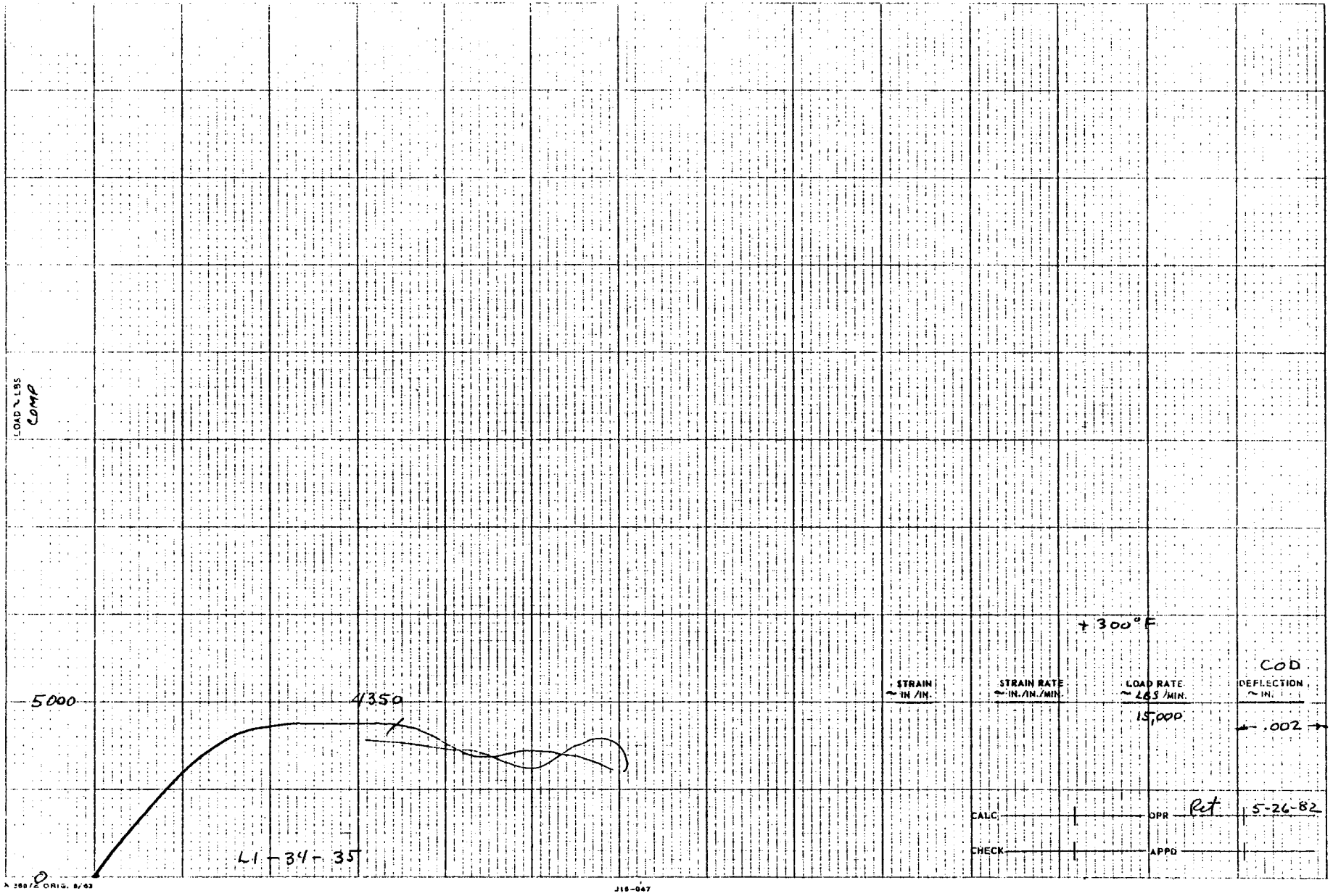
LOAD ~ LBS
COMP
5000
0
4350
L1-34-35
+300°F
STRAIN ~ IN/IN.
STRAIN RATE ~ IN./IN./MIN.
LOAD RATE ~ LBS/MIN.
15,000
COD DEFLECTION ~ IN.
.002
CALC
OPR
Ret
5-26-82
CHECK
APPD
A 288/2 ORIG. 8/63
J18-047

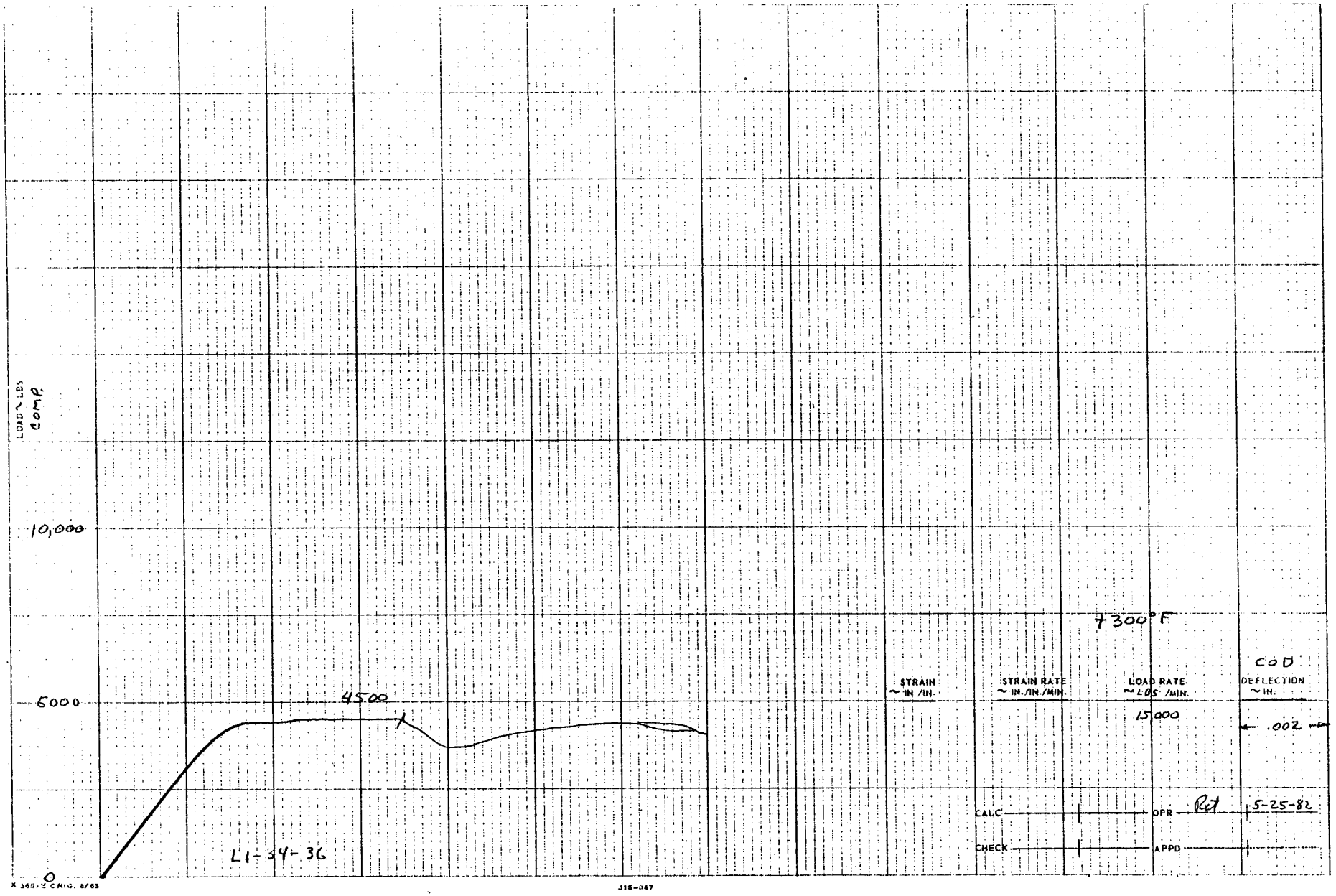
LOADS
comp
10,000
5000
0
4500
L1-34-36
7300°F
STRAIN
~ IN /IN.
STRAIN RATE
~ IN./IN./MIN.
LOAD RATE
~ LBS /MIN.
15,000
COD
DEFLECTION
~ IN.
.002
CALC
OPR
Ret
5-25-82
CHECK
APPD
X 365/2 ORIG. 8/63
315-047

COMP. LEAF N. LBS

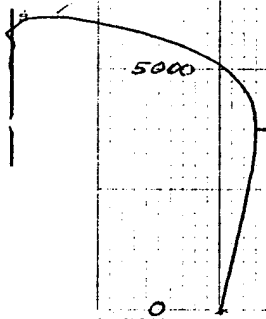

6075

EDI Cmp Adhesive Failure

.0006 @ 3750

STRAIN ~ IN /in.	STRAIN RATE ~ IN./IN./MIN.	LOAD RATE ~ /MIN.	C.O.D. DEFLECTION ~ IN.
		15,000	.002

CALC M 2-6-87 OPR Rat 2-8-82

CHECK APPD

L1-34-37 300°F

A 3057E CR14. 5/83

J15-047

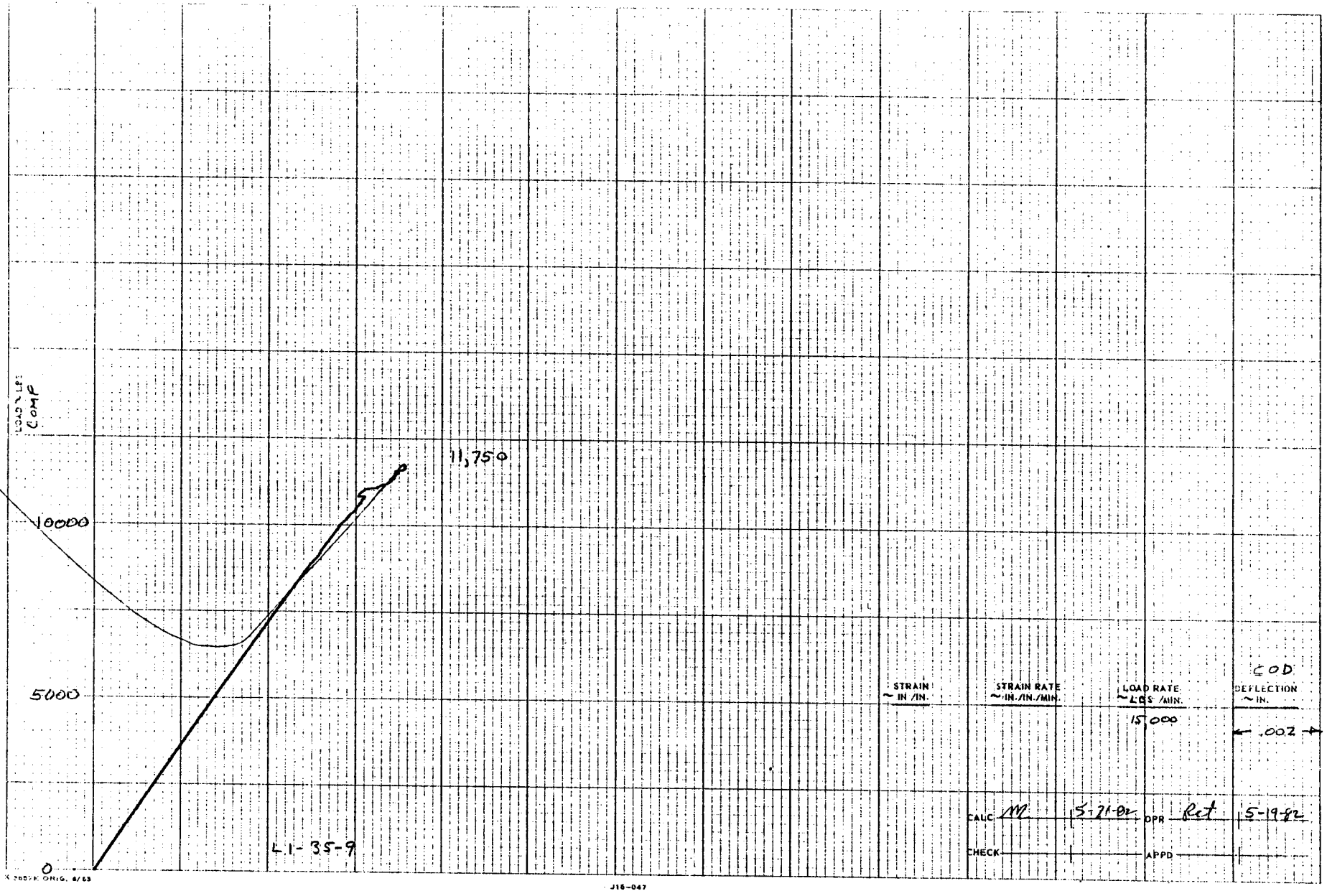
COMP
11,750
10000
5000
0
L1-35-9
STRAIN ~ IN /IN.
STRAIN RATE ~ IN./IN./MIN.
LOAD RATE ~ LBS /MIN.
15,000
COD
DEFLECTION ~ IN.
.002
CALC M 5-21-62
DPR Rct 5-19-62
CHECK
APPD
J18-047

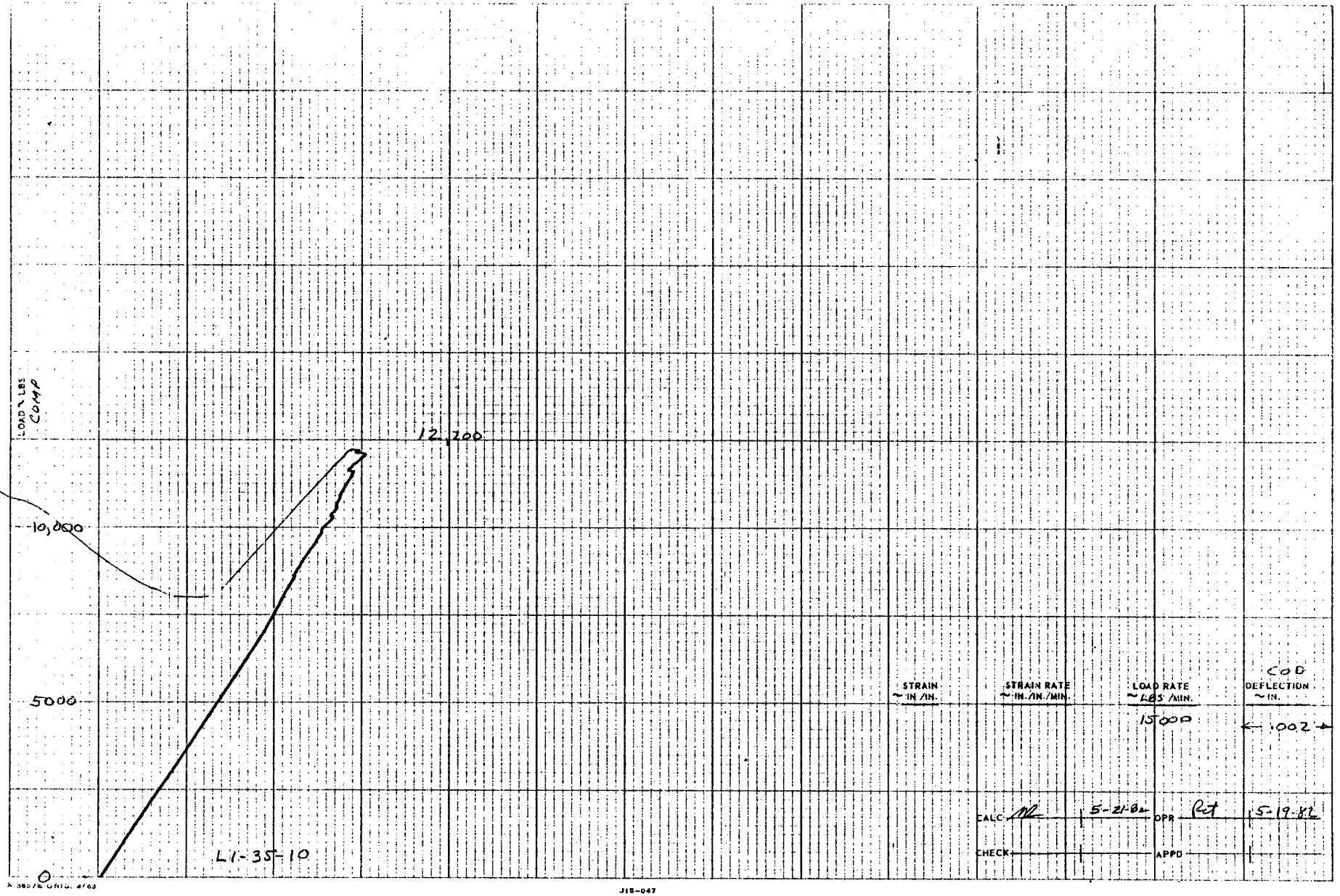
LOAD ~ LBS COMP
12,200
10,000
5000
0
L1-35-10
STRAIN ~ IN /IN.
STRAIN RATE ~ IN./IN./MIN.
LOAD RATE ~ LBS /MIN.
15000
COD DEFLECTION ~ IN.
.002
CALC
5-21-82
OPR
Ret
5-19-82
CHECK
APPD

J15-047

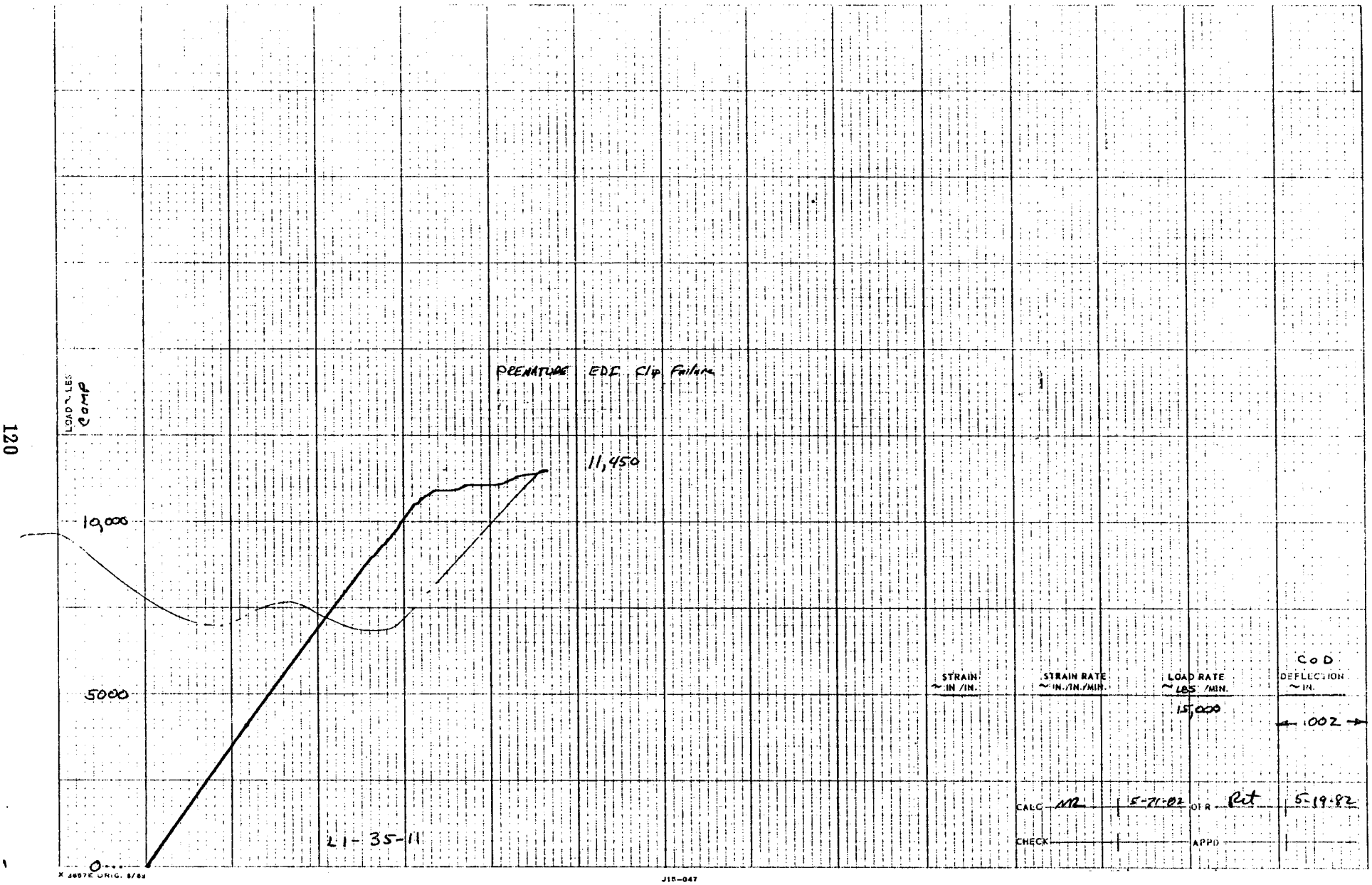
LOAD ~ LBS
Comp
PREMATURE EDI Clip Failure
11,450
19,000
5000
0
21-35-11
STRAIN
~IN /IN.
STRAIN RATE
~IN./IN./MIN.
LOAD RATE
~LBS /MIN.
15,000
COD
DEFLECTION
~IN.
.002
CALC MR 5-21-82 DR Rct 5-19-82
CHECK APPD
X 3657E ORIG. 8/81
J15-047

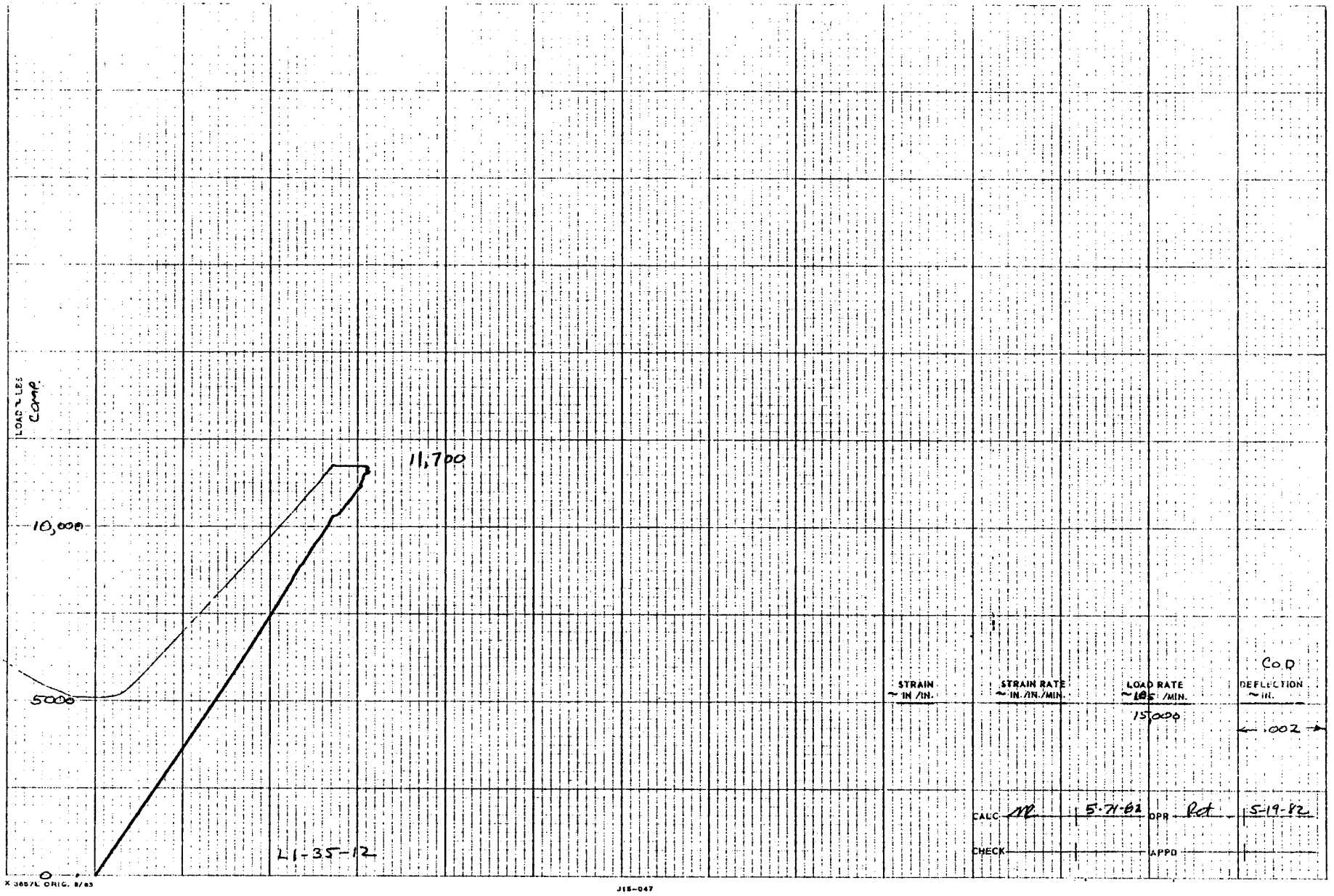
LOAD ~ LBS
Comp
11,700
10,000
5000
0
L1-35-12
STRAIN ~ IN /IN.
STRAIN RATE ~ IN./IN./MIN.
LOAD RATE ~ LBS /MIN.
150000
Co.D
DEFLECTION ~ IN.
.002
CALC
5-21-82
OPR
Rct
5-19-82
CHECK
APPD
X 3687/L ORIG. 8/83
J15-047

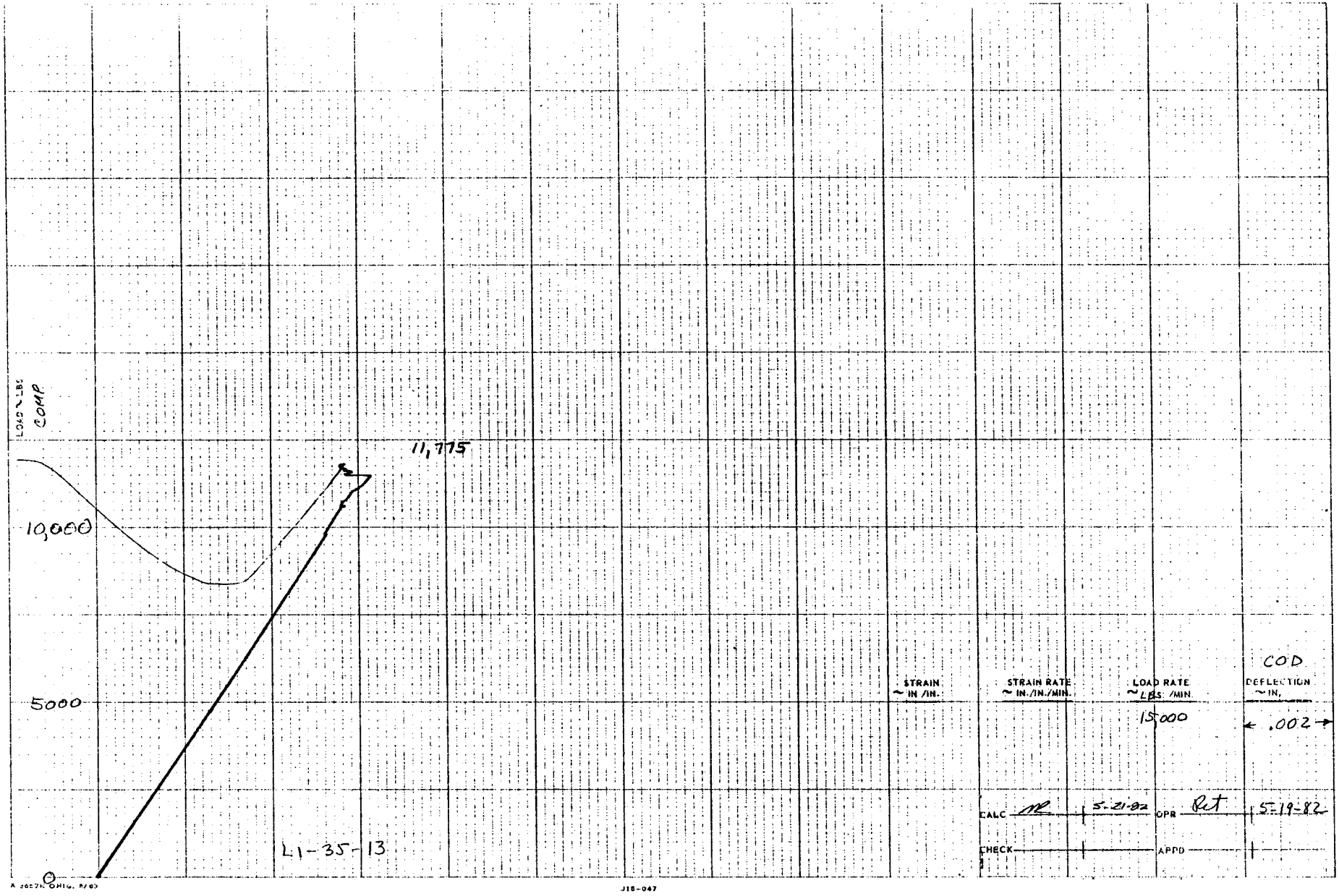
LOAD ~ LBS
COMP
11,775
10,000
5000
L1-35-13
STRAIN ~ IN /IN.
STRAIN RATE ~ IN./IN./MIN.
LOAD RATE ~ LBS /MIN
15,000
COD
DEFLECTION ~ IN.
.002
CALC
5-21-82
OPR
Ret
5-19-82
CHECK
APPD
J18-047

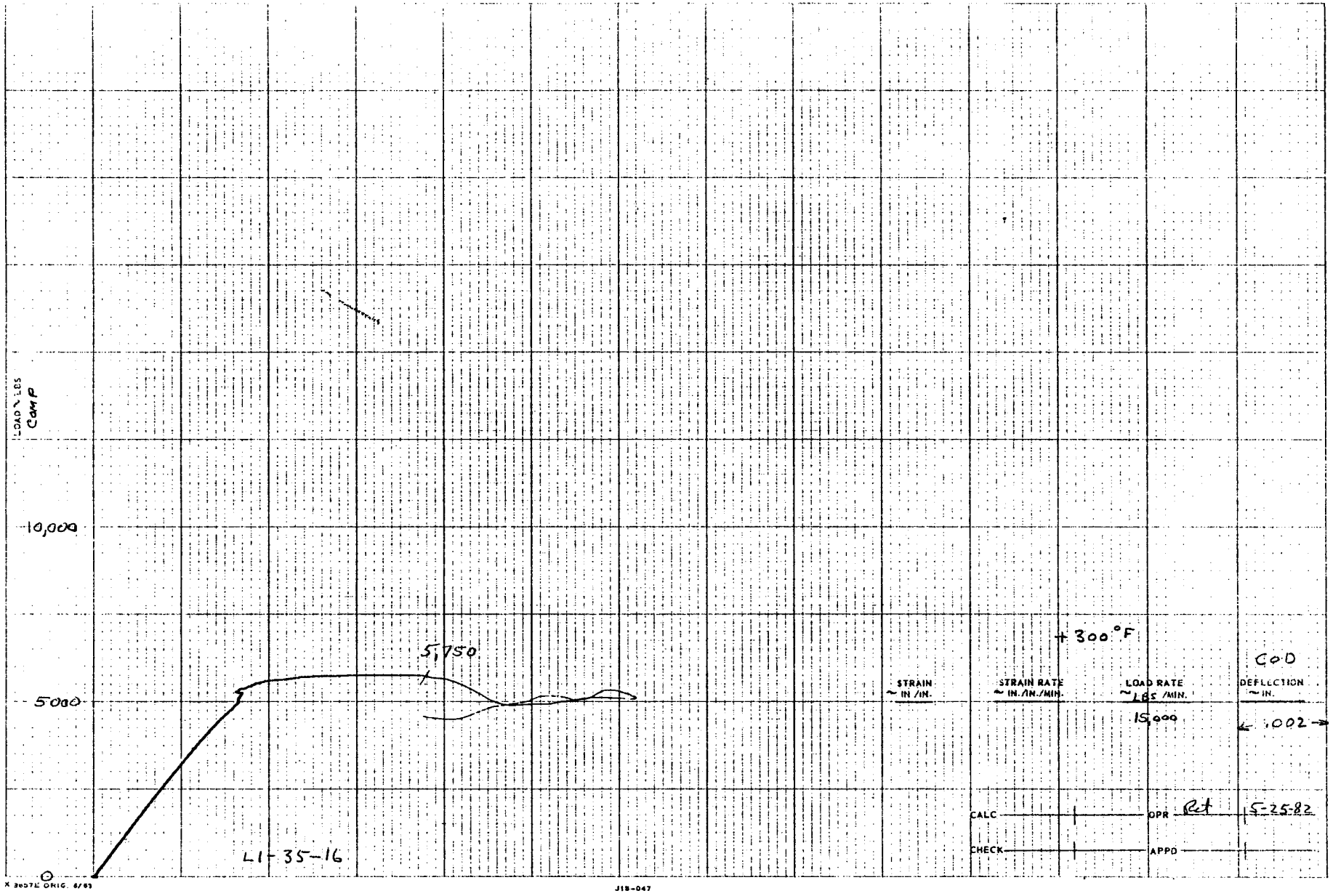
LOAD ~ LBS
Comp
10,000
5000
5,750
+300°F
C.O.D
STRAIN ~ IN/IN.
STRAIN RATE ~ IN./IN./MIN.
LOAD RATE ~ LBS/MIN.
15,000
DEFLECTION ~ IN.
.002
CALC
OPR
Rt
5-25-82
CHECK
APPD
L1-35-16
X 36578 ORIG. 6/63
J18-047

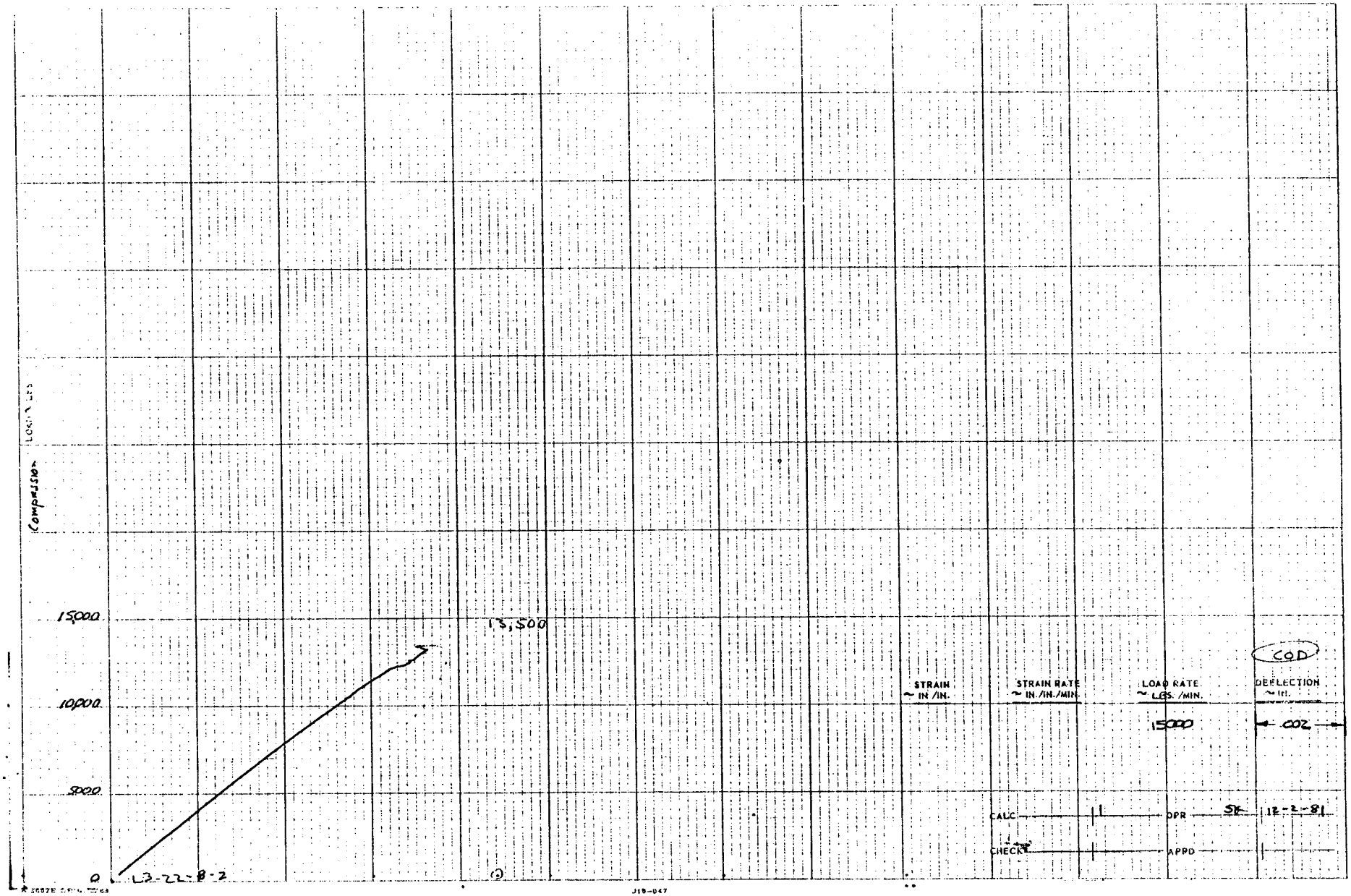
Compression
15000
10000
5000
0
15,500
L3-22-8-2
STRAIN ~ IN /IN.
STRAIN RATE ~ IN./IN./MIN.
LOAD RATE ~ LBS. /MIN.
15000
DEFLECTION ~ in.
COD
.002
CALC
DPR
SE
12-2-81
CHECK
APPD

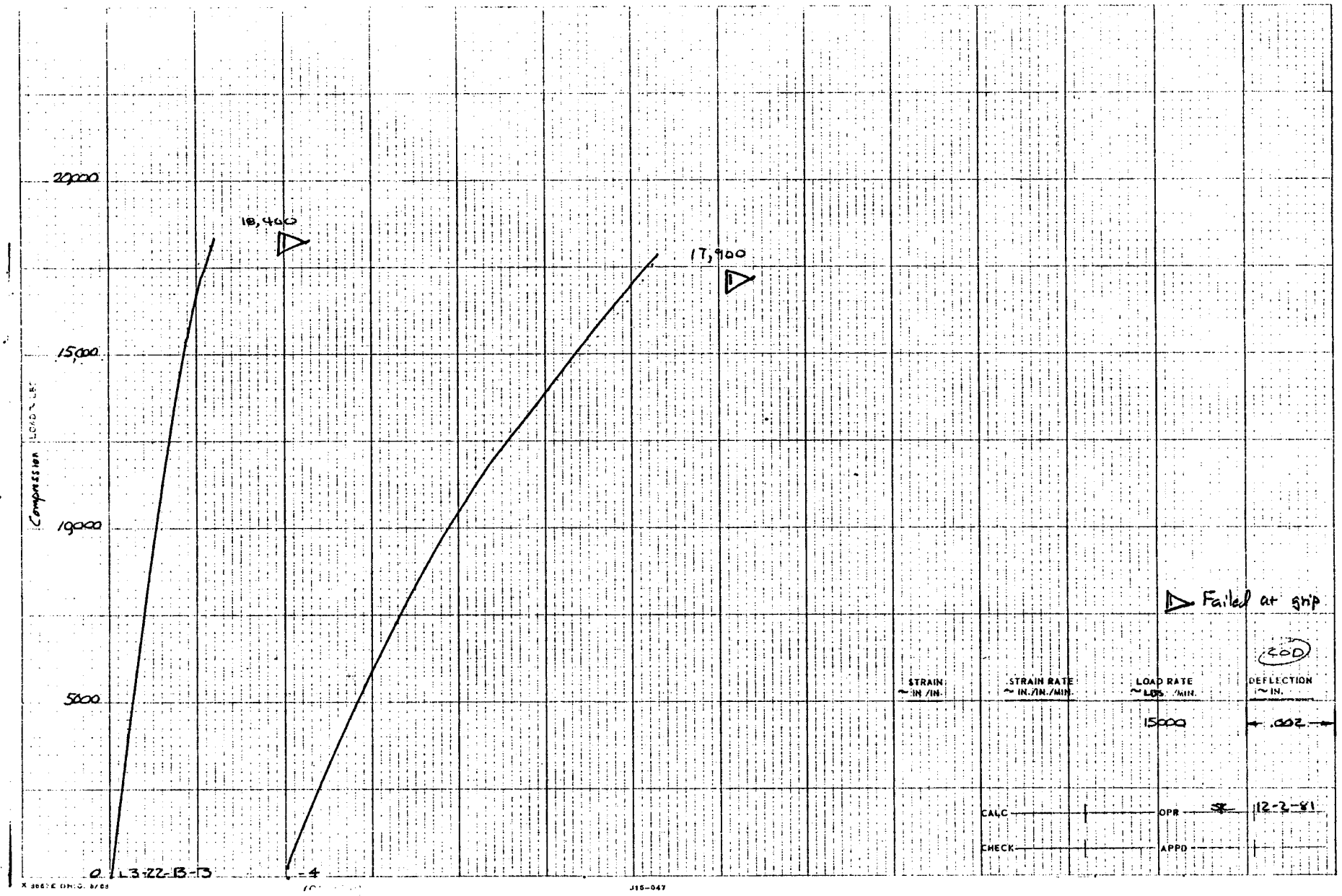
20000
15,000
10000
5000
0
Compression LOAD ~ LBS
18,400
17,900
Failed at grip
L3-22-13-13
-4
STRAIN ~ IN/IN.
STRAIN RATE ~ IN./IN./MIN.
LOAD RATE ~ LBS./MIN.
15000
DEFLECTION ~ IN.
.002
CALC
OPR
12-3-81
CHECK
APPD
J15-047

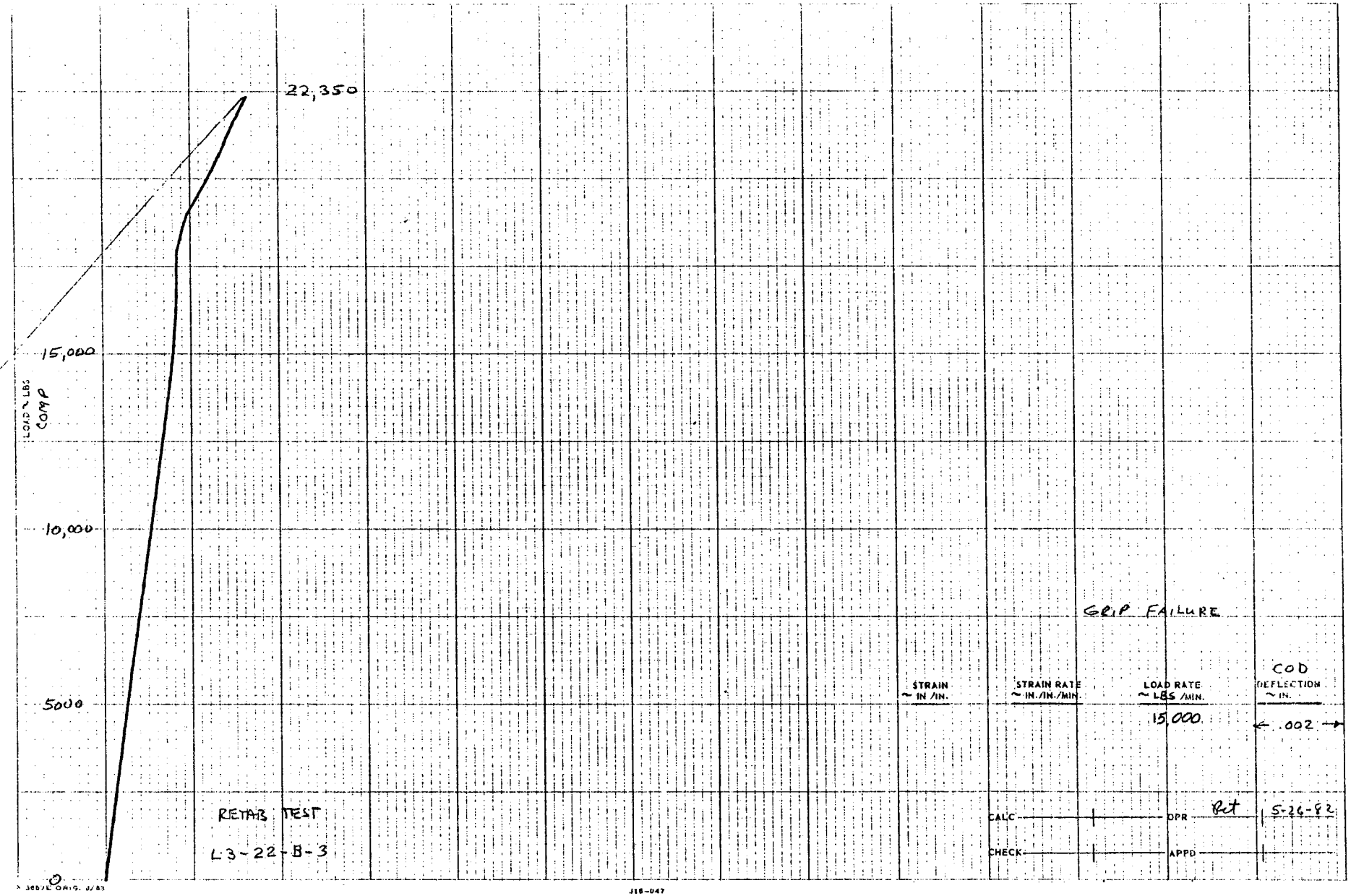
22,350
15,000
10,000
5000
0
LOAD ~ LBS
COMP
GRIP FAILURE
STRAIN ~ IN /IN.
STRAIN RATE ~ IN./IN./MIN.
LOAD RATE ~ LBS /MIN.
15,000
COD DEFLECTION ~ IN.
← .002 →
RETAB TEST
L3-22-B-3
CALC
DPR
Rct
5-26-82
CHECK
APPD

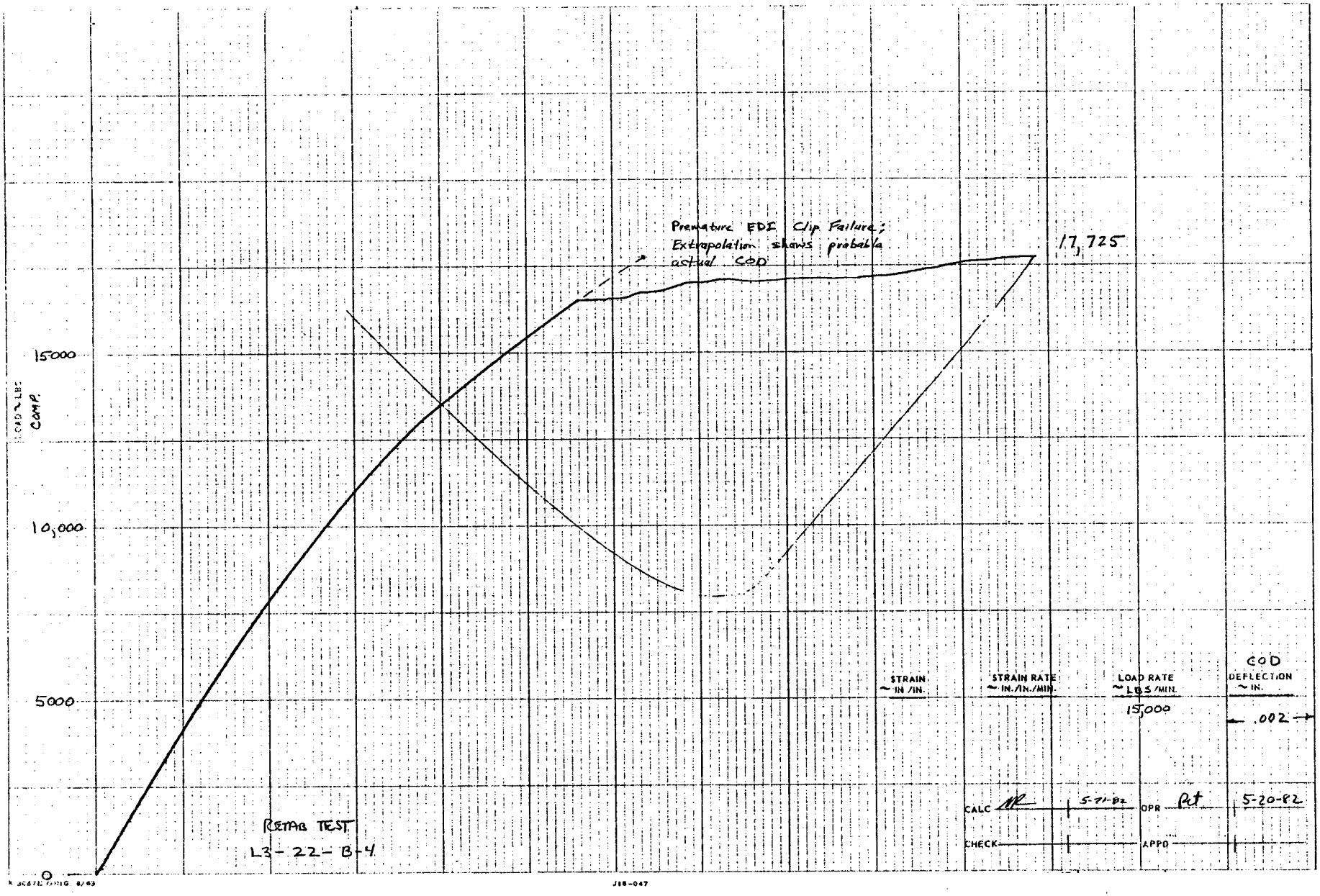
Premature EDF Clip Failure;
Extrapolation shows probable
actual COD
17,725
15000
10,000
5000
0
LOAD ~ LBS
COMP.
RETAB TEST
L3-22-B-4
STRAIN
~ IN /IN.
STRAIN RATE
~ IN./IN./MIN.
LOAD RATE
~ LBS/MIN.
15,000
COD
DEFLECTION
~ IN.
.002
CALC
5-21-82
OPR
Pat
5-20-82
CHECK
APPD
J18-047

1. Report No.	2. Government Accession No.	3. Recipient's Catalog No.
NASA CR-168023		

4. Title and Subtitle	5. Report Date
COMPRESSION AND COMPRESSION FATIGUE TESTING OF COMPOSITE LAMINATES	JULY 1982
	6. Performing Organization Code
7. Author(s)	8. Performing Organization Report No.
T. R. PORTER	D180-27619-1
	10. Work Unit No.
9. Performing Organization Name and Address Boeing Military Airplane Company P.O. Box 3707 Seattle, Washington 98124	11. Contract or Grant No. NAS3-22812
	13. Type of Report and Period Covered Final: 6-1-81 to 8-31-82
12. Sponsoring Agency Name and Address National Aeronautics and Space Administration Lewis Research Center/21000 Brookpark Road Cleveland, Ohio 44135	14. Sponsoring Agency Code

15. Supplementary Notes
Project Manager, Gordon T. Smith
Structures Branch
NASA Lewis Research Center
Cleveland, Ohio 44135

16. Abstract

This report presents the results of a program with the objective to experimentally investigate the effects of moisture and temperature on the fatigue and fracture response of composite laminates under compression loads. The structural laminates investigated were a typical angle ply laminate and a typical turbine-engine fan blade laminate. Defects investigated were: full- and half-penetration slits and impact delaminations. Results are presented showing the effects of moisture on the fracture and fatigue strength at room temperature 394K (250°F) and 422K (300°F). Static test results are presented that show the effects of defect size and type on the compression-fracture strength under moisture and thermal environments. The cyclic test results compare the fatigue lives and residual-compression strength under compression only and under tension-compression fatigue loading.

17. Key Words (Suggested by Author(s))		18. Distribution Statement
Composite Materials	Moisture Absorption	Unclassified-Unlimited
Graphite/Epoxy	Delamination Growth	
Fracture	Impact Damage	
Fatigue	Experimental Data	
Flaws		

19. Security Classif. (of this report)	20. Security Classif. (of this page)	21. No. of Pages	22. Price
Unclassified	Unclassified	127	

Available: NASA's Industrial Applications Centers

N-305